The Integrity of Compartmentation in Buildings During a Fire

The authors of this report are employed by BRE. The work reported herein was carried out under a Contract placed by the ODPM. Any views expressed are not necessarily those of the ODPM.

Executive Summary

The research reported here was commissioned by ODPM Buildings Division because of concern that modern methods of design and construction which utilised longer spans, resulting in the increasing use of unprotected steel members, could lead to a premature loss of integrity of fire resisting compartment walls.

This work will be of particular interest to regulators, designers, architects, manufacturers of proprietary fire protection and members of the fire and rescue services.

The overall aim of the work was to provide improved guidance, where appropriate, to ensure the integrity of compartmentation, typically walls and floors, in buildings during a fire. There is currently no quantitative guidance on the levels of deflection to be accommodated by fire resisting compartment walls.

It was also intended that the findings would be fed into the current review of the guidance contained in Approved Document B of the Building Regulations.

This research was led by BRE and included contributions by experts from Buro Happold and University of Ulster. Buro Happold were responsible for the structural modelling while the University of Ulster provided information in relation to the performance of fire resisting walls.

The work consisted of a review of information currently in the public domain, consultation with stakeholders, analysis of existing data and a limited parametric study using non-linear finite element methods to predict the response of a typical framework to a range of different parameters. This study included the location of compartment walls, the relationship between standard and parametric fire exposures, the effect of increasing spans, the impact of imposed loads and the influence of applied fire protection.

The findings of this work have shown that traditional methods for ensuring the integrity of compartment walls have provided acceptable levels of safety. Quantitative information on typical levels of deflection for different forms of construction have however been derived based on the location of the compartment wall and the floor span. This takes into account the concerns of longer spans and the increasing use of unprotected steel in buildings.

If the designer chooses to adopt a system that is incapable of accommodating the levels of displacement anticipated then he or she has the option of designing the compartment wall to resist the additional loading imposed due to movement of the floor.

Contents

Introduction

There is a need for more rigorous guidance in relation to the integrity of compartmentation during a fire.

The fire resistance of loadbearing and non-loadbearing components that form compartment walls and floors are typically assessed in isolation, using the standard fire test procedures in BS476 Parts 20, 21 and 22, EN1363 Part 1. It is assumed that the construction will provide this level of resistance in an actual fire in a real building. However, the mode of failure may be different to that experienced in the isolated tests. In the case of loadbearing walls and infill masonry panels, horizontal thermal expansion of the surrounding structure could cause instability of the wall, leading to premature failure. For non-loadbearing walls, the vertical displacement of the structure during a fire is not directly considered when assessing its performance and may lead to premature failure when used in actual buildings.

There is a need to estimate the anticipated vertical and horizontal deformations during a fire for a range of typical design scenarios and accommodate these deformations within the total design of the compartmentation.

BRE undertook a research programme for ODPM Buildings Division to consider all of the relevant issues in order to bring forward, where appropriate, proposals for improvements to the current guidance.

The work involved:

- A review of the current situation in relation to maintaining the integrity of compartmentation during a fire for which typical deflection limits associated with standard test procedures were identified.
- A study of the levels of displacement associated with real buildings through an analysis of available large-scale test data.
- Gathering information on the relevant parameters (design fire scenarios, compartment geometry, construction details) for subsequent analysis. Validation of the analytical methods adopted based on comparisons with existing experimental data.
- A parametric study using non-linear finite element methods to determine suitable levels of deflection to be accommodated by compartment walls during a fire.

A summary of the work follows and the full and comprehensive details are presented in the Appendices.

bre

Project summary

The summary of this work is presented as a series of discrete tasks:

Review of existing information

A review was undertaken which considered the current situation in terms of the regulatory requirements and the results from standard fire tests. It looked at the classification for walls in buildings and provided information on new design methods and existing guidance. Details of typical deflection heads provided by manufacturers of compartment walls were included in this review.. In this way the current means of meeting the regulatory requirement could be assessed alongside typical forms of construction. The work highlighted the fact that levels of deflection in standard fire tests are, in part, a function of the form of construction and that any guidance needs to account for the differences in forms of construction. The essential information from this work is included in Appendix A.

Collate existing data on the magnitude of displacements from full-scale fire tests

An investigation was undertaken into the time-temperature-deflection relationships from a number of full-scale fire tests on different forms of construction. The results from eleven full-scale tests carried out over a period of approximately six years were investigated to ascertain the deflections associated with real fires in real buildings. Again this work demonstrated the different levels of deflection associated with different forms of construction. Lightly reinforced composite floor slabs with unprotected beams achieved a maximum deflection of almost span/10 with only slight recovery on cooling while precast concrete units reached a maximum deflection of span/60 with residual displacement in excess of span/150. The results from flat slab concrete floors indicated a residual deflection of approximately span/100. The relevant information from this work is included in Appendix B.

Evaluate existing analytical methods

It was necessary to consider which parameters would be investigated in subsequent parametric studies. An initial choice of frame layout for analysis, compartment geometry, imposed loads, design fire scenarios and location of compartment walls was made. In addition detailed validation is presented for both the thermal (THELMA) and structural (VULCAN) numerical models used to undertake the parametric studies...The relevant information from this work is included in Appendix C.

Description of existing data for subsequent analysis

This involved the use of test data, from a full-scale European test carried out on the steel framed building at BRE's Cardington laboratory. The results had not previously been used for model development or validation and had not been released in the public domain. The utilisation of this data enabled the analysis and validation of the thermal and structural models used in this work.. The relevant information from this work is included in Appendix D.

Parametric studies

A parametric study consists of an analysis of the influence of individual factors on the outcome of a particular event. In this case the individual factors (or parameters) are the location of compartment walls, the fire exposure, the amount of fire protection, the span of the supporting beam and the level of the design load condition. A parametric study looking at the effects of variations in these critical parameters was undertaken using a CFD model to determine the thermal response of the building linked to a finite element model to determine structural response. A comparison of predictions was made against the Cardington full-scale test data which provided confidence in the analytical tools. There was a very close correlation between observed and predicted behaviour. The significant findings from the parametric study are summarised below:

- When all beams are protected in accordance with the requirements of BS476, the maximum deflections that are likely to occur are approximately span/40.
- The maximum deflection that is likely to occur directly above a compartment wall is approximately span/100.
- When intermediate beams are unprotected, the maximum deflection that is likely to occur within the fire compartment is approximately span/20. The maximum deflection that is likely to occur under protected beams is approximately span/100.

The relevant information from this work is included in Appendix E.

Produce guidance for regulatory authorities on the acceptance criteria to be applied to fire safety engineering solutions

Specific recommendations have been produced based on the results from this project and consultation with industry representatives. The recommendations have been reported separately to the project sponsors (ODPM) and are therefore not included in this final factual report. One issue that was not part of the parametric study was the performance of connections in fire and their influence on the integrity of compartmentation. Evidence from a number of full-scale tests investigated through this project has shown that satisfactory performance of wall and floor elements tested in isolation is not sufficient to ensure stability at the fire limit state. The robustness of connections must be assessed when considering compartmentation even where the robustness requirements of Approved Document B do not apply.

General discussion

This work has enabled a few general points may be made.

- Standard fire tests are based on deflection limits of span/30 or span/20 (depending on rate of deflection). From a consideration of available fire test data this value is reasonable for protected steel beams but rarely achieved for elements such as concrete floor slabs where the insulation criteria generally governs.
- Standard deflection head details for non-loadbearing fire-resistant partitions generally provide a deflection allowance of up to 50mm.
- The deformations associated with real fires are often much higher than the limits imposed through the standard fire test. However, the magnitude of the deflection is in part a function of the form of construction and the presence or absence of passive fire protection. For unprotected composite beams deflections of span/10 are not uncommon. For other forms of construction such as precast hollow core slabs mid-span deflections of span/60 are more common. Any limitation on compartmentation must reflect the different behaviour of different forms of construction.
- The comparisons with full-scale test results show that properly validated thermal and structural models are capable of predicting the complex non-linear behaviour associated with the deformation of buildings during and following a fire. The work has highlighted a number of areas where there is insufficient validation to provide confidence in the output.
- The parametric study has concentrated on those areas where the models can provide accurate predictions of behaviour. The recommendations are based largely on the results from the parametric study.

Concluding Remarks

This project has investigated a number of the parameters influencing the integrity of compartmentation in buildings during a fire. The work carried out has provided a rational basis for the recommendations to be made to ODPM for changes to the guidance in support of AD-B.

Appendix A – Review of existing methods to ensure the effectiveness of compartmentation

Regulatory Requirements and Standard Fire Tests

The starting point for a review of current approaches to maintaining the integrity of compartmentation is to consider the provisions of AD-B. Section 9 deals with the issue of compartmentation and is related to the requirement B3 dealing with internal fire spread within the structure. Compartmentation has traditionally been assumed based on the concept of fire resistance and measured in relation to resistance to collapse, resistance to fire penetration, and resistance to the transfer of excessive heat.

The purpose of sub-dividing spaces into separate fire compartments is twofold. Firstly to prevent rapid fire spread which could trap occupants of the building and secondly to restrict the overall size of the fire. According to the guidance in AD-B there should be continuity at the junctions of the fire resisting elements enclosing a compartment. Typically this would be the junction between a wall (either loadbearing or non-loadbearing) and a floor. The general method for elements of structure (including compartment floors and walls) is to rely on the prescribed values in Tables A1 and A2 of AD-B. The values relate to a minimum period for which the element must survive in the standard fire test measured against the relevant performance criteria of stability, integrity and insulation. Given that the standard test relates to single elements it is difficult to see how such a reliance can achieve the requirement related to the provision of continuity at the junction between two elements.

In this project the principal area of concern is related to separating elements required to satisfy the criteria of integrity and insulation in addition to loadbearing capacity where appropriate. It is therefore necessary to investigate in detail the methods used to assess performance against the defined criteria for both floor and wall elements.

Loadbearing Capacity

Floors

For horizontal members failure in a standard test is assumed to have occurred when the deflection reaches a value of L/20 where L is the clear span of the specimen or where the rate of deflection (mm/min) exceeds a value of $L^2/9000d$ where d is the distance from the top of the section to the bottom of the design tension zone (mm). The rate of deflection criteria only applies once the deflection has reached a value of L/30.

The origin of the deflection limits are unclear but they, at least in part, are based on the limitations of test furnaces and the requirement to avoid damage to the furnace. This is not a logical basis on which to assess loadbearing capacity. The full-scale tests carried out on the steel framed building at Cardington have demonstrated that loadbearing capacity can be maintained when deflections much greater than those used to measure “failure” in a standard test have been mobilised. For concrete floor elements failure is generally a function of the insulation capacity rather than loadbearing capacity.

Walls

For vertical loadbearing elements failure of the test specimen is deemed to occur when the specimen can no longer support the applied load. There is no clear definition of failure in relation to the standard test. Laboratories are only required to provide for maximum deformations of 120mm and values over and above this limit would require the test to be terminated. The state of failure is characterised by a rapid increase in the rate of deformation tending towards infinity. It is therefore recommended that laboratories monitor the rate of deformation to predict the onset of failure and support the test load.

Integrity

Floors and Walls

The basic criteria for integrity failure of floor and wall elements is the same. An integrity failure is deemed to occur when either collapse, sustained flaming or impermeability have occurred. Impermeability, that is the presence of gaps and fissures, should be assessed using either a cotton pad or gap gauges. After the first 5 minutes of heating all gaps are subject to periodic evaluation using a cotton pad 100mm square by 20mm thick mounted in a wire holder which is held against the surface of the specimen. If the pad fails to ignite or glow the procedure is repeated at intervals determined by the condition of the element. For vertical elements where the gaps appear below the neutral pressure axis position gap gauges will be used to evaluate the integrity of the specimen. If the 25mm gauge can penetrate the gap to its full length (25mm + thickness of the specimen as a minimum value) or the 6mm gauge can be moved in any one opening for a distance of 150mm then integrity failure is recorded. The cotton pad is no longer used when the temperature of the unexposed face in the vicinity of the gap exceeds 300°C. At this point the gap gauges are used.

Again the origins of the measures used to determine performance are unclear.

Insulation

Floors and Walls

The basic criteria for insulation failure of floors and wall elements is the same. Insulation failure is deemed to occur when either the mean unexposed face temperature increases by more than 140ºC above its initial value or the temperature at any position on the unexposed face exceeds 180°C above its initial value.

The effect of these localised temperature rises on the unexposed face is unclear. For timber products ignition by a pilot flame can occur between 270ºC and 290ºC whilst spontaneous ignition (required if there is no integrity failure) occurs between 330ºC and 500ºC depending on species. These figures suggest that the temperatures used to define insulation failure may be too low particularly for structural elements passing through compartment walls where storage of combustible materials on the unexposed side is unlikely.

BS476 Part 21 states specifically that the standard test method is not applicable to assemblies of elements such as wall and floor combinations. There is some limited guidance to suggest that the test method may be used as the basis for the evaluation of three-dimensional constructions with each element loaded according to the practical application and each element monitored with respect to compliance with the relevant criteria.

Results from Standard Tests

A comprehensive series of fire resistance tests carried out by the Fire Research Station during the period 1936-1946 has been reported in National Building Studies Research Paper No. 12[1].

There are issues to be considered about the allowable deflection to be accommodated in relation to fire resisting construction on the fire floor itself, the floor below and the floor above. Compartment walls are often built under existing lines of compartmentation. For residential buildings where the requirements for compartmentation are particularly stringent the building layout is generally regular with compartment walls running continuously from floor to floor. In such cases the anticipated deflection is likely to be quite small where structural elements span from compartment wall to compartment wall. However, there is no guarantee that compartment walls will always be located in such an advantageous arrangement and there is nothing in the regulations to prevent a compartment wall being constructed immediately underneath or immediately above the mid-span of the supporting element. A useful starting point would therefore be a review of the likely range of deflections to be accommodated for a number of different forms of construction both in terms of standard fire tests and measured results from natural fire tests.

The information produced in reference 1, although comprehensive, is based on fire resistance tests carried out some sixty years ago. However, there is some useful information on the levels of deflection associated with timber and reinforced concrete floors and the deflection of protected and unprotected steel beams and concrete beams. Figure A1 below shows the spread of results for the maximum deflection of tested reinforced concrete floors in the centre of the span.

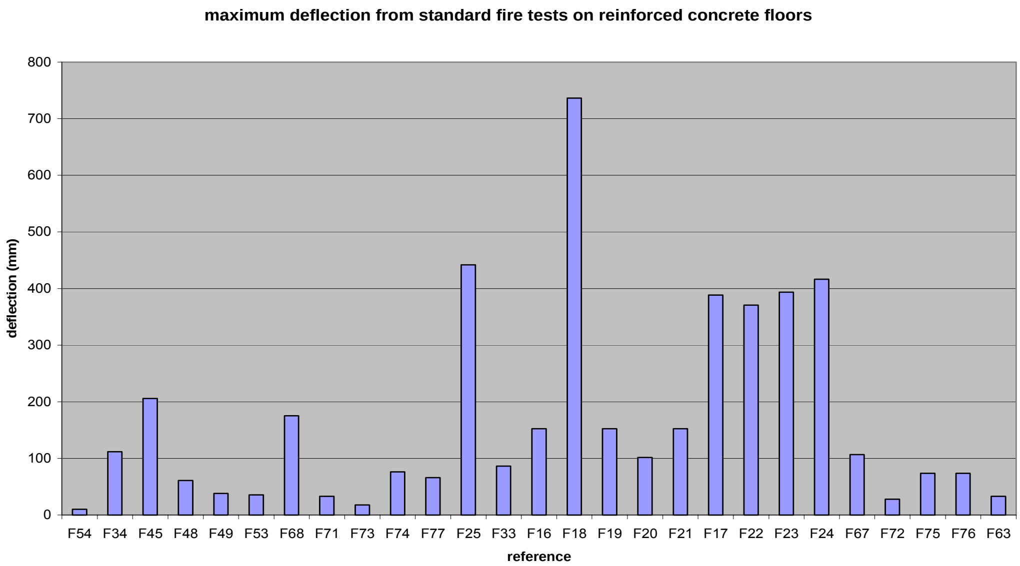

Figure A1 Maximum mid-span deflection of reinforced concrete floors in standard fire tests

In general the fire resistance of concrete floors in the absence of spalling is governed by the insulation requirement. Therefore, excluding those values above where overall collapse took place and limiting the results to those elements that either survived for the entire duration of the test or failed by an insulation failure the displacement at the centre of the slab is shown below.

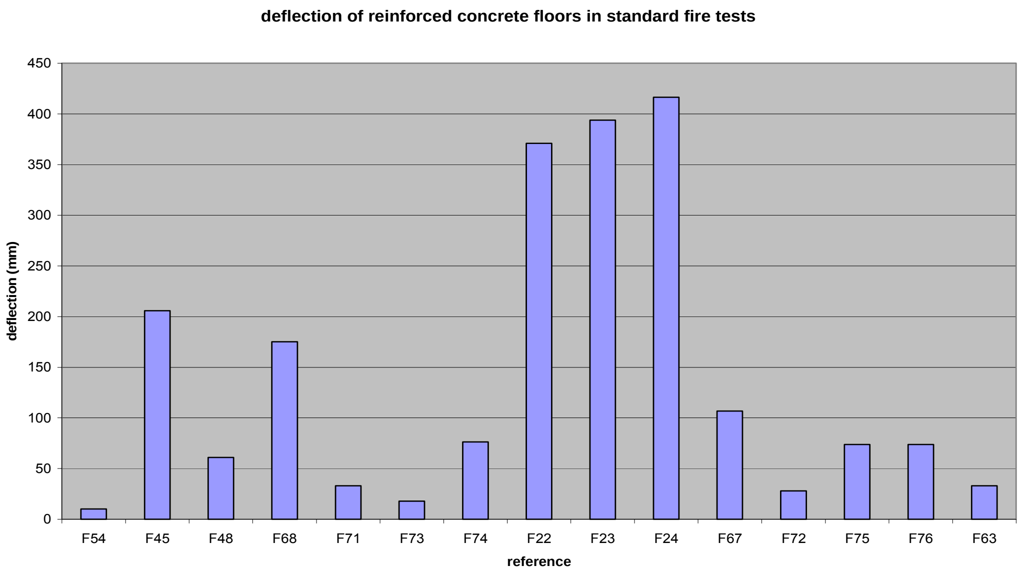

Figure A2 Maximum deflection of reinforced concrete slabs excluding loadbearing and integrity failure

Figure A3 shows the maximum displacement recorded for a variety of protected beam sections for a variety of durations ranging from 40 minutes to just over 120 minutes. All tests were carried out on a 4.25m span with simple supports.

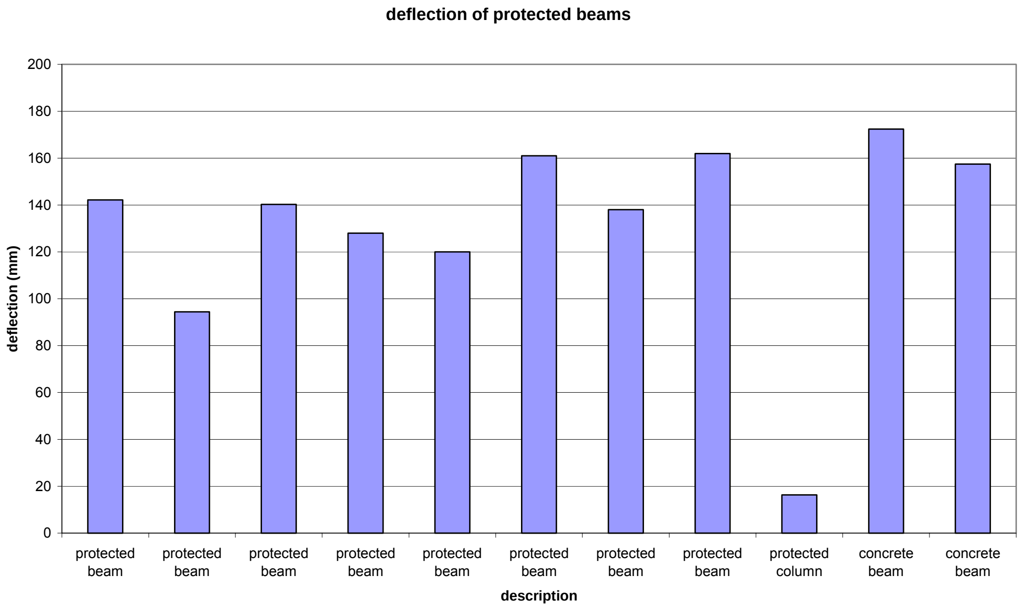

Figure A3 Maximum deflection of protected beams in standard fire tests

There is an assumption that the current method of meeting the regulatory requirement provides acceptable results. In general the tests referred to above were carried out on specimens spanning 4m. Limiting the deflection to a value of L/20 should exclude results greater than 200mm for a 4m span. The values quoted are for the maximum deflection recorded and do not provide any information on the time-deflection history throughout the test.

The “allowable” deflection of floor slabs and beams should be seen alongside the requirements for both loadbearing and non-loadbearing walls and partitions. For loadbearing walls there is a requirement to measure vertical deformation and lateral deflection. For non-loadbearing wall elements (partitions) there is a requirement to measure the lateral movement and record the maximum value. The nature of the deformation of walls in standard tests is very much a function of the test set-up. For non-loadbearing walls they are restrained in a frame and therefore can only move laterally due to thermal bowing. For loadbearing walls they are retained along the free edges but free to move in the direction of load.

The results for non-loadbearing brick walls are summarised in figure A4 below. The measurements generally relate to a time period of 120 minutes.

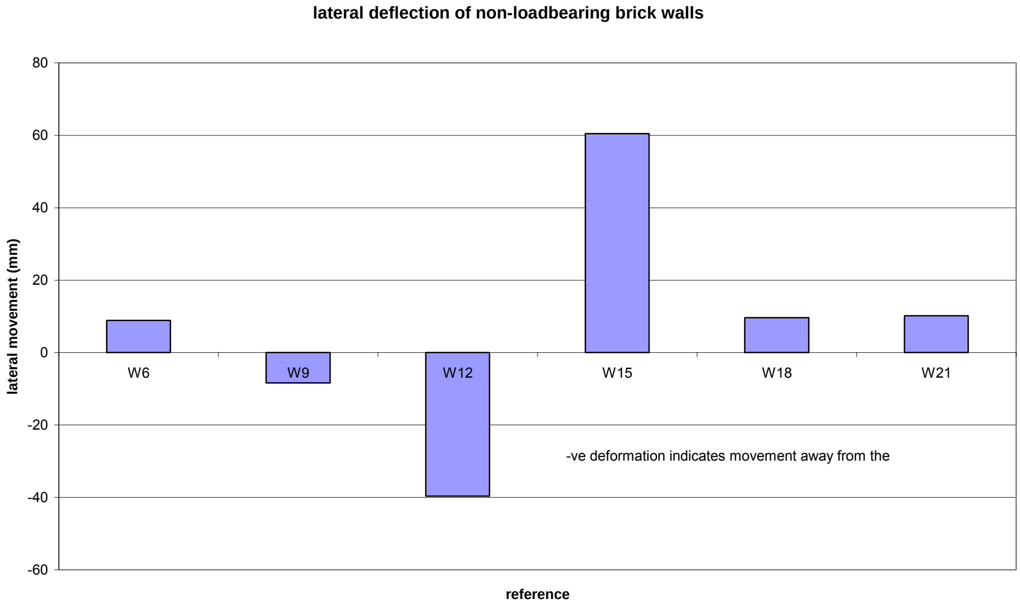

Figure A4 Lateral movement of non-loadbearing brick walls subject to a standard fire curve

The corresponding figure for loadbearing walls is indicated in figure A5 below. The loaded specimens are generally twice the thickness of those shown in figure A4 and the test duration is 360 minutes for all cases.

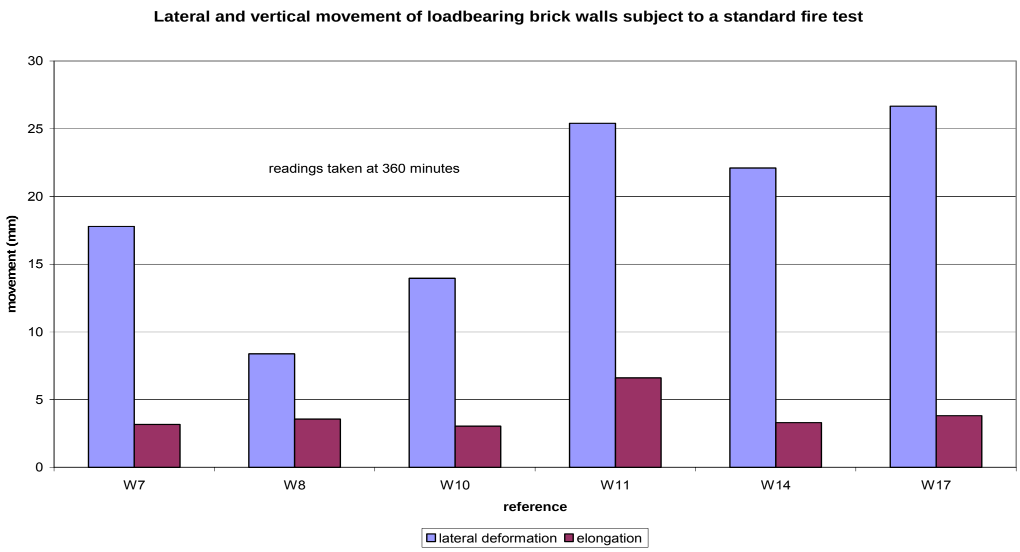

Figure A5 lateral and vertical movement of loadbearing brick walls subject to a standard fire test

The values for vertical movement are a result of the balance between thermal expansion of the heated face and a reduction in the load carrying capacity of the member due to the corresponding reduction in material properties at the heated face.

The values above provide some indication of the magnitude of the deformation associated with floors, beams and walls in the standard fire test. However, there is no direct relationship between the deflection limits applied to floors and beams and the deformation criteria applied to walls.

Although fire resisting compartment walls are often built on the main structural gridlines there is no requirement for this to be the case. Architectural and commercial requirements require flexibility in order to optimise the available space. Therefore compartment walls may be located at any location within the span. If the assumption from standard fire tests is that supporting elements may deflect as much as span/20 and that non-loadbearing compartment walls can be located anywhere within the span of the beam then there is clearly a potential for premature failure of compartmentation. This potential for failure applies to existing prescriptive methods (i.e. a reliance on the results from standard fire tests) of providing the necessary fire resistance to ensure the integrity of compartmentation.

Classification of Walls in Buildings

Walls in buildings are designed and constructed with many different end conditions. There appears to be little or no uniformity in this regard. Most if not all these walls, as constructed, would meet accepted structural design criteria. Many of the details of the edges of the wall which may have only a marginal influence structurally, would have a significant influence on the stability of the wall in a fire.

A non-load bearing partition wall will usually have gaps of about 10 mm along the vertical sides and top edge to allow for movement of the wall or columns. Ties on the vertical edges hold the wall to the columns. If the infill mastic is destroyed and the fire attacks the ties the wall may not have any support. The self-weight will give the wall some fixity along the bottom edge while the ties along the vertical edges will simulate a pin-ended condition. The top edge would be free. This would correspond to the wall type (h) in Table A1.

Type	End Restraints
(a)	All four sides fixed
(b)	Bottom edge and the vertical sides fixed and top edge pinned
(c)	Bottom edge fixed and the vertical sides and the top edge pinned
(d)	Top and bottom edges fixed and the vertical sides free
(e)	Bottom edge fixed, top edge pinned and the vertical sides free
(f)	Bottom edge fixed and the top edge and the vertical sides free
(g)	Bottom and top edges fixed and the vertical sides pinned
(h)	Bottom edge fixed, top edge free and the vertical sides pinned

Table A1. End restraints on Single Leaf Walls

The loading on a loadbearing wall would ensure some fixity along the top and bottom edges. Depending on the length, the wall may have movement joints or it might directly abut onto the columns. This will correspond to type (d) or (g) respectively of Table A1.

Walls required to resist shear will be in contact with other loadbearing construction on all four sides of the wall. This would correspond to type (a) of Table A1.

For both loadbearing and non-loadbearing walls horizontal and/or vertical gaps are often present to accommodate movement (expansion gaps). Irrespective of the reason for their presence, these gaps will have a profound influence on the fire behaviour of walls. Most structural codes specify minimum values for expansion or movement gaps and the general tendency is to go beyond the minimum value. The larger the gap the greater the chances are that the wall will deflect freely without interlocking. Larger gaps also provide less protection to the metal ties from the fire. The coefficient of thermal expansion would affect the closing of the gaps and in conjunction with the thermal gradient through the wall, would largely determine the deflection of the wall. Thus the behaviour of a wall with gaps, fillers and ties exposed to fire is a complex problem involving the interaction of many factors such as thermal expansion, thermal gradient, modulus of elasticity and strength of the wall, insulation and fire properties of the mastic, capacity of the wall ties and the relative dimensions of the walls and the gaps. The problem is further complicated by the fact most of theses factors vary with temperature.

Non-loadbearing walls

Detailing of non-load bearing walls fall into three general categories. In the first category, the walls are built with a nominal gap of 10mm on the vertical sides and top edge as shown in Figure A6a. The wall is tied to the columns on the sides with metal ties to provide lateral stability. Some engineers require these ties to be flexible to accommodate in-plane movement. Mastic filler along the edges covers the ties on the side though in a few special cases ceramic fibre has been used to thermally insulate the ties. These walls correspond to type (h) of table A1. When such a wall is exposed to fire, the wall would behave in one of the following ways:

- The expansion of the wall would close the gaps at the top and sides. The end restraints which initially corresponded to type (h) would change to type (g) or (c) and finally to type (a). In such an event, the high initial rate of deflection would be arrested and it is likely that the behaviour of the wall under fire conditions would be consistent with the results of a fire resistance test on a non-load bearing wall.
- Before the expansion of the wall could close the gaps, the deflection of the wall would impose loads on the ties already weakened by the fire, causing the ties to fail. The wall starts as type (h) and with the loss the effectiveness of the ties in the side would behave as a type (f) wall. With further increases in deflection with temperature, it is probable that the wall would collapse.
- The expansion of the wall is insufficient to close the gap. The ties being insulated by the mastic filler and the narrow gap retain their strength. Such a situation corresponds to wall type (h).

In the second category, walls are built with a 10 mm nominal gap at the top and the sides. Metal cleats from the floor above provided to support suspended ceilings also function to stabilise the wall as in Figure A6b. These walls correspond to type (e) of Table A1. These walls would lose the support at the top when the ceiling is damaged by fire.

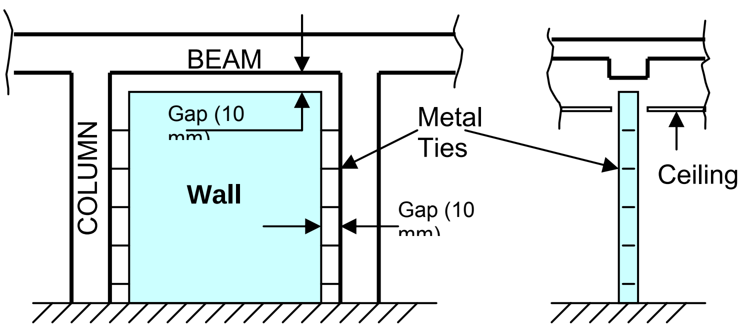

Type (a)

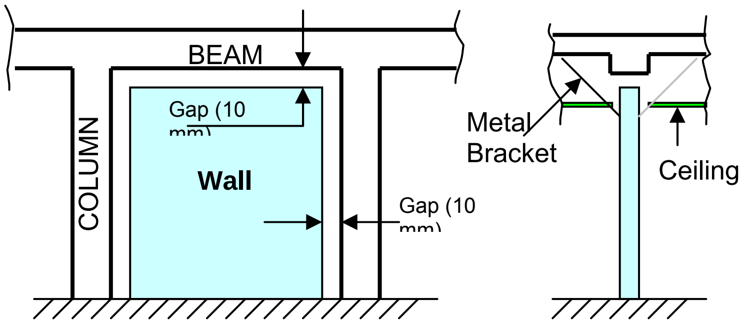

Type (b)

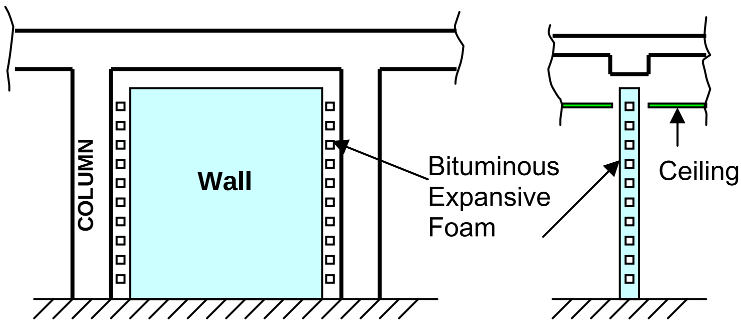

Type (c)

Figure A6 End restraints on non load bearing walls in the field

In the third category, the walls are built with foamed expansion-control material on the two edges and with a gap at the top as Figure A6c. Friction at the edges provided the required forces for stability. This category of walls would correspond to something between type (f) and (g) of Table A1.

Loadbearing Walls

Load bearing walls generally fall into three categories. In the first category, the vertical sides of the walls are free because of the incorporation of expansion joints as shown in Figure A7a and would correspond to type (d) in table A1. The end restraint on the wall in the field and the test specimen in the laboratory are similar.

Long lengths of load bearing wall forms the second category. The wall deforms into a series of corrugations in the horizontal direction and curve in the vertical direction. The end restraint on the wall in the field and on the specimen in the laboratory are quite compatible.

Load bearing walls, which abut on to other load bearing walls, form the third category. Walls of a fire compartment will deflect towards the fire as shown in figure A7b.

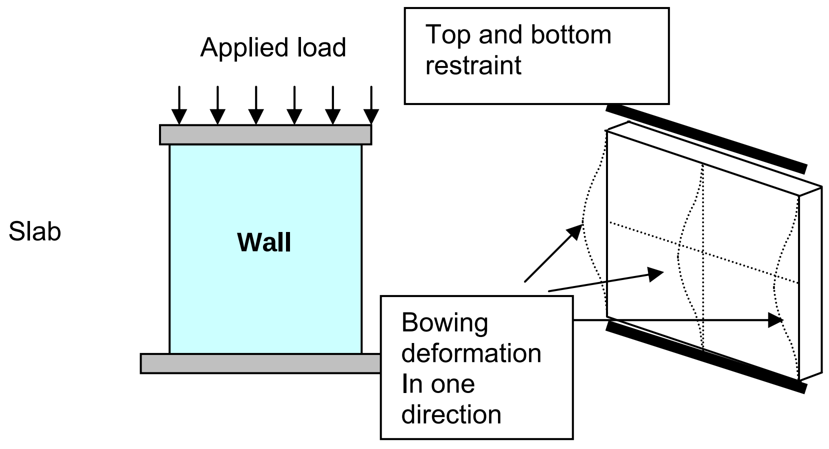

Type (a)

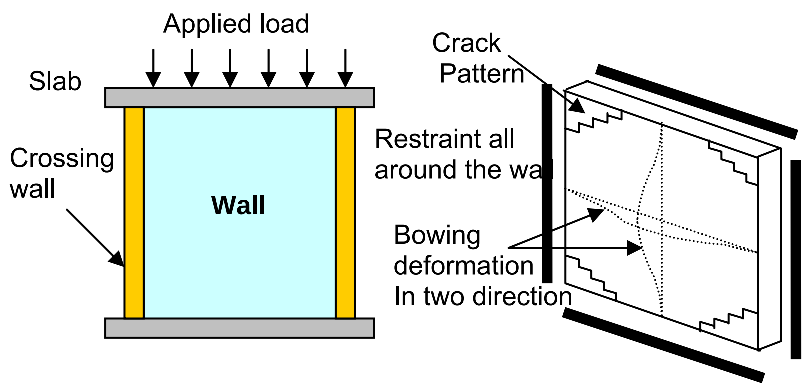

Type (b)

Figure A7 End restraints on loadbearing walls in practice

New Design Methods and Existing Guidance

Over the last few years, new design approaches[2] have been developed based on whole building behaviour in fire. The use of such methods generally leads to a reduction in the levels of passive fire protection applied to steel beams with a subsequent increase in the deformation of the structure during a fire. There is general concern that the use of calculation methods will result in an increased risk of damage to compartment walls. However, this is not the case for two reasons:

- Current methods to ensure the integrity of compartment walls during a fire do not make adequate allowance for deformation of the structure during a fire.
- The application of new design methods is limited by a displacement criteria (assumed to correspond to failure of the system) that is within the acceptable limits for deformation of structural elements in a standard fire test.

The work carried out on the full-scale steel building at Cardington that underpins the new design guidance highlighted the issue of compartmentation through the need to accommodate the anticipated large deformation of the structure. The guidance produced from the work[2,3] highlighted the issue of compartment walls and made the recommendation that, whenever possible, compartment walls should be located beneath and in line with beams. The performance of two compartment wall systems is illustrated in figures A8 to A11 below. Figures A8 and A9 show the limited deformation to be accommodated where the walls are built underneath the secondary and primary beams, while figures A10 and A11 provide dramatic illustrations of the potential impact of large deformations on the stability of non-loadbearing partitions built off the main beam gridlines. In order to maintain insulation and integrity requirements for the beam and wall construction acting together, beams over compartment walls will need to be protected and therefore the anticipated deformation will be less than that shown in figure A9.

Where beams pass through or over compartment walls (see figures A10 and A11) the design recommendations in reference 2 are that either the beams are protected or that a deflection allowance of span/30 should be accommodated by walls located within the middle half of an unprotected beam, reducing linearly to zero at the supports for walls constructed in the end quarters of the beam. According to the guidance in AD-B the junction between the compartment wall and compartment floor should maintain the fire resistance of the compartmentation. There would therefore be a need to fire protect the beam at the position where it passes over the compartment wall and to extend the protection to a point where conduction of heat along the beam could not lead to an insulation failure on the unexposed face. These requirements will have a great impact on the potential savings (in terms of reduction passive fire protection) that can be derived from the use of the new design methods. It should be borne in mind that had the requirements above in relation to the location of compartment walls within the end quarters of the beam been used for the design situation corresponding to the BRE large compartment test then the deformation allowed for in design would be somewhere in the region of 67mm for the fire design situation illustrated in figures A10 and A11. The division of the floor plate into protected areas would have resulted in the central primary beams remaining protected (unlike the test) and it is quite feasible that a design solution based on the traditional concept of deflection heads could have been used to maintain the integrity of the wall.

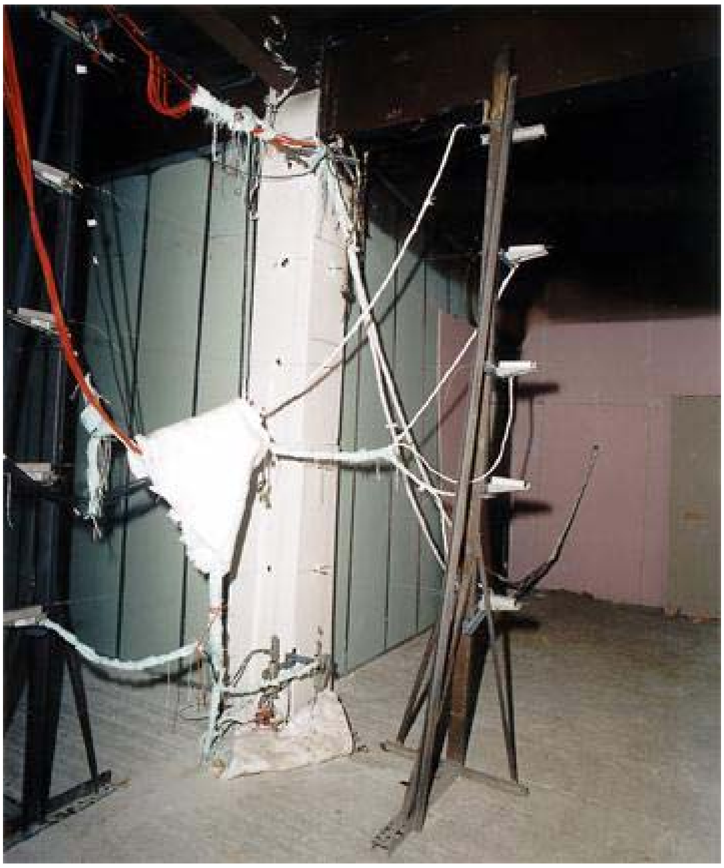

Figure A8 Compartment walls built to underside of main gridlines – BRE corner fire test

Figure A9 Maintenance of integrity of compartment walls – BRE corner fire test

Figure A10 Stability failure of compartment wall (unexposed face) – BRE large compartment test

Figure A11 Integrity failure of compartment wall – BRE large compartment test

For compartment walls made from lightweight plasterboard systems, the manufacturer can supply a range of standard details to accommodate movement from the floor above. In general, the deflection heads are there to accommodate movement at ambient temperature and have not been designed for the large levels of vertical deflection typically occurring during fires.

The limited guidance available[2,3] on maintaining the integrity of compartmentation during a fire makes mention of deformable blanket and sliding joints without providing any specific details of how to design or install such products whilst maintaining the required insulation and integrity characteristics of the wall.

The code of practice for the use of masonry[4] mentions that consideration should be given to the interaction of the whole structure of which the masonry forms a part. The connections of other elements with the walls should be sufficient to transmit all vertical and horizontal loads. For internal walls and partitions not designed for imposed loading, the code provides guidance on the ratio of length to thickness and height to thickness dependent on the degree of restraint present.

If the wall is restrained at both ends but not at the top (a common scenario for non-loadbearing walls), then $t>L/40$ and $t>H/15$with no restriction on the value of L. Where restraint is present at both the ends and the top, then the same restriction on length to thickness applies and there is a restriction on the height to thickness ratio of 30 with no restriction on the value of L. If the wall is restrained at the top but not at the edges then the height to thickness ratio should be greater than 30.

Where a wall is supported by a structural member it is suggested that a separation joint may be included at the base of the wall or bed joint reinforcement should be included in the lower part of the wall.

Where a partition is located below a structural member and is not designed to carry any vertical load from the structure above it should be separated by a gap or by a layer of resilient material to accommodate deformation. Mention is also made of the need to consider lateral restraint and fire integrity in such situations.

For masonry walls whether loadbearing or not one of the most important aspects of behaviour in fire is the impact of thermal bowing. Some guidance is available in BRE Information Paper 21/88[5]. This is the basis of the calculation of the thermal bowing component of the displacement criteria adopted by Bailey[6] who applied a calibration factor based on the results from the full-scale fire tests to apply the equation to composite floor slabs. The original equations apply to metallic elements.

Concrete, brickwork and blockwork have a lower thermal conductivity than steel and the temperature distribution is therefore highly non-linear with a large thermal gradient across the section. Cooke[5] presented data for free-standing (cantilever) walls subject to a standard fire exposure. Two thicknesses of wall were tested (225mm and 337mm) with corresponding slenderness (height/thickness) of approximately 13 and 9. The horizontal deflections at the top of the wall were 70mm and 55mm after just 30 minutes fire exposure. Given that the thickness of the walls was well within the limits set by the code of practice[4] this provides some cause for concern. Walls built to the limits of the code would deflect considerably more than the test values.

A number of design factors can be used to alleviate the effects of thermal bowing. These include:

- The choice of a material with a low coefficient of thermal expansion
- Increasing the thickness of the element
- Providing restraint at the top wherever possible (even for non-loadbearing walls) as the mid-span deflection of simply supported members is a quarter of that at the free end
- Providing edge support

Cooke's paper also pointed to the importance of the thermal exposure in determining the extent of thermal bowing highlighting the need to consider time/temperature regimes other than the standard curve.

References for Appendix A

1. Davey N and Ashton L A, National building Studies Research Paper No. 12, Investigations on Building Fires, Part V. Fire Tests on Structural Elements, HMSO, London, 1953

2. Newman G M, Robinson J T and Bailey C G, Fire Safe design: A New Approach to Multi-Storey Steel-Framed Buildings, SCI Publication P288, The Steel Construction Institute, Ascot, 2000

3. Design recommendations for composite steel framed buildings in fire, ECSC Research Project 7210PA, PB, PC, PD112, December 2002

4. BS 5628-3:2001, Code of practice for use of masonry – Part 3: Materials and components, design and workmanship, British Standards Institution, London

5. Cooke G M E, Thermal bowing in fire and how it affects building design, BRE Information Paper 21/88, Garston, December 1988

6. Bailey C G, New fire design method for steel frames with composite floor slabs, FBE Report 5, Foundation for the Built Environment, BRE Bookshop, January 2003

Appendix B Experimental data to be used for validation of numerical models

Large-Scale Tests

BRE have been involved in a number of large fire tests over the last ten years. Where the primary purpose of the tests was to investigate structural performance vertical and horizontal movement was monitored for the duration of the test. Table B1 below identifies the individual tests and provides information on the type of structure and the magnitude of maximum displacement recorded.

Test reference/ date	Test description	Type of construction	Maximum vertical displacement (mm)	Maximum horizontal displacement (mm)
1/January 95	British Steel Restrained beam test	Steel framed building – composite floor slab	230	3
2/April 95	British Steel plane frame test	Steel framed building – composite floor slab	445	20
3/Oct 95	BRE corner test	Steel framed building – composite floor slab	270	
4/Nov 95	British Steel corner test	Steel framed building – composite floor slab	425	26
5/April 96	BRE large compartment test	Steel framed building – composite floor slab	557	
6/Sept 96	British Steel Demonstration test	Steel framed building – composite floor slab	610	
7/Jan 03	European connection test	Steel framed building – composite floor slab	919	58
8/Nov 98	Slimdek fire test	Steel framed structure deep deck composite floor slab	387	
9/Sept 01	Hollow core fire test 1&2	Steel framed structure precast floor units	100/15	7/10
10/Sept 01	Concrete building fire test	Concrete framed structure	78 (residual)	67 (residual)

Table B1 Large-scale tests

The accurate measurement of displacement of a fire compartment during a fully-developed fire is a difficult task. When analysing the results from full-scale tests the following factors should be borne in mind:

- The reference position for measurement may have a significant impact on the values obtained. Wherever possible an independent reference frame has been used. However, in many cases the only suitable reference position is the floor above. If, as in the British Steel plane frame test, significant deformation takes place on floors above the fire compartment, this needs to be taken into account.
- The measurement of the horizontal movement of restrained floor slabs is complex. The value will be dependent on not only the reference frame used, which may be either part of the structure or separate, but also on the location adopted for measurement. The maximum movement will occur at unrestrained edges in two directions.
- External flaming around window openings or gaps and fissures in the fire compartment may have an impact on the magnitude of the measured deflections if the heat from the flames causes the measuring device itself to elongate. In general the cables chosen to connect to displacement devices have a very low coefficient of thermal expansion to minimise these effects.

Over the last ten years the vast majority of work related to the fire resistance of large-scale structures has been instigated and supported by the steel industry. They have viewed the costs of passive fire protection as a major obstacle to increased market share in construction. It is for this reason that the large scale test results available relate principally to steel framed construction. The single fire test undertaken on the concrete building at Cardington does not provide sufficient information on thermal profiles or structural behaviour to provide a full and comprehensive validation for numerical modelling. Consequently numerical studies for concrete structures subject to natural fires require a number of simplifying assumptions to be made to predict structural behaviour at elevated temperature.

Test parameters

The prediction of displacement is a function of the thermal curvature of the member and the mechanical strain. In order to evaluate deformation for a given scenario it is necessary to calculate the thermal profile of the heated member based on the design fire scenario adopted. For each of the tests considered above the time/temperature history and the time/displacement history is known.

In order to evaluate the structural response of a building to a fire there are 3 steps that need to be undertaken. The process is illustrated schematically in figure B1 below.

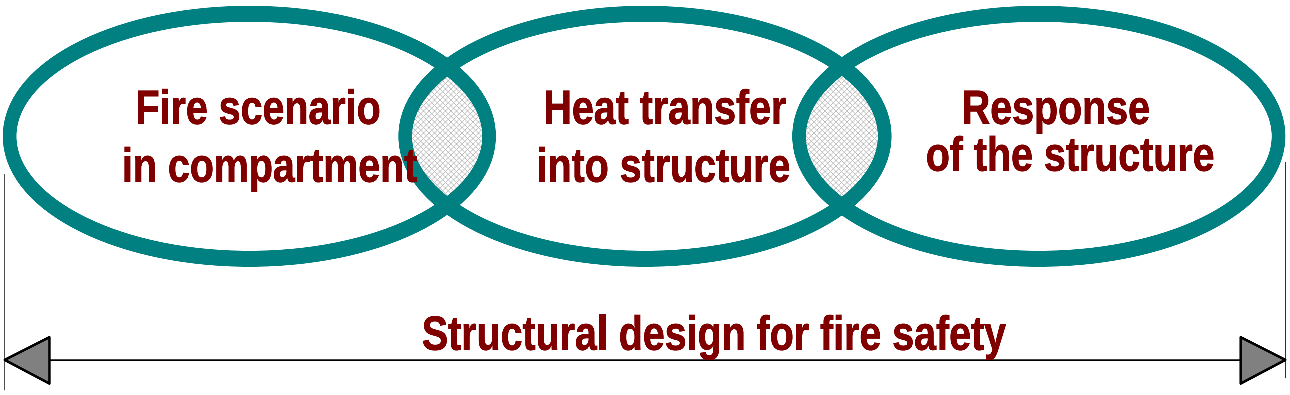

Fire load	Element geometry	Mechanical load
Room geometry	Thermal properties	Element properties
Fire characteristics	Heat transfer coefficients	Element restraint

Figure B1 Process of structural fire engineering design illustrating relevant input parameters

For the calculation of the atmosphere time/temperature response the most significant parameters are the geometry of the fire compartment (length, width and height), the fire load density (expressed in terms of energy per unit floor area), the area and location of openings allowing the free passage of oxygen into the fire compartment and providing a route out for the products of combustion and the thermal properties of the compartment boundaries.

For the calculation of the structural response the most significant factor is the imposed load assumed for design. For most of the fire tests on the steel building only a single load level was used. However, an increased load was applied in the most recent test to provide some indication of the effect of increased load on structural performance.

The most significant parameters for each test are summarised in table B2 below.

Test reference	Fire load density (MJ/m²)	Opening factor (m^{-1})	Thermal properties of compartment boundaries ($J/m^2s^{1/2}K$)	Area of fire compartment (m²)	time to maximum temperature (mins)	max gas temperature °C	max steel temperature °C	maximum vertical deflection (mm)	residual deflection (mm)	Loading – dead and imposed (kN/m²)
1	gas	n/a	n/a	24	170	913	875	232	113	4.94
2	gas	n/a	n/a	53	125	820	800	445	265	4.94
3	720	0.183	720	54	114	1000	903	269	160	4.94
4	810	0.05	1600	76	75	1020	950	325	425	4.94
5	720	0.164	720	342	70	762	691	557	481	4.94
6	828	0.07	1600	136	40	1150	1060	641	544	4.94
7	720	0.043	714	77	55	1108	1088	1200	925	5.51
8	900	0.03-0.04	720	144	74	1118	1084	387	314	
9	540	0.065	945	36	21	1079/1129	n/a	100/115	32/40	7.53/6.33
10	720	0.0795	1104	225	21	950	n/a		78	9.25

Table B2 Significant test parameters

Detailed test results

Test No. 1 British Steel Restrained Beam Test

Figure B2 below illustrates the time-temperature-displacement relationship for the restrained beam test. The test was carried out on the 7th floor of the steel framed building at Cardington (figure B3). A gas fired furnace 8m long by 3m wide was built up to the underside of the composite floor to incorporate the majority of a 305x165mm UB spanning 9m between the minor axis of 254x254 universal columns. The objective of the test was to provide validation for structural models by carrying out a controlled test on a single element with realistic boundary conditions.

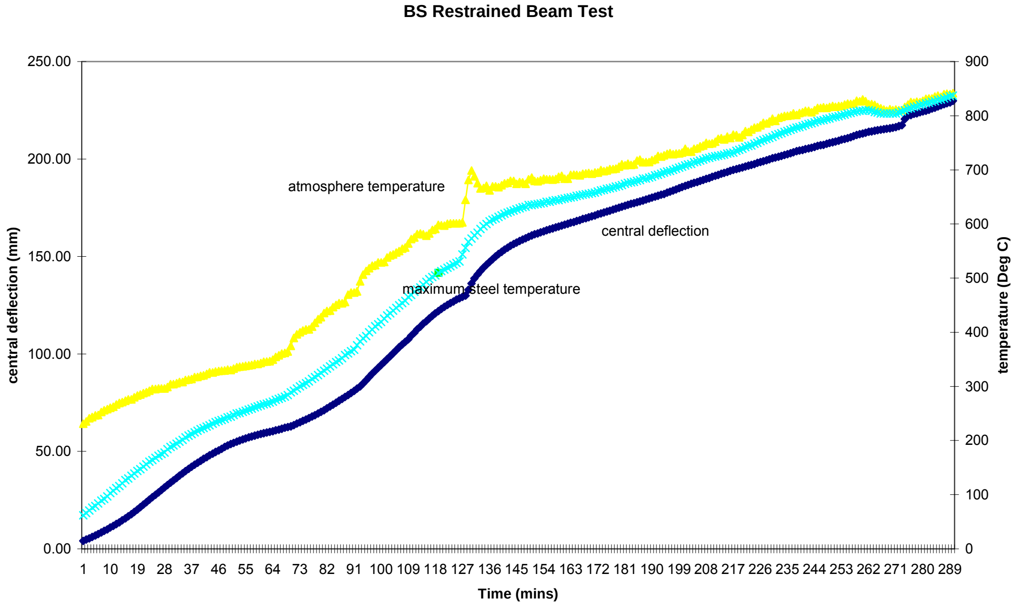

Figure B2 Relationship between time, air temperature, steel temperature and vertical deflection at mid-span – restrained beam fire test

The furnace is shown in position in figure B3 and the beam following the test is illustrated in figure B4. All the required data on the temperature profile along the beam and through the depth of the slab is available and accessible to those responsible for carrying out subsequent structural analysis.

Figure B3 British Steel Restrained Beam Test

Figure B4 Restrained beam post-test

Test Number 2 British Steel Plane Frame Test

The objective of the second test was to extend the model validation to a complete sub-frame consisting of a slice across the full width of the building incorporating two partially protected internal columns and two partially protected perimeter columns within the heated area. A gas fired furnace 21m long by 4m high was constructed to form a 2.5m wide corridor. The furnace is illustrated in figure B5 below.

Figure B5 Gas fired furnace – Plane frame test

The relationship between time, atmosphere temperature, maximum steel temperature and mid-span displacement is shown in figure B6. The rapid increase in deflection at approximately 51 minutes was a function of the shortening (localised buckling failure) of the unprotected portion of the internal columns. The post-buckled state of the area close to the connection (figure B7) also accounts for the relatively high residual deflection indicated in figure B6. Again all relevant data related to the thermal gradients along and across the structure and the associated deformations are accessible to those involved in subsequent structural analysis.

bre

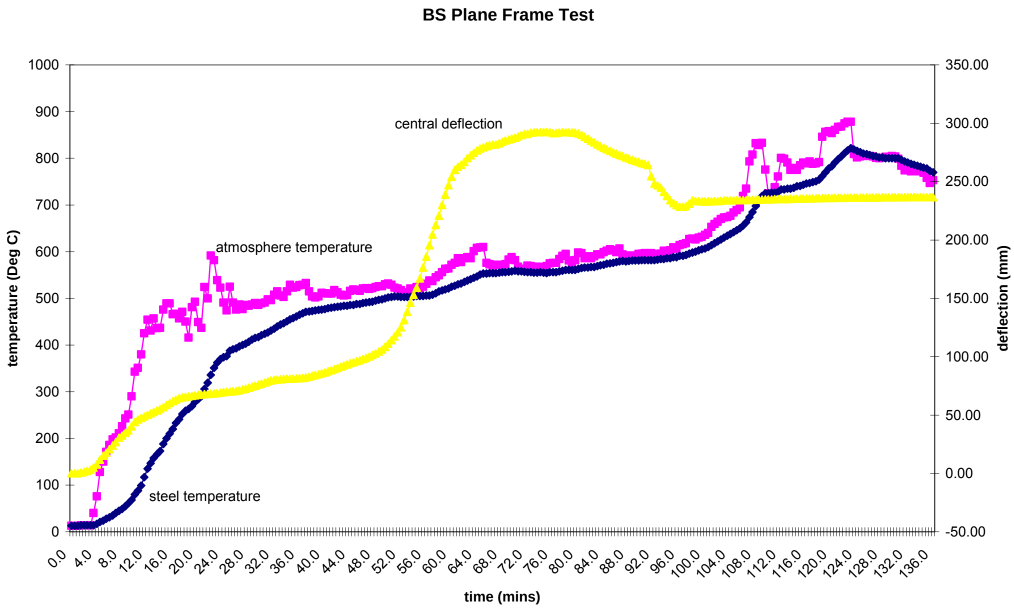

Figure B6 Relationship between time, air temperature, steel temperature and vertical deflection at mid-span – plane frame fire test

Figure B7 Plane frame – post test (note: localised buckling at top of column)

Test 3 BRE corner fire test

The BRE corner fire test took place in a 9m x 6m compartment on the second floor of the steel framed building at Cardington. The compartment was formed using British Gypsum fire resistant partitions designed to give a notional fire resistance of 2 hours to the columns and the compartment walls. The basic layout of the compartment is illustrated in figure B8 below.

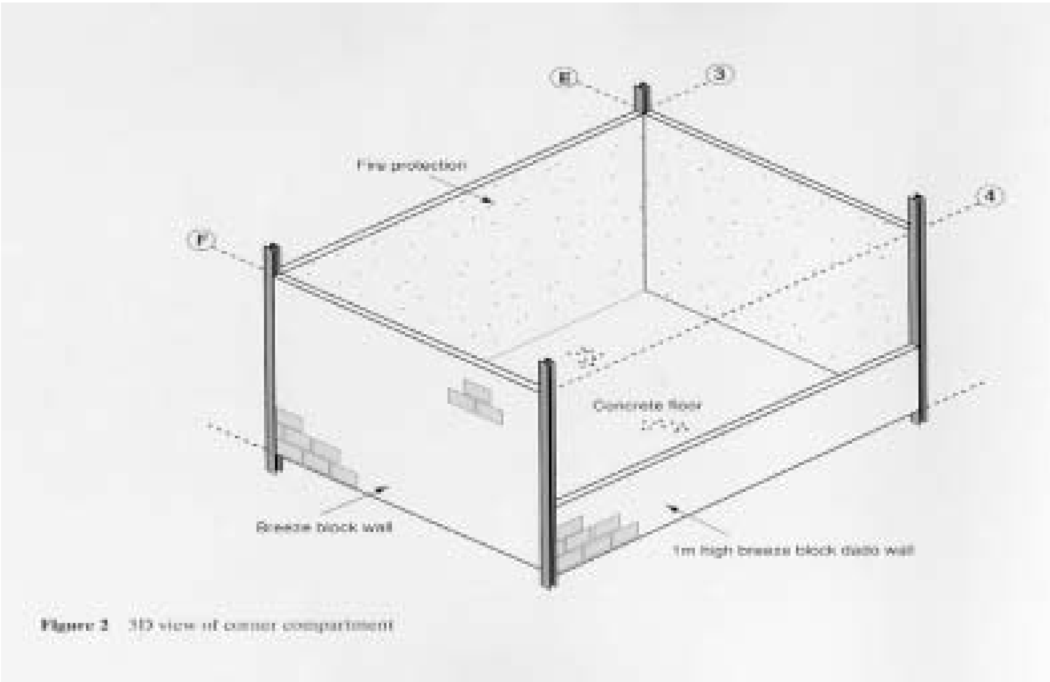

Figure B8 schematic of BRE corner fire test

The use of a practical compartment wall configuration without any additional measures to accommodate the anticipated deformation of the structure makes the results from this test of particular significance for this project.

The time/temperature/deflection relationship is illustrated in figure B9 below.

bre

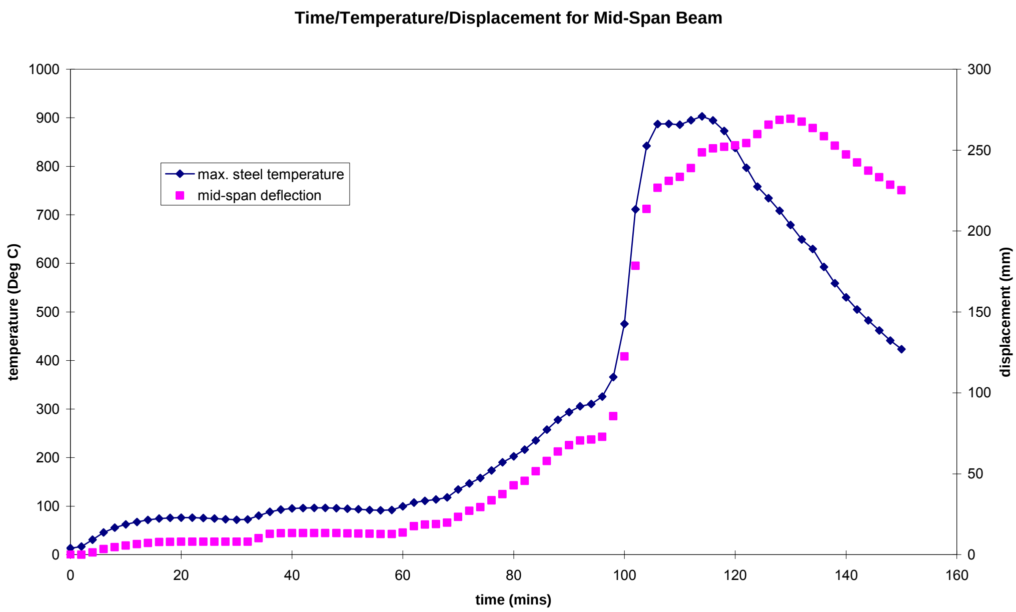

Figure B9 Time/temperature/deflection relationship – BRE corner fire test

In this case the compartment walls were built up to the underside of the primary and secondary beams to provide partial protection to the elements with a normal allowance for deflection. The UK code of practice for the fire resistant design of steel structures[1] recommends an allowance of span/100 for the anticipated vertical movement of a beam at mid-span. For the primary beam used in this test the corresponding figure is 60mm. This is generally in excess of the limits used in traditional deflection heads.

A schematic of the main steel members forming the boundaries of the fire compartment is shown in figure B10 below. The internal columns were completely protected using a 2 hour British Gypsum Glasroc system. The edge beam B5 was partially protected by the infill masonry wall on the end elevation, the internal primary and secondary beams B4 and B3 were partially protected by the fire resistant compartment wall. Beam B3 was fully protected for some of its length as it was located behind the shaft wall system forming the protection to the stairway. Therefore the only members left unprotected were the internal beam B2 and the edge beam B1. The edge beam received support during the fire from the non-structural wind posts on the floor above. As mentioned in the previous report the compartmentation performed very well with respect to the deformation of the structure. The general construction of the compartment is illustrated in figure B11 while figures B12 and B13 show the condition of the plasterboard from both the outside and inside of the compartment after the fire.

bre

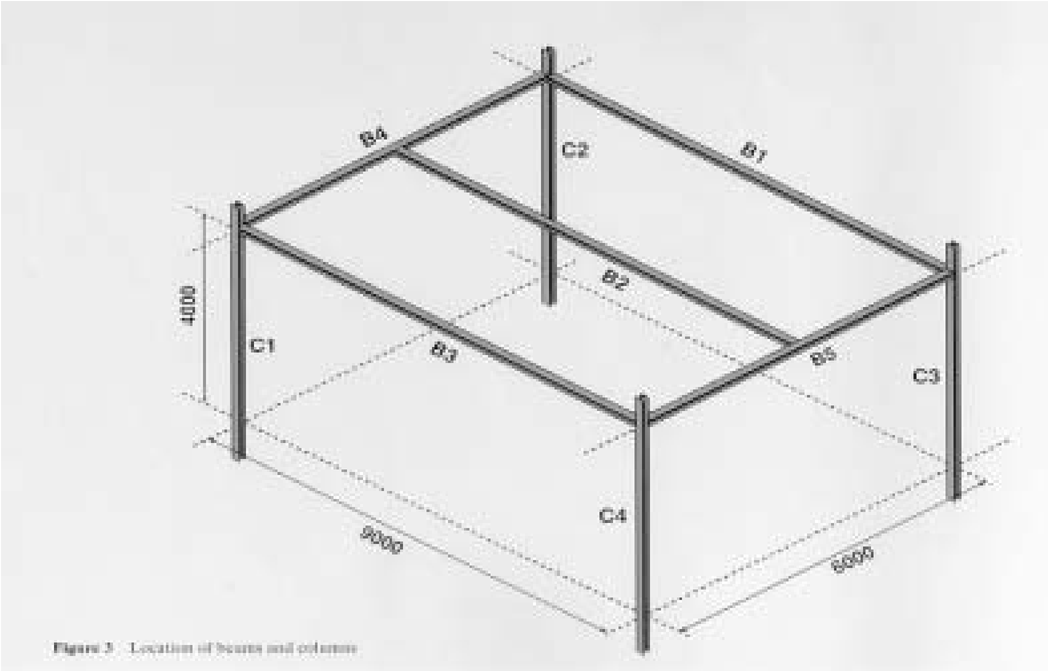

Figure B10 Schematic of structural steelwork – BRE corner fire test

Figure B11 BRE corner compartment – General arrangement

Figure B12 BRE corner compartment – interior view post-test

Figure B13 BRE corner fire test – exterior view post-test

During the test the lateral and axial movement of the columns C1 and C2 was measured. However, further interpretation of the data is required before the data can be used. Also measurements of the movement of the blockwork infill panel between C3 and C4 were taken using a laser system. Again more analysis is required before the test results can be presented and the data is not particularly reliable due to difficulties in seeing the laser targets through the smoke produced during the test.

Test 4 British Steel Corner Compartment

A compartment with a floor area of approximately 80m² was built on the first floor of the Cardington steel building. Unlike the previous test all existing restraint from the gable wall and the wind posts connected to the edge beams was removed. The compartment walls were built from loadbearing blocks with a suitable allowance for deformation of the floor slab (400mm). All the columns were protected to their full height including the area around the beam to column connections. The edge beams were also protected with the remaining primary and secondary beams unprotected.

The time-temperature-displacement relationship is shown in figure B14 below. The condition of the steelwork and the floor slab following the test is illustrated in figure B15. The detailed test results are available for those involved in subsequent modelling.

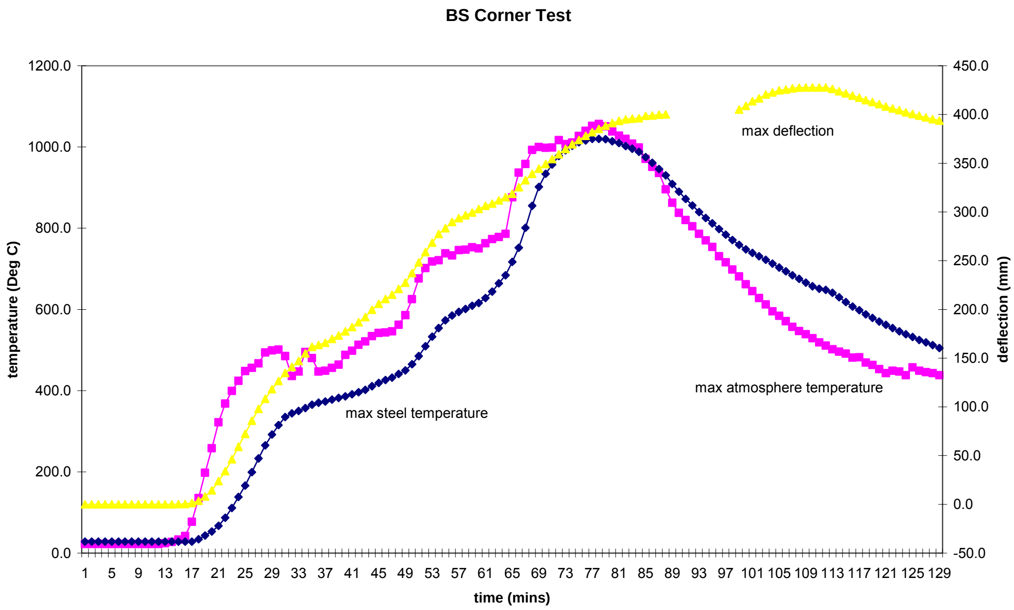

Figure B14 Time-temperature-deflection relationship – British Steel corner fire test

Figure B15 British Steel corner fire test – damage to steelwork and displacement of floor slab

<u>Test 5 BRE Large compartment test</u>

This test was carried out on the second floor and covered an area of approximately 340m² extending across the full width of the building. The compartment was constructed by erecting a fire resistant stud and plasterboard wall across the full width of the building and by constructing additional protection over the shaft wall system protecting the lift shaft. Double glazing was installed on both sides of the building with the middle third of the glazing left open. The internal and external columns were protected up to and including the connections with all edge and internal beams left unprotected. The time-temperature-deflection relationship is illustrated in figure B16.

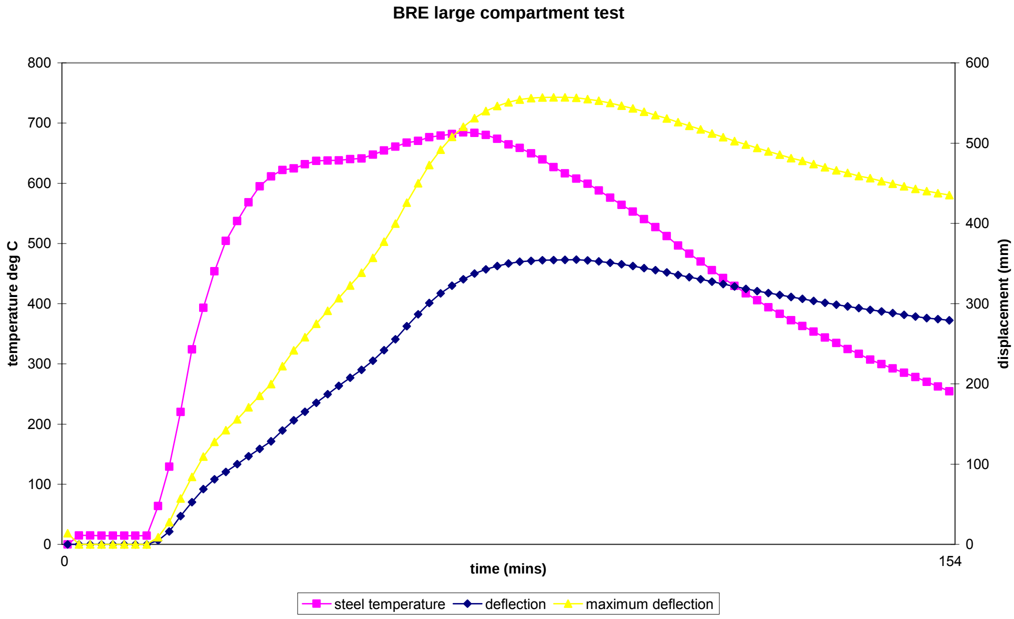

Figure B16 Time-temperature-deflection relationship – BRE large compartment fire test

For this test the maximum atmosphere temperature was relatively low (746°C) although the overall duration of the fire was greater than previous tests (approximately 70 minutes to maximum temperature). There are two main reasons for this. Firstly the cross-ventilation achieved from openings on either side of the compartment may have lowered the temperature of the compartment. Secondly although the fire load density was the same as that used in the BRE corner test (40kg/m²) the actual distribution of the fire load was somewhat different. In the corner test the crib porosity adopted was a 1:1 spacing for maximum combustion efficiency (see figure B17). However, due to concerns over the effect of heat transfer from the fire compartment to the structure of the Cardington hangar the crib design was altered for the large compartment test to try and reduce the burning rate. The modified design used 340 individual sticks in each crib compared to 200 in the corner test. As the fire load density was the same this resulted in a larger space between the cribs (see figure B18) and the cribs tended to burn as individual fires.

Figure B17 Crib layout (1:1 spacing) – BRE corner fire test

Figure B18 crib layout BRE large compartment test

The effect of the large deflections on the performance of the compartment wall has been highlighted in the previous report produced under this contract. The large deflections caused a stability failure of the compartment wall as illustrated in figure B19.

Figure B19 Deformation of floor slab causing instability of compartment wall – BRE large compartment fire test

In addition to the direct effect on the compartment wall the large deflections led to significant cracking of the floor slab (figure B20). This did not lead to an integrity failure as the profiled decking remained intact. However, at the column sections large fissures in the floor slab were noted which would allow the passage of flames and hot gases (figure B21). The importance of ensuring the mesh reinforcement is properly overlapped at the intersection of the column and the floor slab has been highlighted in design guidance arising from the full-scale tests[2].

Figure B20 Cracking of floor slab – BRE large compartment test

Figure B21 Integrity crack around column – BRE large compartment fire test

Test 6 British Steel Demonstration Test

This test consisted of a compartment up to 18m wide and 10m deep on the first floor of the steel framed building at Cardington. The blockwork wall forming the compartment boundaries was similar in construction to that used for the British Steel corner test with a similar allowance for vertical deflection. However, in this test no attempt was made to decouple the existing wind posts and connections between the edge beams and external blockwork wall.

The compartment was fitted out with office furniture, computers and filing systems typical of a modern office. The total fire load available for combustion was equivalent to 45.6kg of wood/m²of floor area. The columns were protected up to their full height including the main beam to column connections. The height of the external dado wall was increased to restrict the available oxygen for combustion.

The relationship between time, temperature and displacement is illustrated in figure B22.

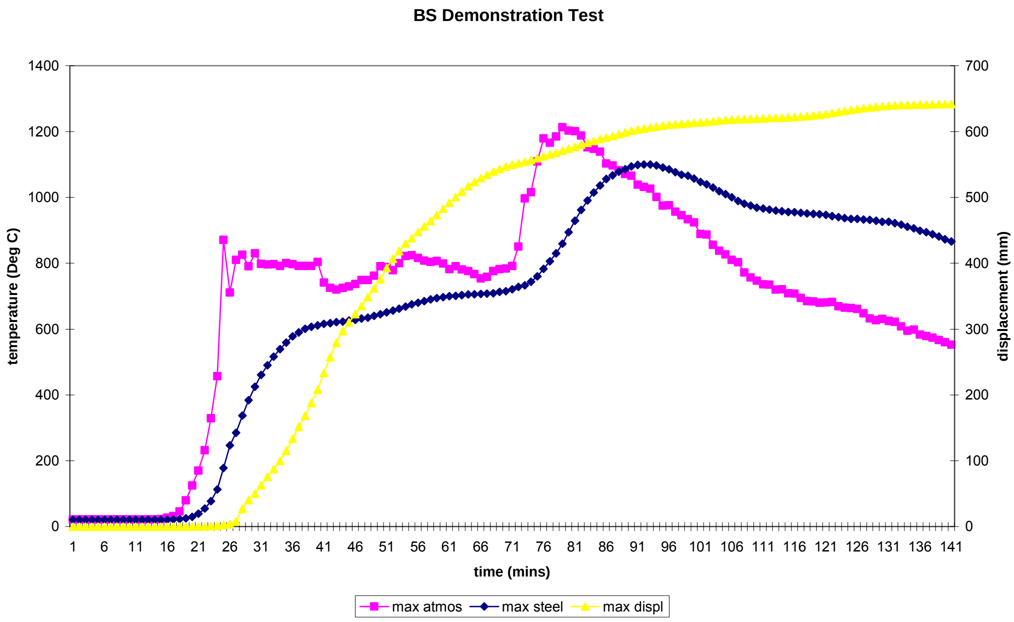

Figure B22 time-temperature-displacement relationship – British Steel Demonstration test

The nature of the compartment construction for the two British Steel natural fire tests means that there is no direct information on the performance of the walls although obviously the information on displacement of the floor slab is extremely significant. As with the large compartment fire test cracking took place around the internal columns leading to a possible integrity failure of the horizontal compartmentation. Subsequent analysis has suggested that the cracks may have opened up on cooling possibly at the time of localised fracture of the steel beam to column connections. The localised cracking around the interior column is illustrated in figure B23.

Figure B23 Cracking around column E3 – British Steel Demonstration Test

Test 7 European Connection Test

The general arrangement of the most recent test to be carried out on the Cardington steel framed building is shown in figure B24. The compartment floor area was 11 metres by 7 metres and the height of the compartment was approximately 4m. Ventilation was provided from the window opening on the South face of the building as shown in figure B24. The original window height of 2.77m was reduced to 1.27m for the test to restrict the amount of oxygen available for combustion and therefore increase the duration of the fire. The compartment walls were built from plasterboard extending from the floor to a position approximately 500mm from the underside of the ceiling. The gap between the top of the wall and the underside of the ceiling was sealed with compressible fibre to allow for the anticipated large displacement of the floor above. Allowance was made for the deformation of the beams supporting the floor. The opening on the floor above was sealed off using inconel reinforced ceramic blanket to prevent the flames from entering the building on the fourth floor and damaging the instrumentation. The internal and external columns were protected using a sprayed protection system.

bre

Figure B24 European connection fire test

The test demonstrated that a compartment wall can be designed and built to accommodate very large deflections without collapse. The time-temperature-deflection relationship is illustrated in figure B25 below.

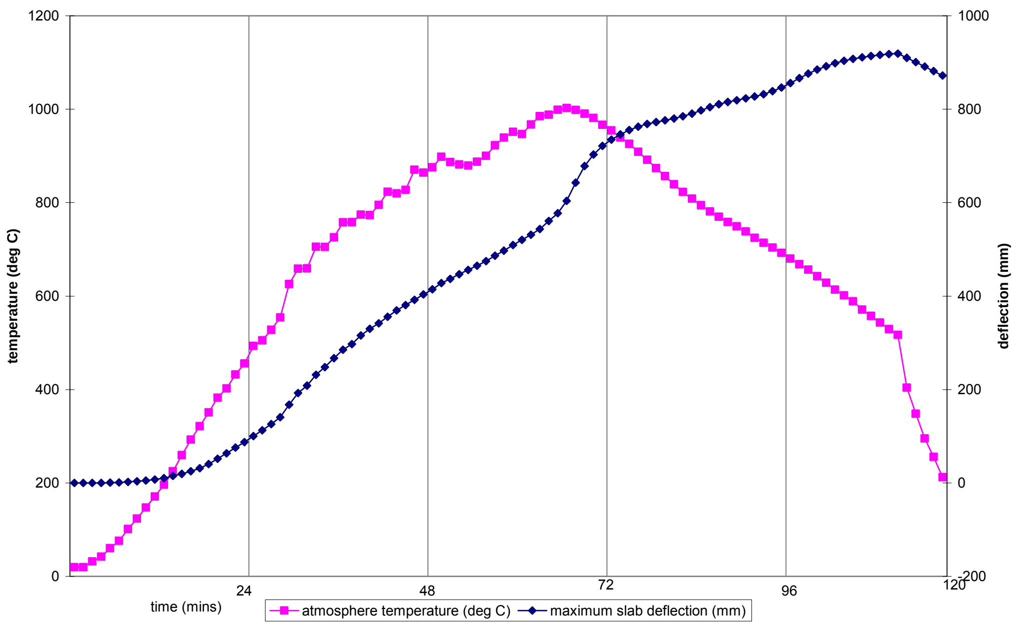

Figure B25 time-temperature-deflection relationship – European connection fire test

bre

For this test the measured values of displacement in the critical areas in the centre of the floor panel are not the maximum values. During the test a number of the displacement transducers reached the end of their travel (approximately 1 m) and were left hanging from the beams above as the floor moved beyond their limit of measurement.

As both the value of the imposed load and the extent of the unprotected steel was greater than in previous tests the deflections were much greater than recorded in any of the previous tests. The BRE design method[2] includes deflection limits based on uncertainties as to the mode of failure of composite floor slabs in fire. The results from this test suggest that the BRE design method is extremely conservative and that there is scope to extend the use of the method. This would have implications for the design and positioning of compartment walls.

Again the issue of cracking around the column and the possibility of a localised integrity failure requires further investigation to identify whether this occurs during heating or cooling. Figure B26 illustrates extensive cracking around the internal column.

Figure B26 Cracking around internal column – European connection fire test

Test 8 Slimdek Fire Test

This test took place in a 12mx12m compartment 4m high. Adjustable screens were used to provide some control over the burning rates and the fire load consisted of 50kg of wood per m². The test considered the structural response of a deep deck composite floor system. The time-temperature-displacement response is shown in figures B27 and B28 below. Analysis of the data was complicated by problems with some of the thermocouples during the test.

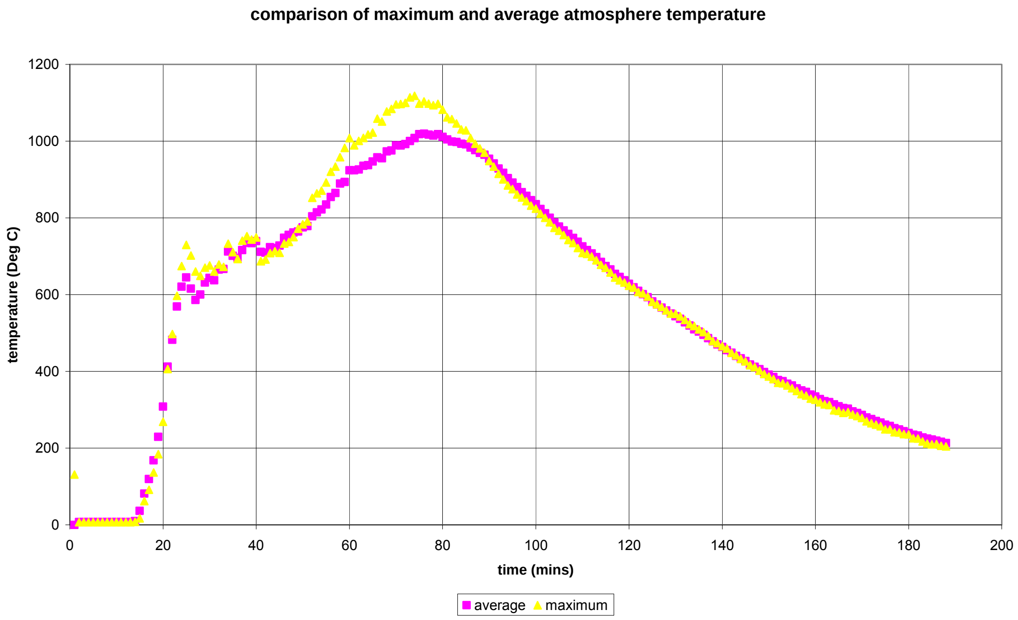

Figure B27 maximum and average compartment temperatures – Slimdek Fire Test

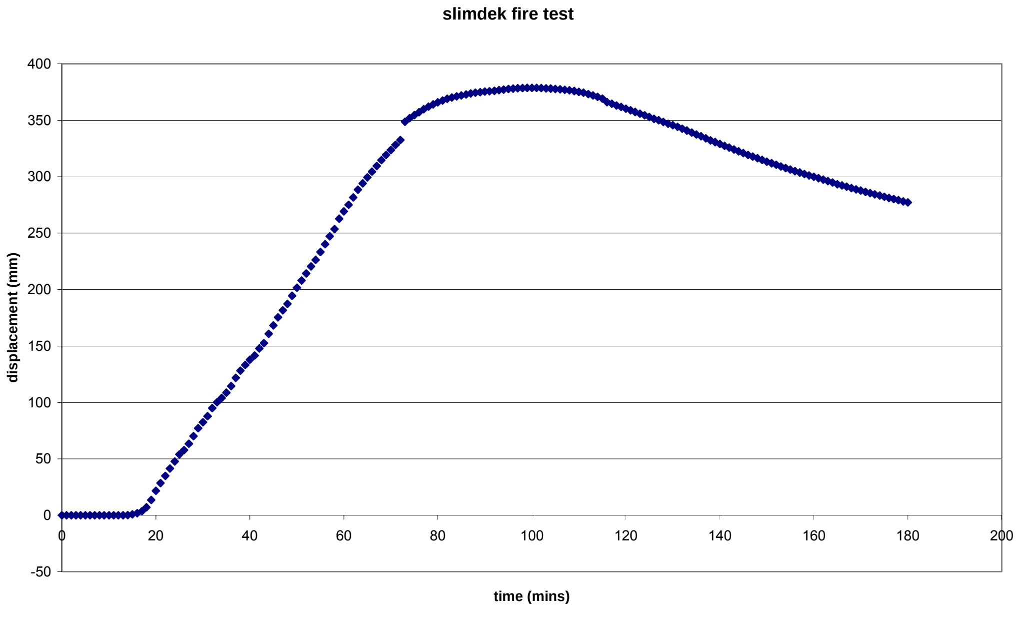

Figure B28 Maximum deflection – Slimdek Fire Test

<u>Test 9(a) Hollow Core Fire Test 1</u>

This project was carried out in a 6m x 6m compartment modified from that used to carry out the test above. The object of the test programme was to investigate the structural performance of hollow core slabs subject to natural fires. The fire load was 30kg of wood per m². The floor units were loaded with sandbags from above providing an imposed loading of 3.66kn/m². The compartment is shown in figure B29. The time-temperature-deflection history is shown in figures B30, B31 and B32 below.

Figure B29 Fire compartment – hollow core fire tests

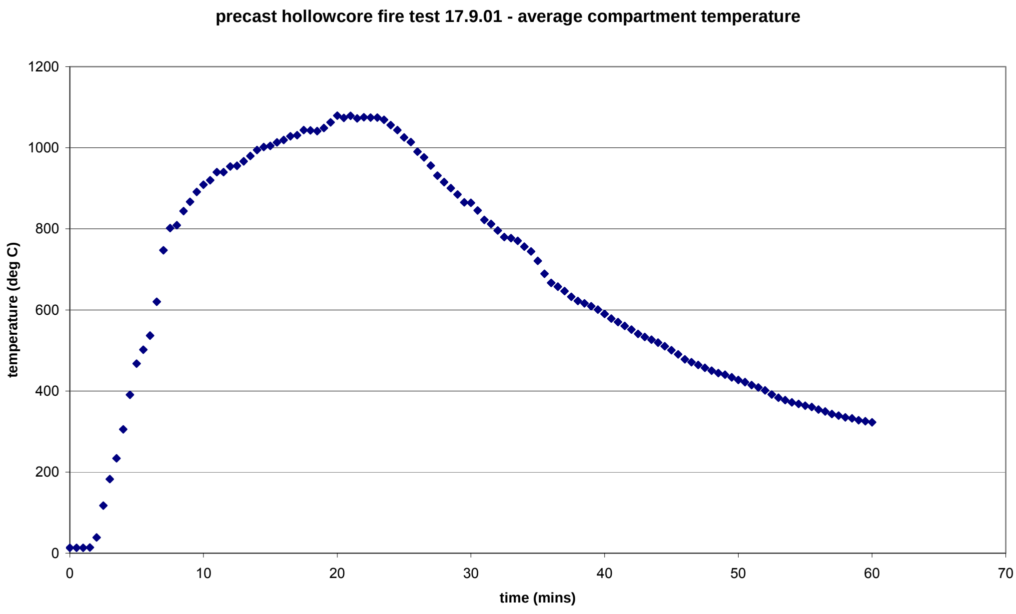

Figure B30 Average compartment temperature – hollow core fire test 1

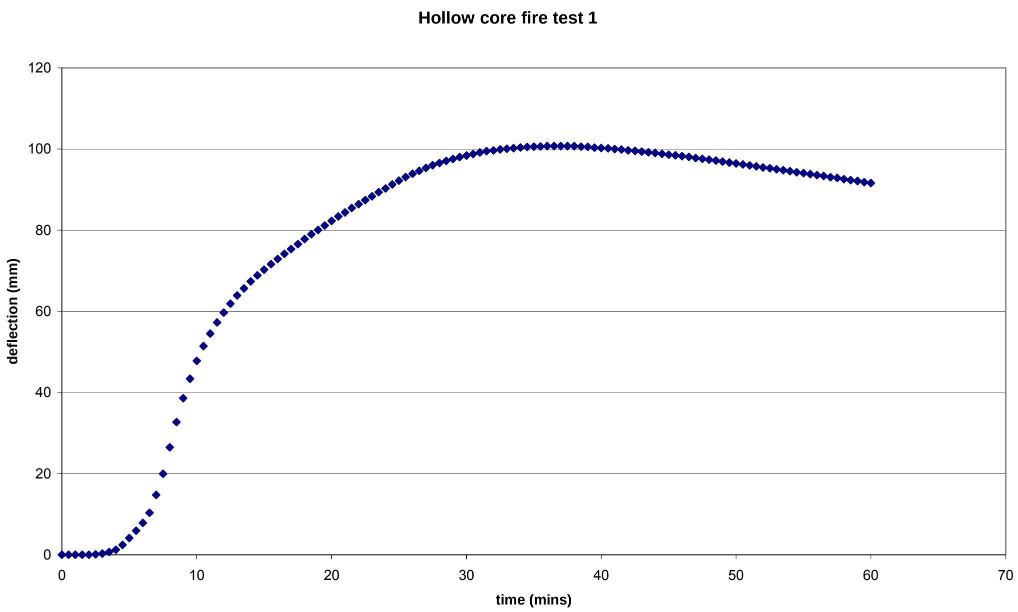

Figure B31 Maximum vertical deflection – hollow core fire test 1

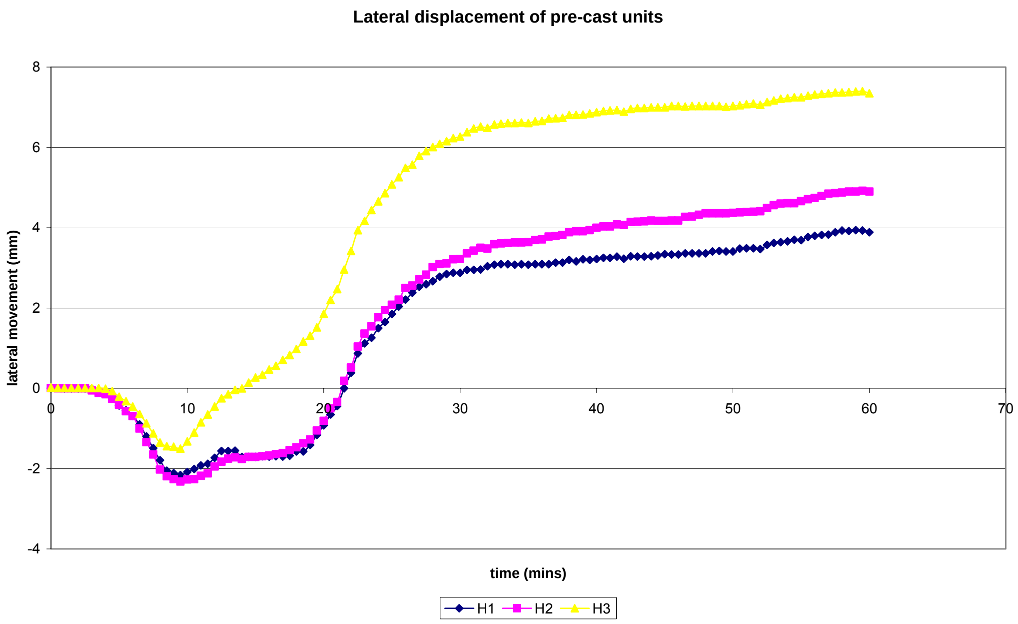

Figure B32 Lateral movement of floor units – hollow core fire test 1

<u>Test 9(b) Hollow Core Fire Test 2</u>

For the second test the fire design scenario for the previous test was replicated with the same level of imposed floor load. The only difference was in the construction details of the precast unit and the absence of a structural screed laid over the precast units. Again the temperature and deflection history are illustrated in figures B33, B34 and B35.

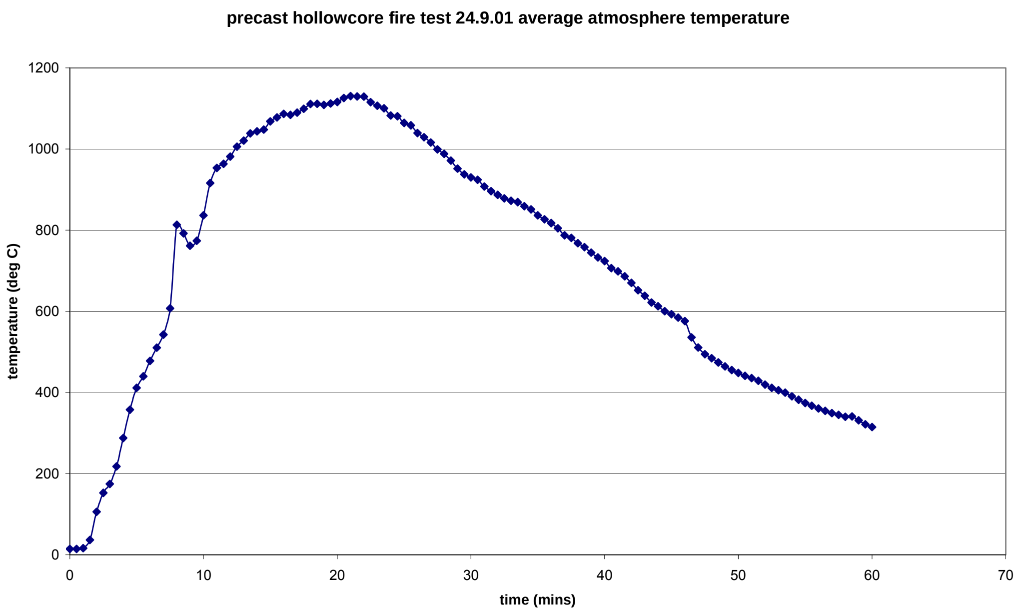

Figure B33 Average compartment temperature – hollow core fire test 2

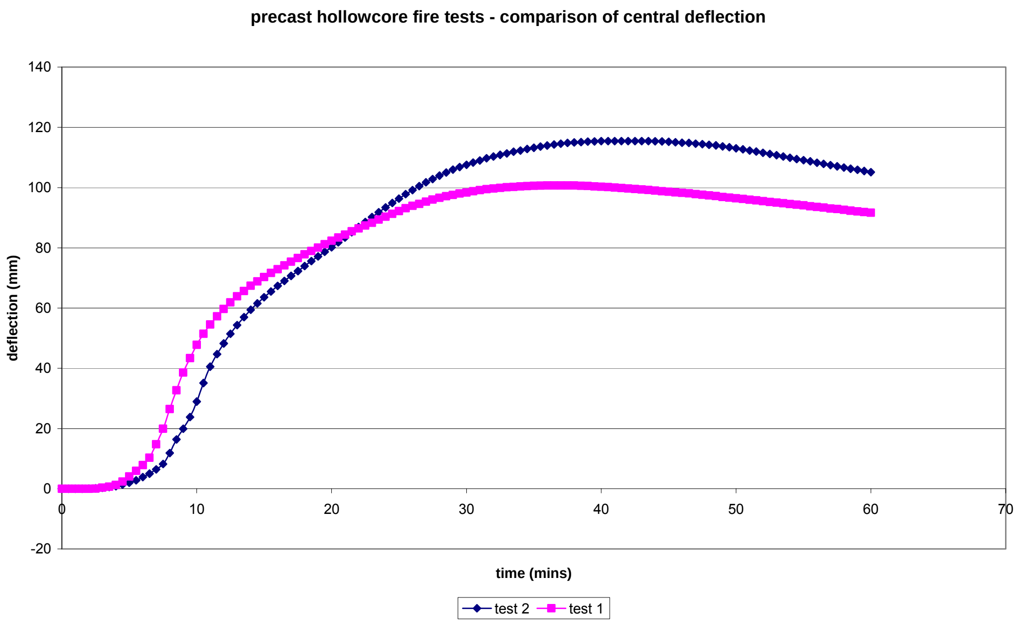

Figure B34 Central deflection hollow core fire tests – comparison between tests 1 and 2

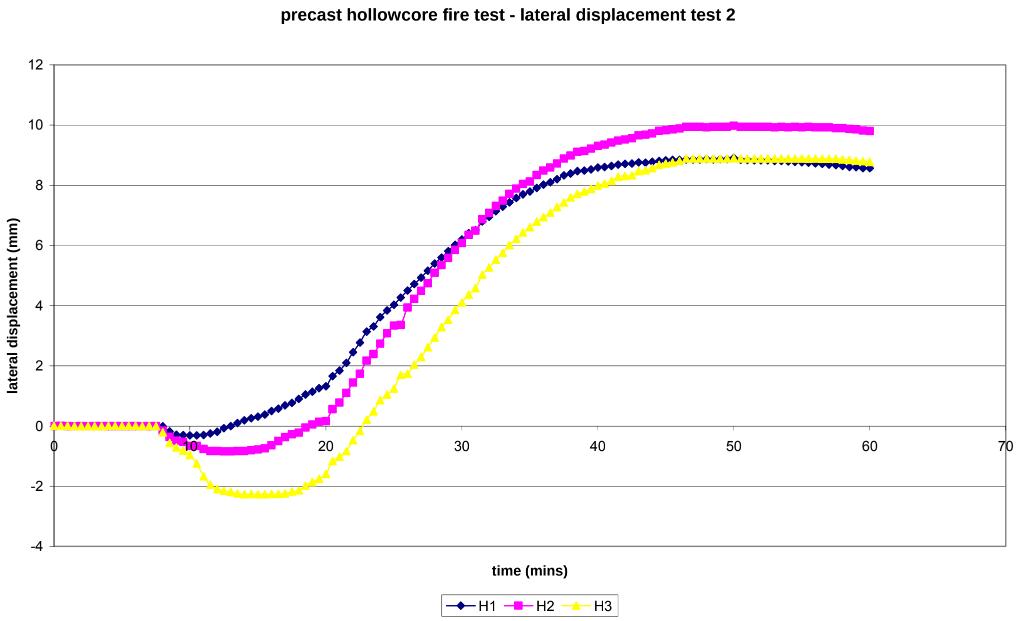

Figure B35 Lateral movement of floor slab – hollow core fire test 2

Although the supporting frame of beams and columns was steel the purpose of the tests was to investigate the performance of the hollow core slabs and, in particular, the tendency of the units to spall in an explosive manner. More information on the background to the tests and the detailed test results may be found in reference 3.

Test 10 Concrete Building Fire Test

The fire test on the concrete building at Cardington took place in a ground floor compartment with an area of 15m by 15m and a height of 4.25m. The fire load was 40kg of wood per m² of floor area. Figure B36 shows the front elevation of the compartment during the test. Interpretation of the results is complicated by the loss of instrumentation caused by fire damage to the data acquisition cable during the test. However, residual deflections were recorded the following day and these are illustrated in figure B37.


Figure B36 Concrete building fire test

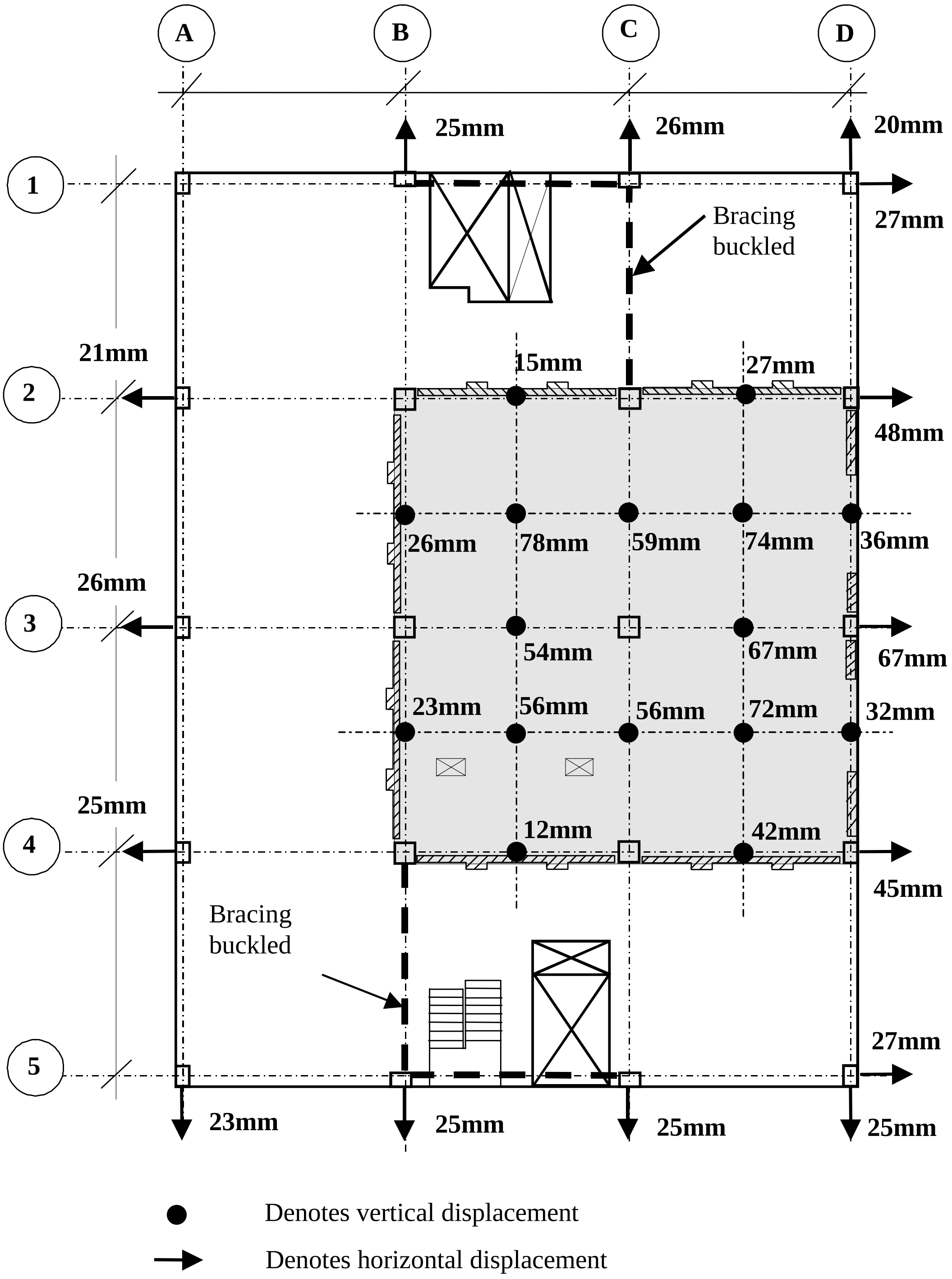

Figure B37 Residual horizontal and vertical displacements – concrete building fire test

References for Appendix B

1. BS5950-8:1990, Structural use of steelwork in building – Part 8: Code of practice for fire resistant design, British Standards Institution, London
2. Newman G M, Robinson J T and Bailey C G, Fire Safe design: A New Approach to Multi-Storey Steel-Framed Buildings, SCI Publication P288, The Steel Construction Institute, Ascot, 2000
3. Lennon T, Precast Hollow core slabs in fire, BRE Information Paper 5/03, BRE, Garston

Appendix C Design fire scenarios, frame layout and validation of numerical methods

Design fire scenarios

The analysis to be carried out for this project will consider standard fire resistance periods and a limited number of natural fire scenarios. Traditionally, the fire protection requirements for structural elements and assemblies are determined in accordance with Standard Fire Tests. In such tests, the furnace temperature is controlled in accordance with the Standard Fire Curve. Whilst these tests provide valuable information, the Standard Fire Curve does not necessarily represent reality. Therefore, in the context of this project, it is important to consider the deflections that would occur under realistic fire scenarios as well as under the Standard Fire Curve exposure.

It is impossible and impracticable to consider all realistic fire scenarios. Therefore, three parametric fires will be adopted for all analyses; low severity, medium severity and high severity. The severity of real fires is a function of the fuel load, ventilation conditions and room geometry. The fire load densities for a given occupancy are generally fixed values relating to the results from fire load surveys of buildings. Therefore for a given occupancy the fire load will be assumed to be a constant value equal to the 80% fractile value taken from BS7974 PD1[1]. As the compartment geometry is fixed according to the frame layout (see below) it is intended that the design fire scenarios adopted will be related to the ratio of the ventilation area to the compartment floor area. In this way three values will be adopted ranging from a ventilation condition designed to provide a severe fire of short duration to a situation resulting in a fire of longer duration and lower peak compartment gas temperatures (for the same value of fire load and compartment floor area). The ratios of ventilation area to floor area to be considered are as follows:

- $A_v < 2.5\% A_f$
- A_v/A_f 2.5% to 5%
- $A_v > 5\% A_f$

Frame layout

In order to carry out the necessary comparisons between different forms of construction and the effects of locating compartment walls in different locations a basic floor plan has been adopted.

Several sub-frames will be modelled to determine the realistic deflection heads to which compartment walls may be subjected in real fires. The modelling process is as below:

1. Determine appropriate design fires.
2. Conduct thermal analyses to determine the temperature distribution of the structure when exposed to the design fires defined in step 1.
3. Define appropriate sub-frames for analysis.
4. Determine the structural response of the sub-frames under the temperature distributions as determined in step 2.

Appropriate Sub-frames

The project brief requires that following variables and conditions be considered:

steel and concrete frames,
different flooring systems,
location of compartmentation,
level of fire protection, and
required fire resistance.

The following sections discuss these in more detail.

Frames and Flooring Systems

Three frames/floor systems will be analysed:

Composite Steel and Metal Deck (see figure C1)
SlimflorTM using Precast Planks (figure C2)
Reinforced Concrete – Solid Slab (figure C3)

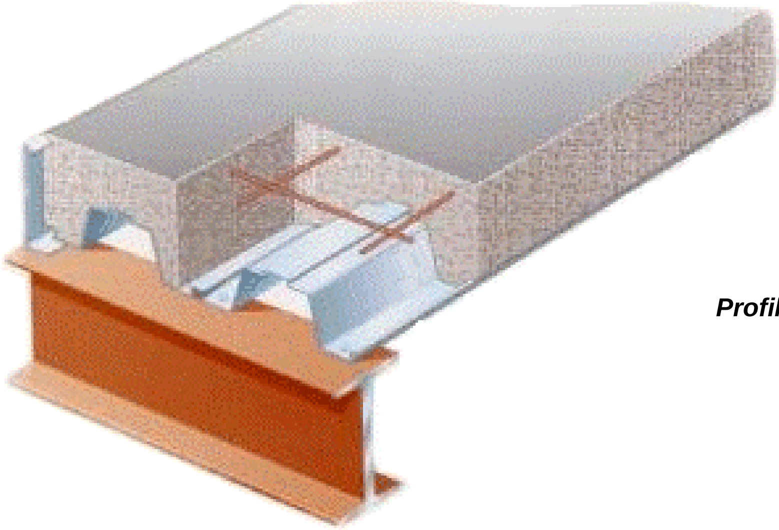

Figure C1 Composite steel and metal decking details

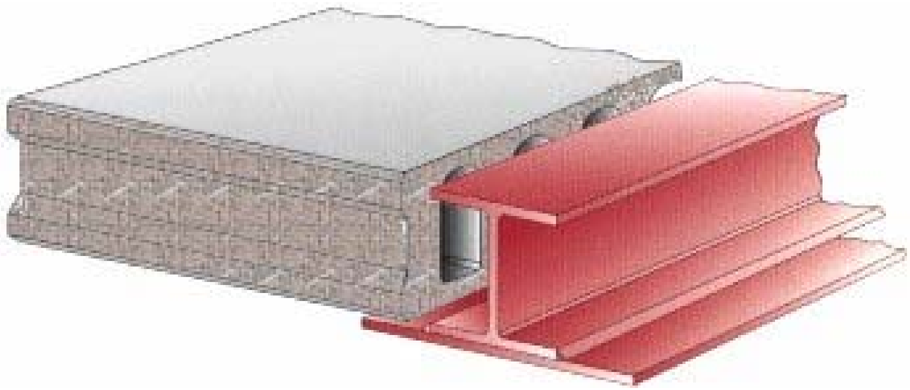

Figure C2 SlimFlor system with a wide flange plate welded to the underside of the beam

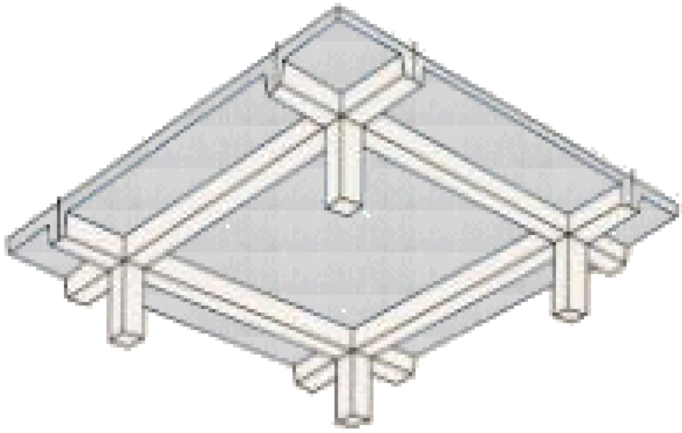

Figure C3 Two-way spanning in-situ suspended slab

Within each of these systems, four grid arrangements will be analysed.

9.0m x 7.5m
9.0m x 6.0m
9.0m x 9.0m
12.0m x 6.0m

For the composite steel and metal deck systems the following assumptions are made regarding the form of construction and the loading.

- MD60 metal deck slab thickness = 140mm
- Concrete grade C30 (30 N/mm²)
- Steel grade S275 (σ_y = 275N/mm²)
- Applied load for finishes and services = 1.0 kN/m²

The initial boundary condition assumes simple supports along the four edges. The layout of the frame together with designed values for the primary and secondary beam sizes dependent on the value of the imposed loading are illustrated in figures C4 and C5.

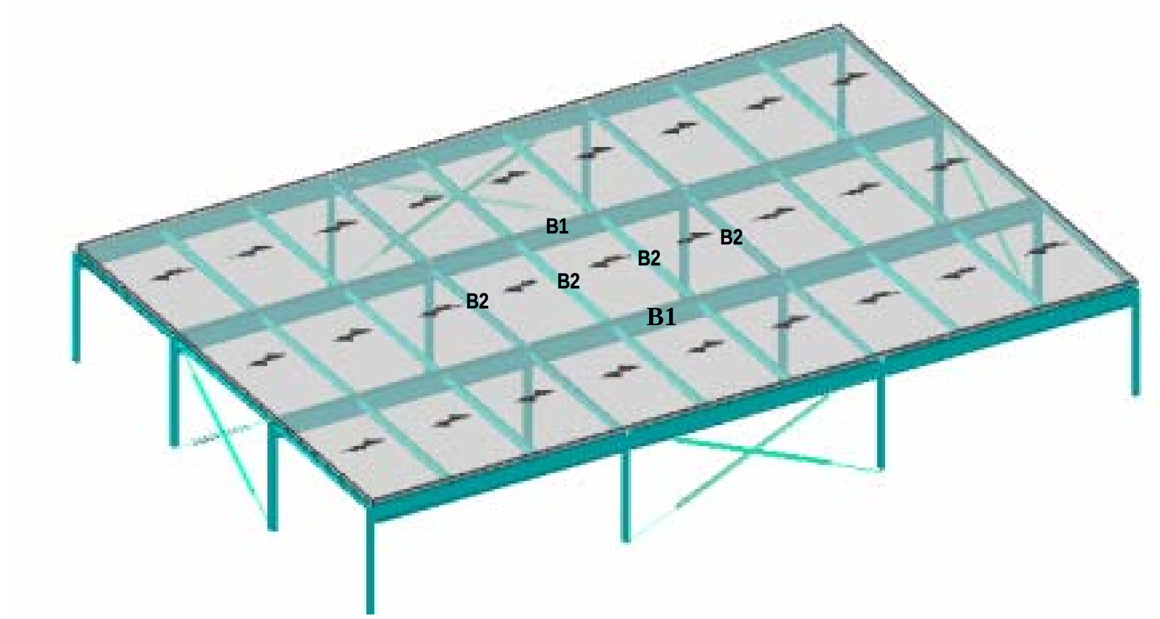

Figure C4 Frame layout for composite slab

9m x 6m (MD60, 140mm with A142 mesh reinforcement)			
Dead load (kN/m²)	Live load (kN/m²)	B1	B2
4.36	2.5+1	610x305x238UB	305x102x28UB
4.36	4+1	610x305x238UB	305x102x28UB
4.36	7.5+1	610x305x238UB	356x127x33UB
9m x 7.5m (MD60, 140mm with A142 mesh)			
4.36	2.5+1	610x305x238UB	406x140x39UB
4.36	4+1	610x305x238UB	406x140x39UB
4.36	7.5+1	610x305x238UB	406x178x54UB
9m x 9m (MD60, 140mm with A142 mesh)			
4.36	2.5+1	533x210x92UB	406x140x46UB
4.36	4+1	610x229x101UB	406x178x54UB
4.36	7.5+1	762x267x134UB	457x191x67UB

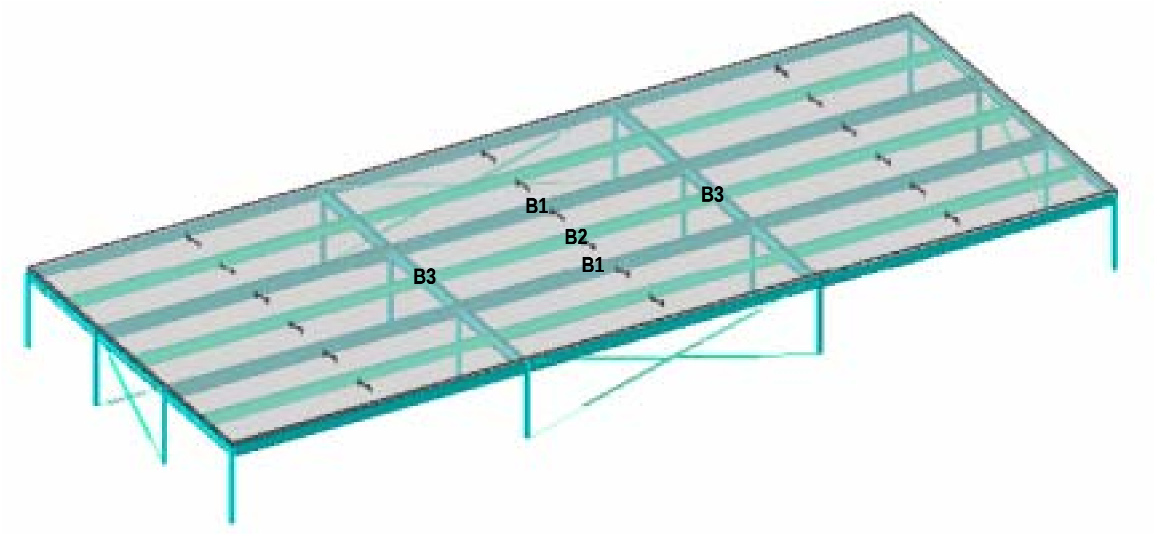

Figure C5 Frame layout for composite slab

15m x 6m (MD60, 140mm with A142 mesh)				
Dead load (kN/m²)	Live load (kN/m²)	B1	B2	B3
4.36	2.5+1	686x254x125UB	610x229x113UB	686x254x125UB
4.36	4+1	686x254x125UB	610x229x125UB	686x254x125UB
4.36	7.5+1	762x267x134UB	762x267x134UB	686x254x170UB

Location of Compartmentation

Six compartmentation locations will be considered for each grid. These are defined by placing the compartmentation under primary and secondary beams. Examples of describing the location of compartment walls are shown below for a typical floor plate.

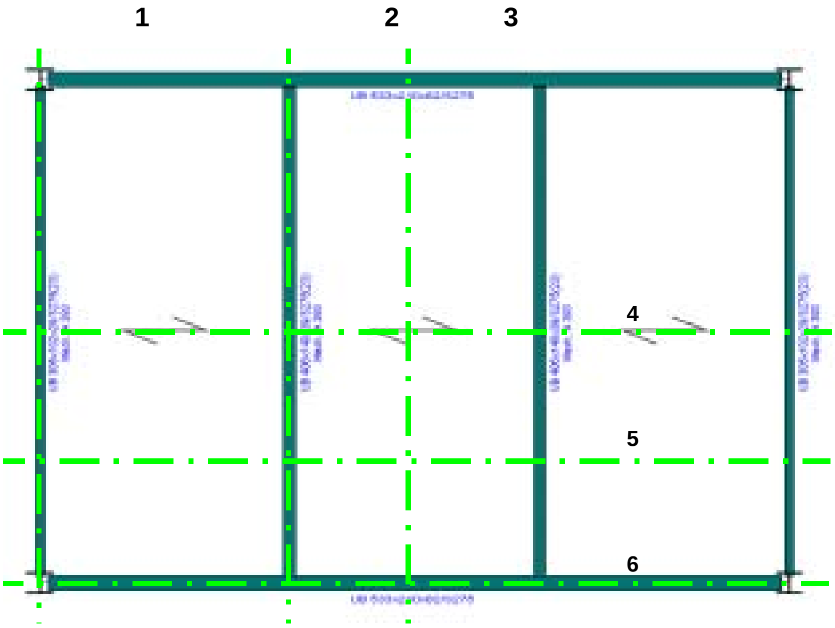

Figure C6 Location of compartment walls

Level of Protection

For the steel and composite frames two protection regimes will be considered corresponding to realistic design scenarios. In the first case all beams will be considered to be protected (to the appropriate fire resistance period) and in the second case intermediate beams will be left unprotected.

Required Fire Resistance

Fire resistance periods of 30, 60, 90 and 120 minutes will be considered.

Validation of numerical models

Structural model - VULCAN

The computer program VULCAN has been developed at the University of Sheffield for the structural analysis of steel and composite framed buildings in fire. *Vulcan* is a three-dimensional frame analysis program, which has been developed for the purpose of modelling the behaviour of skeletal frames, together with floor slabs, under fire conditions. Temperature distributions across members can be non-uniform, causing differential thermal expansion and a spread of elastic and inelastic properties across the section, and a range of cross-sections can be defined allowing different shapes and materials to be represented.

The structure is modelled as an assembly of finite beam-column, spring, shear connector and slab elements. It is assumed that the nodes of these different types of element are defined in a common fixed reference plane, which is assumed to coincide with the mid-surface of the concrete slab element. The beam-columns are represented by 2-noded line elements. The cross-section of each element is divided into a number of segments to allow variations in the temperature, stress and strain through the cross-section to be represented. Both geometric and material non-linearities are included. To represent the characteristics of steel-to-steel connections in a frame, a 2-noded spring element of zero length, with the same nodal degrees of freedom as a beam-column element, is used. The interaction of steel beams and concrete slabs within a composite floor is represented using a linking two-noded shear-connector element of zero length, with three translational and two rotational degrees of freedom at each node.

The analysis includes geometric non-linearity in the slabs, using a quadrilateral 9-noded higher-order isoparametric element. This includes a modified layered orthotropic formulation based on Mindlin/Reissner theory, and using an effective stiffness model in each slab layer to model the ribbed nature of typical composite slabs. The temperature and temperature dependent material properties can be specified independently. A maximum-strain failure criterion has been adopted for the concrete, and a smeared model has been used in calculating element properties after cracking or crushing. After the initiation of cracking in a single direction, concrete is treated as an orthotropic material with principal axes parallel and perpendicular to the cracking direction. Upon further loading of singly cracked concrete, if the tensile strain in the direction parallel to the first set of smeared cracks is greater than the maximum tensile strain then a second set of cracks forms. After compressive crushing, concrete is assumed to lose all stiffness. The uniaxial properties of concrete and reinforcing steel at elevated temperatures, specified in EC4, have been adopted in this model.

Vulcan has been extensively validated against both ambient temperature and elevated temperature tests, which includes, for example, comparison of the predicted results from Vulcan with two standard fire resistance tests on simply supported composite beams[4], and three of the fire tests undertaken on the steel framed building at Cardington.

The results of two ISO 834 standard fire tests on simply supported composite beams are compared with analytical results in figures C7 and C8. These show reasonable agreement, particularly in view of the uncertainties associated with fire testing. For example, there is little data concerning temperature variation along the length of the beam, simple support conditions are very difficult to produce in a furnace at high temperatures and high deflections, and some assumptions have been made concerning material properties. The nominal ambient temperature values of material properties reported were: compressive strength of concrete 30N/mm^2; yield strength of steel 255 N/mm^2; and yield strength of reinforcing steel 600 N/mm^2. The ultimate shear strength of the studs was assumed as 350 N/mm^2.

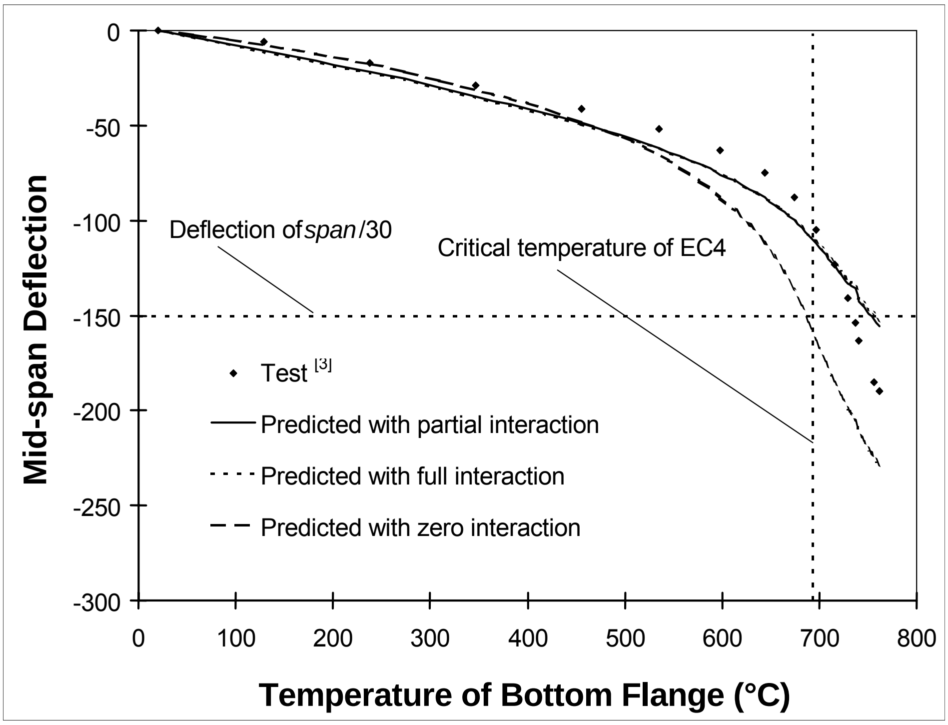

Figure C7 Comparison of temperature-deflection behaviour for 254 × 146 × 43UB composite with a 130mm reinforced concrete slab, subject to a standard fire test[2].

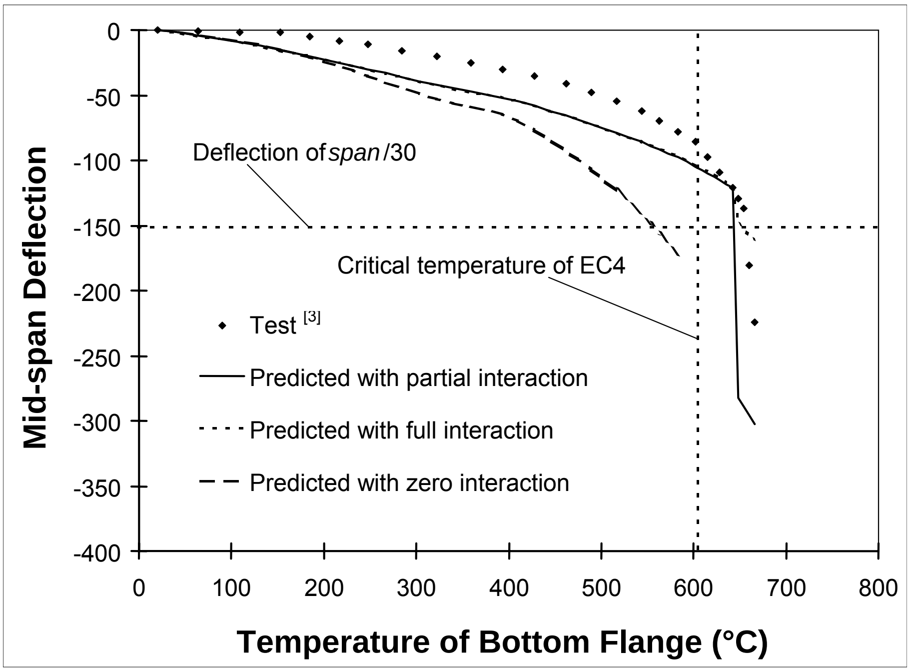

Figure C8 Comparison of temperature-deflection behaviour for 254 × 146 × 43UB composite with a 130mm reinforced concrete slab, subject to a standard fire test[2].

In 1995-96 six large fire tests, in all of which the internal steel beams were unprotected against heating, were carried out on a full-scale 8-storey composite building constructed in 1994 at the BRE fire research laboratory at Cardington. The test building was constructed as a typical office development, using downstand beams supporting lightweight slabs cast *in-situ* onto ribbed steel decking. Composite action was achieved between both primary and secondary steel beams and the floor slabs using through-welded shear studs. The six fire tests were sited in different types and sizes of fire compartments designed to test a variety of situations, as indicated on the typical floor plan (figure C9). The floors were loaded throughout the testing period using sand-bags, which contributed to an overall floor loading of 5.48kn/m^2. For the secondary composite beams this equates to a load ratio of 0.44.

The most significant qualitative observation was that in none of the six fire tests was there any indication of run-away failure, despite unprotected steel beam temperatures over 1000°C in some tests. Tensile membrane action in the concrete floor slabs may have played an important role in this respect.

The ambient-temperature material properties used in the modelling, based on tested values from the Cardington frame where these were available, are as follows:

- The yield strength of steel members is 308 N/mm^2 for Grade 43 steel (S275) and 390 N/mm^2 for Grade 50 steel (S355);

- The yield strength of the steel used in the anti-crack mesh was assumed to be 460 N/mm^2;
- The elastic modulus of steel was 2.1×10^5 N/mm^2;
- The average compressive strength of concrete test samples was 35 N/mm^2.

In all tests the internal steel beams in the ceiling of the compartment were left unprotected, although columns were mainly protected and in some tests the perimeter beams were protected.

It is not possible to be totally certain of the conditions of these tests, because of inevitable variations in details such as loading, heating, slab thickness and material properties. Nevertheless they represent the most significant source of experimental data for steel structures in fire, and provide a unique basis for comparison with regard to complete structure behaviour.

For current purposes the significant tests in figure C9 are test 1 (British Steel Restrained beam test), test 4 (BRE corner test) and test 5 (BRE large compartment test).

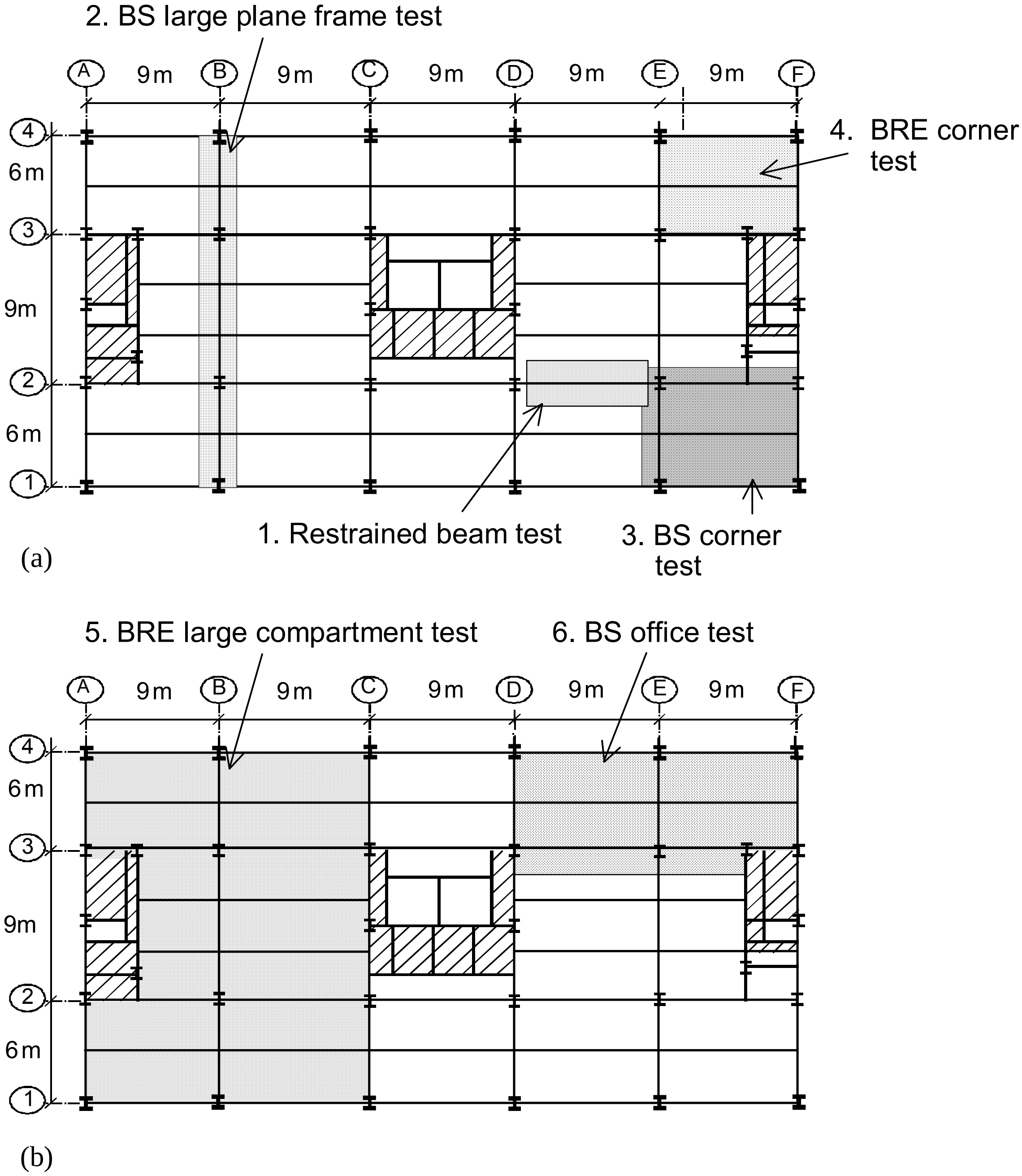

Figure C9 Locations of six fire tests in the Cardington test frame:
(a) test 1 to 4; (b) test 5, 6.

The Restrained Beam Test involved heating a single 305x165UB40 secondary beam and an area of the surrounding slab on the seventh floor. The major objective of this test was to study the effects of restraint from a large area of surrounding cool structure, including floor slabs, on the behaviour of the heated structure. The finite element mesh layout used for the analysis of this test is shown in Figure C10.

The temperature distributions in the steel beam and slab are based on the average values recorded. In order to investigate the structural behaviour up to extremely high temperatures, these temperatures have been extrapolated linearly.

The test results (mid-span deflection against bottom flange temperature) are shown in Figure C11, together with the analytical results. The predictions of the present model, including geometric non-linearity of the slab element, are in remarkably good agreement with the test results, whereas using a linear slab element gives a poor representation above about 500°C.

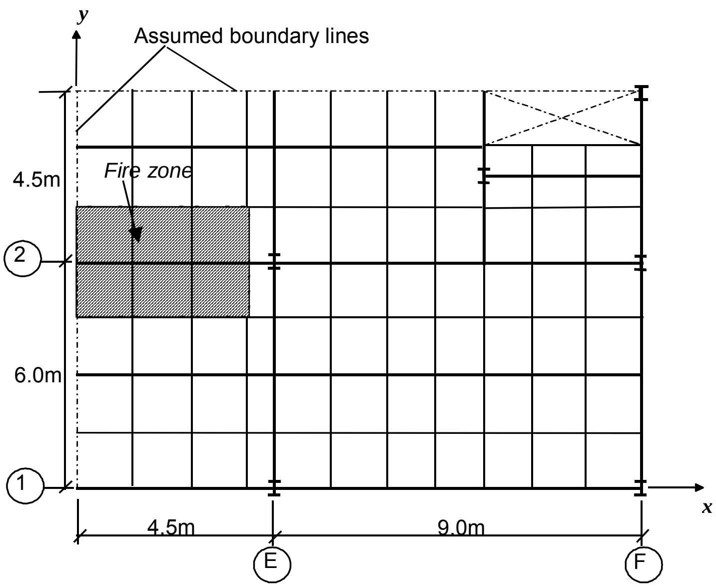

Maximum modelled temperatures

Member(s)	Maximum concurrent temperatures (˚C)		
Heated beam	Top flange 920˚C	Web 983˚C	Bottom flange 1005˚C
Heated slab	Top layer 165˚C		Bottom layer 637˚C

Figure C10 Finite element layout adopted in the analysis of the Restrained Beam test.

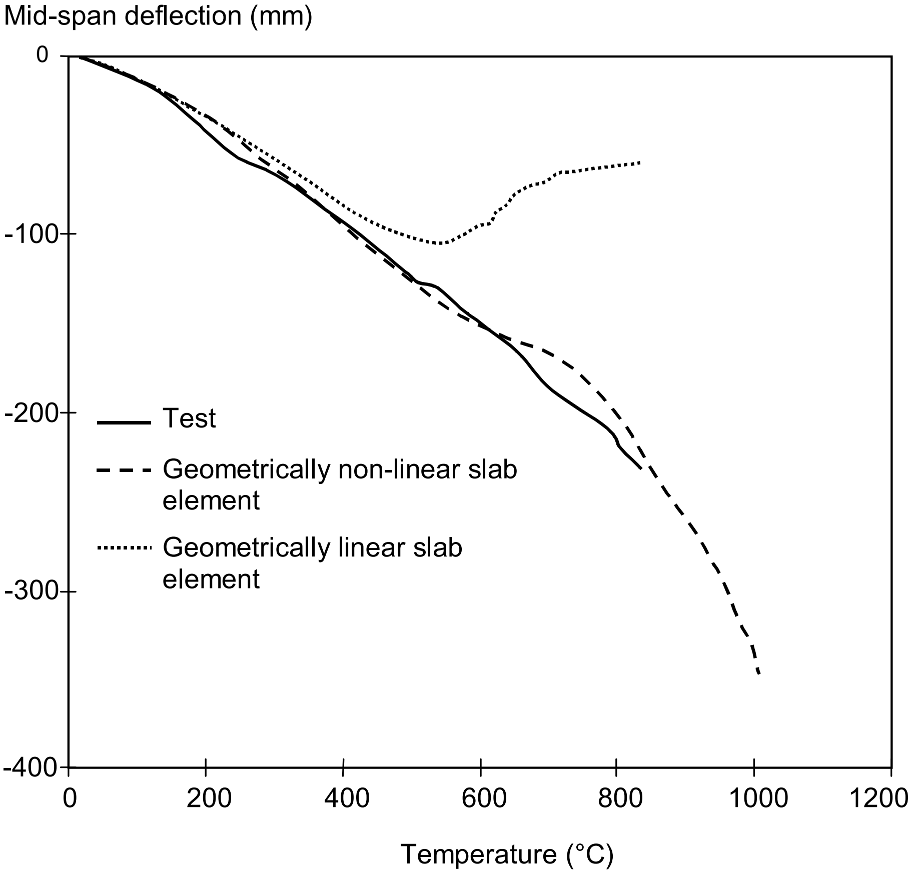

Figure C11 Vertical deflections for the Restrained Beam test

The BRE corner test took place in a rectangular compartment measuring 9m by 6m in plan. Wind-posts effectively restricted vertical downward movement of the edge beams to 80mm. All of the steel beams in the compartment were left unprotected, but the steel columns inside the compartment were protected by insulating material up to the underside of the ceiling slab, including the beam-to-column connections. During the fire test the maximum recorded temperature were 1051°C (atmosphere), 842°C (internal beam), 590°C (edge beam), 285°C (concrete slab), and 150°C (columns). These have been extrapolated to allow structural analysis at higher temperatures.

The finite element mesh layout adopted for the analysis is shown in Figure C12. The comparisons between the predicted and test results for vertical deflection of the central position D19 are plotted in Figure C13. The geometrically linear results give a reasonable representation up to temperatures of about 600°C, but at higher temperatures are unable to model the behaviour of the floor slab adequately. In contrast, the geometric non-linear results provide a very good comparison throughout.

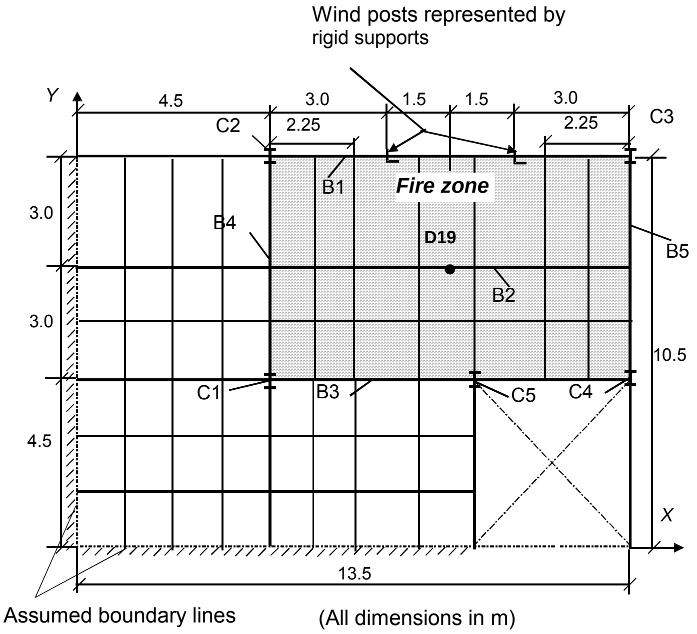

Maximum modelled temperatures

Member(s)	Maximum concurrent temperatures (˚C)					
B2	Top flange	845˚C	Web	1000˚C	Bottom flange	1000˚C
B1, B3, B4, B5	Top flange	530˚C	**Web**	690˚C	Bottom flange	690˚C
Columns	Outer flange	80˚C			Inner flange	150˚C
Slab	Top layer	65˚C			Bottom layer	330˚C

Figure C12 Finite element layout for the BRE Corner Fire Test, with key temperatures.

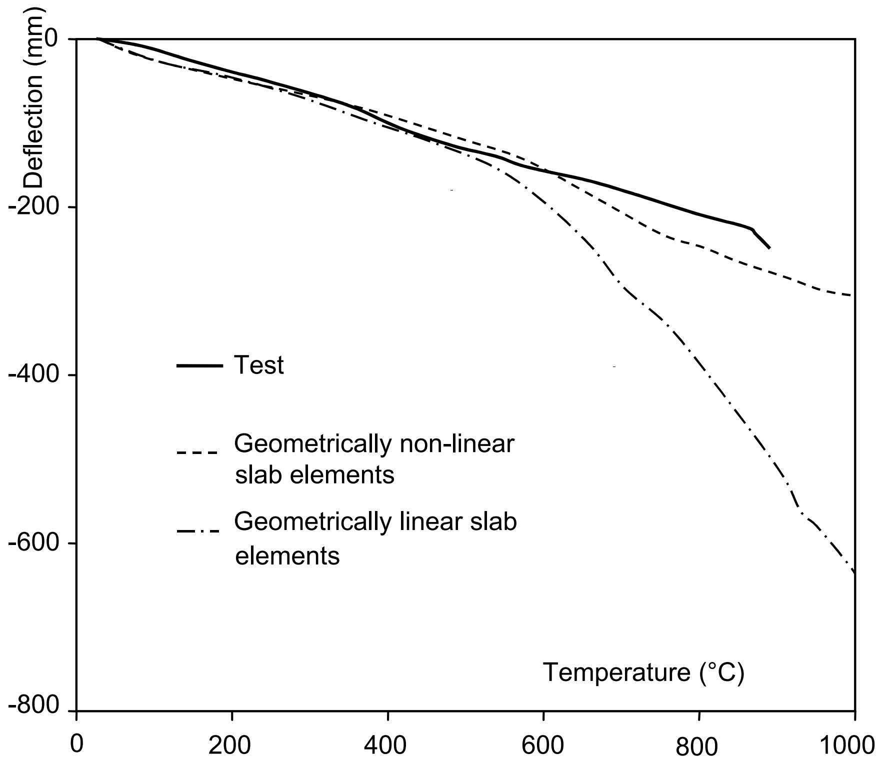

Figure C13 Comparison of predicted and measured deflections for the BRE Corner Fire Test using geometrically linear and non-linear slab elements.

The BRE large compartment test extended across the full width of the building, between Grid-line A and a line 0.5m from Grid-line C, covering an area of $340m^2$. All the internal steel beams were unprotected, but the columns were protected over their full height, including the connections. This fire test was rather cooler than the others, having maximum recorded atmospheric and steelwork temperatures of 763°C and 691°C, respectively. The maximum average measured temperature of the bottom layer of the concrete slab was about 260°C. These have been extrapolated linearly in order to investigate the structural behaviour up to higher temperatures.

The finite element mesh layout adopted for the analysis is shown in Figure C14. The comparisons between the predicted and test results for vertical deflections at key position D32 are shown in Figure C15. The deflection profile of the composite slab, given by the *Vulcan* modelling, is shown in Figure C16 at 1000°C, including the cracking patterns of the top layer of concrete. It can be seen that the predictions are in good agreement with test results over the test temperature range.

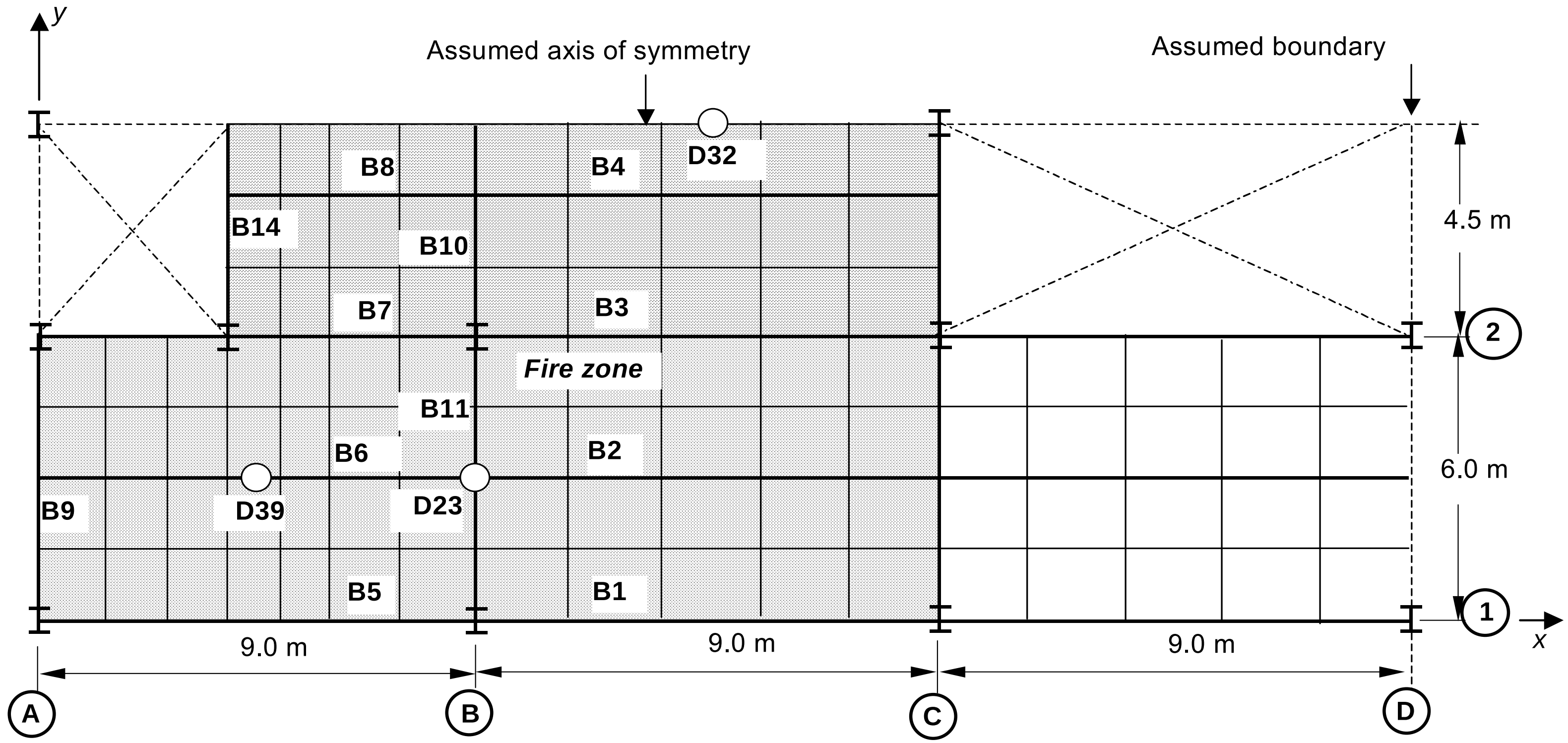

Maximum modelled temperatures

Member(s)	Maximum concurrent temperatures (˚C)					
B2, B3, B4, B6, B7, B8, B10, B11	Top flange	885˚C	Web	957˚C	Bottom flange	1000˚C
B1, B5, B9, B14	Top flange	567˚C	**Web**	640˚C	Bottom flange	640˚C
All columns	Uniform	92˚C				
Slab	Top layer	106˚C			Bottom layer	366˚C

Figure C14 Finite element layout adopted in the analysis of the BRE Large Compartment Fire Test, together with key temperatures

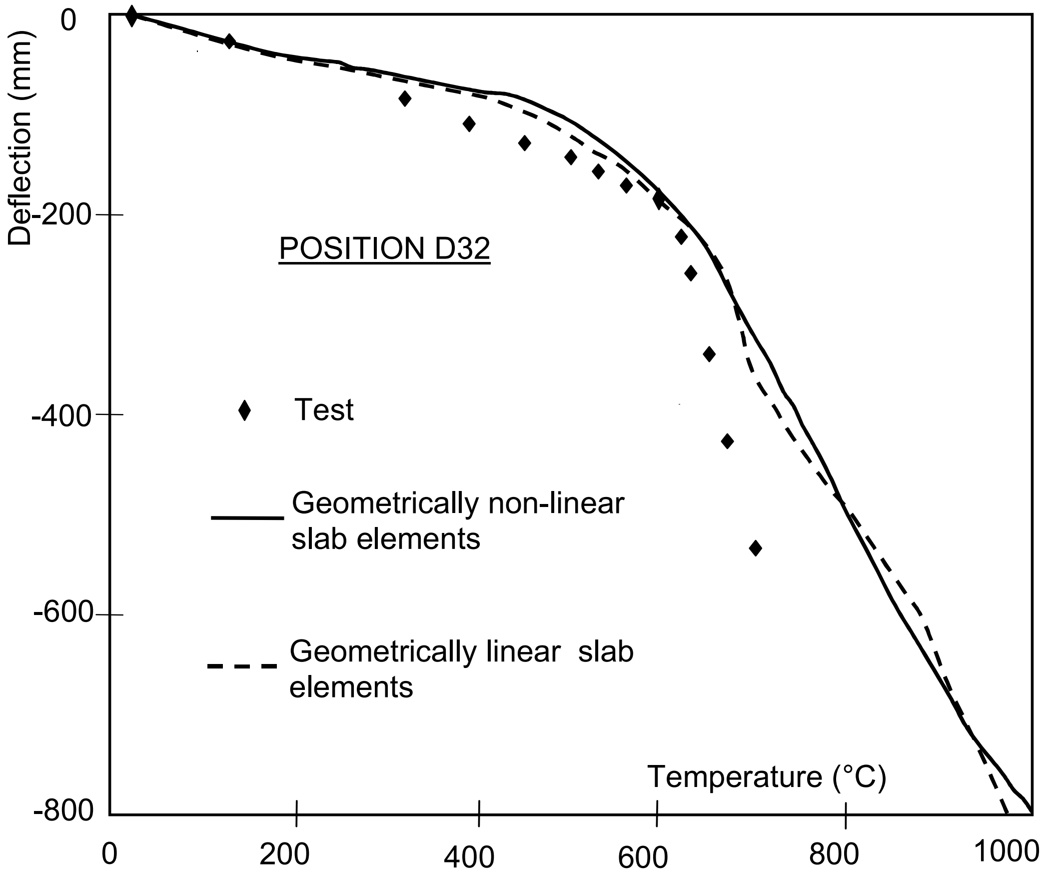

Figure C15 Vertical deflections at position D32 for BRE large compartment test

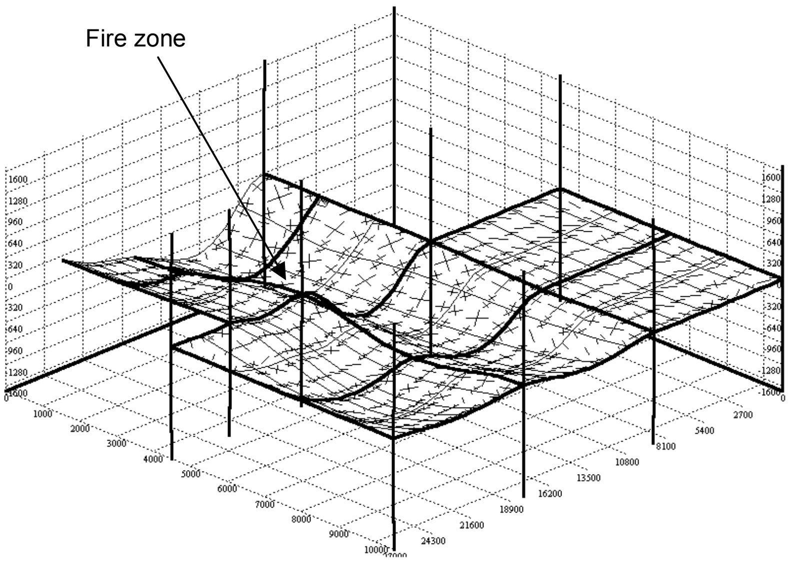

Figure C16 Deflection profiles for 1000°C for BRE large compartment test

From the results presented above it can be concluded that:

Vulcan is capable of modelling the load-deflection behaviour of isolated members, as demonstrated through comparisons with experimental results for composite elements;

Vulcan provides a good model for the temperature-deflection behaviour of isolated members, as demonstrated through comparisons with standard fire tests on single beams and more extensive structures for both steel and composite construction;

Vulcan predicts the structural behaviour of a composite steel-framed building subject to fire with reasonable accuracy.

The influence of membrane action in composite floors can be significant, particularly when the fire compartment is subject to high restraint, because it is surrounded by cool, stiff structure which resists expansion and pull-in, or when slabs of fairly square aspect ratio are vertically supported along their edges by protected beams or by other types of support.

In spite of the uncertainties associated with experimental work generally and fire testing in particular, the *Vulcan* analyses presented here have produced very good predictions.

Structural Model – MasSET

A finite element model MasSET (Masonry Subject to Elevated Temperatures) has been developed[3] taking into consideration material and geometric non-linearity, the cracking and crushing using the stress-strain failure criterion for masonry walls under elevated temperature. The inclusion of geometric non-linearity allows P-Δ effects to be incorporated for axially loaded walls. The interface element, which can predict wall-slab interaction behaviour under elevated temperature is also taken into consideration. Because masonry walls subject to flexure exhibit failure by either cracking or debonding of the mortar layer on the tension side the tensile properties of the wall must be based on the bond strength of the mortar layer in the brick wall.

The finite element model has been validated against the results from a full-scale axially loaded masonry wall with dimensions of 3m x 3m x 90mm thick constructed from clay masonry units[4]. The top and bottom boundary conditions were laterally and rotationally restrained while the vertical edges were unrestrained with sufficient clearance for free thermal expansion. Sandwich platens constructed from ceramic fibre core and laminated by two steel plates were used between the wall top and bottom boundaries and the loading plates. The wall was subject to the Australian standard time-temperature curve and an applied axial stress of 0.877N/mm².

Figure C17 is a comparison between the test results and then numerical simulations yielded by MasSET and clearly show that increasing rotational stiffness produces a decrease in thermal bowing. With free rotation, failure due to buckling occurred at levels below that derived for the test.

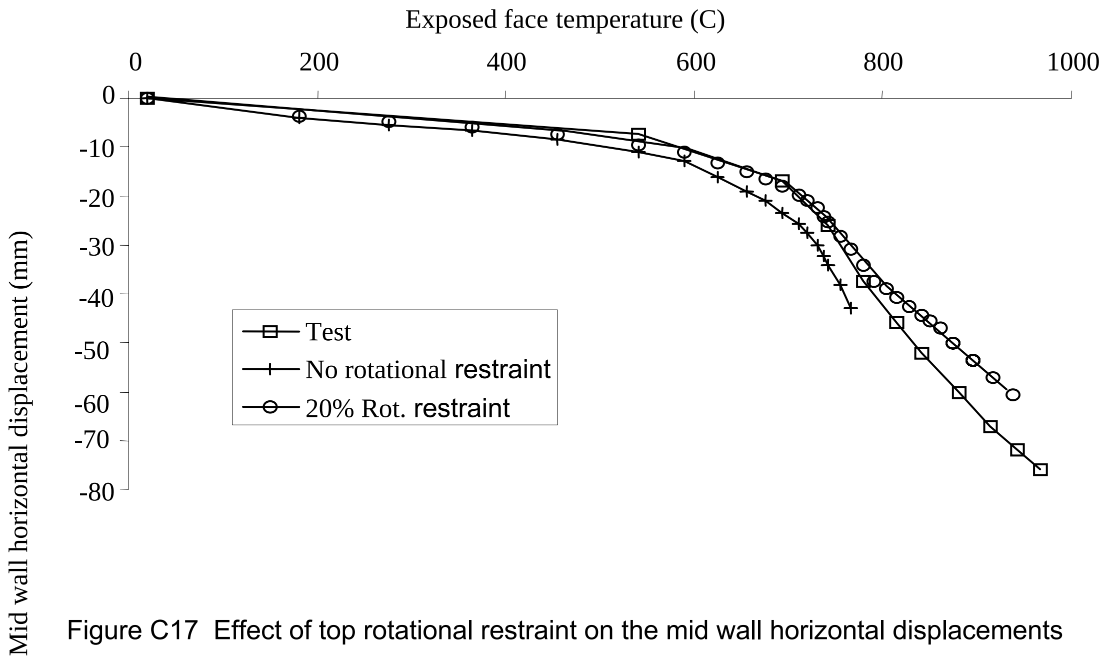

Figure C17 Effect of top rotational restraint on the mid wall horizontal displacements

Additional validation has been carried out using model scale walls tested at the University of Ulster[5]. The model walls were 430mm wide by 1330mm high strip columns with a thickness of 50mm subject to 50% of the design ultimate load. Masonry units consisted of concrete with a specified crushing strength of 20N/mm², bedded on a 1:3 mortar mix using Ordinary Portland Cement. The base of the walls were built on a flat steel plate and the applied axial load was distributed over the width of the panel through a steel loading plate which was restrained against rotational movement, the vertical edges of the wall were unrestrained with sufficient space for free thermal expansion. The axial load was kept constant during all the tests. Lateral deflections were measured at support positions and at mid-span. Temperature was recorded at third points of the wall. The comparison between measured and predicted response is shown in figure C18.

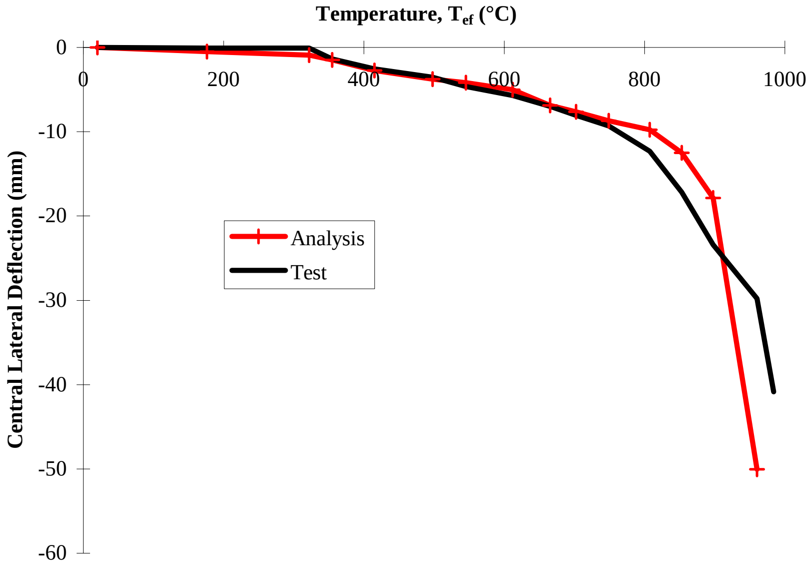

Figure C18 Comparison between experimental and analytical central deflection v exposed face temperature for test FW1

In general, the finite element model MasSET has proved to be very successful in predicting the behaviour of restrained walls at elevated temperature. Areas where experimental simulation proved difficult were due to uncertainties in the precise configuration of the tests. Where controlled rotational stiffness was present MasSET produced close correlation with the measured values.

Thermal Model – THELMA

THELMA was developed at BRE for modelling the thermal response of construction materials to fire. It uses standard finite-element techniques to model the flow of heat through an arbitrary 2-D slice of a material, accommodating cavities as required, and describing boundary condition heat transfer via a convective heat transfer coefficient and a surface emissivity value. Temperature-dependent material properties are available and the latest version of the software includes a simple moisture model.

THELMA incorporates pre-processing facilities to allow the user to enter the geometry of the problem, generate a mesh and to assign material properties and boundary conditions. Standard fire exposure curves can be selected and material properties data is included for many common building materials. The built-in post-processor includes time-temperature and contour plotting facilities.

In early work, THELMA was extensively validated against test data for steel, concrete and composite structures. Recently, the main area of interest has been masonry and a simple preprocessor for generation of the material properties data files has been written which calculates the effective temperature-dependent specific heat and thermal conductivity according to the initial moisture content in the material. In addition, an adaptive meshing feature was developed for the Windows version of the code.

The simple moisture model has been calibrated by comparison with through-thickness temperature data from 18 standard fire-resistance tests on masonry. It was found to be necessary to adopt significantly increased thermal conductivity values below the moisture vaporisation temperature of the material. This is not unreasonable, given the neglect of moisture *transfer* in this simple model, and the implicit assumption of a direct coupling of the moisture concentration and temperature.

Figures C19-C22 below illustrate the predictions of the code for the temperature profile in a voided masonry unit and a comparison with the test data from a fire resistance test.

Figure C23-C24 illustrate application of the model to analysis of heating of a protected steel member in a large (12mx12m) compartment fire test performed at BRE's Cardington laboratory in 1999. The comparison of steel and predicted temperatures is shown in Figure C25.

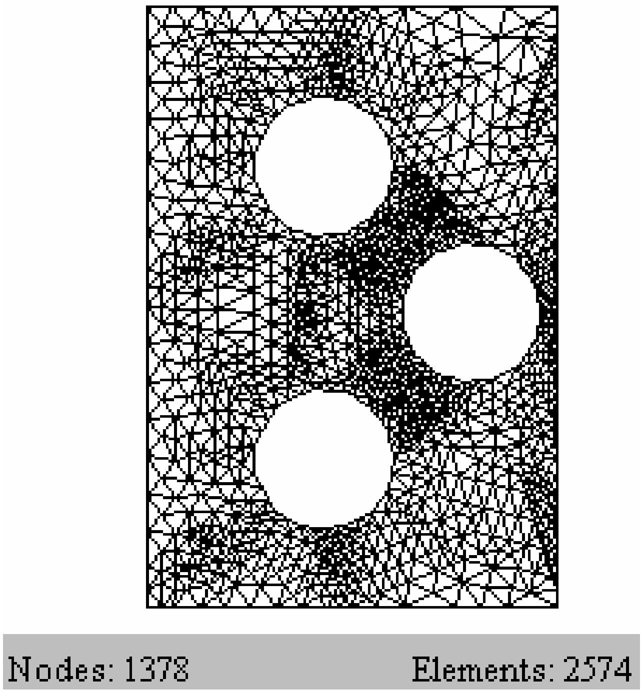

Figure C19 Computational mesh for a voided brick

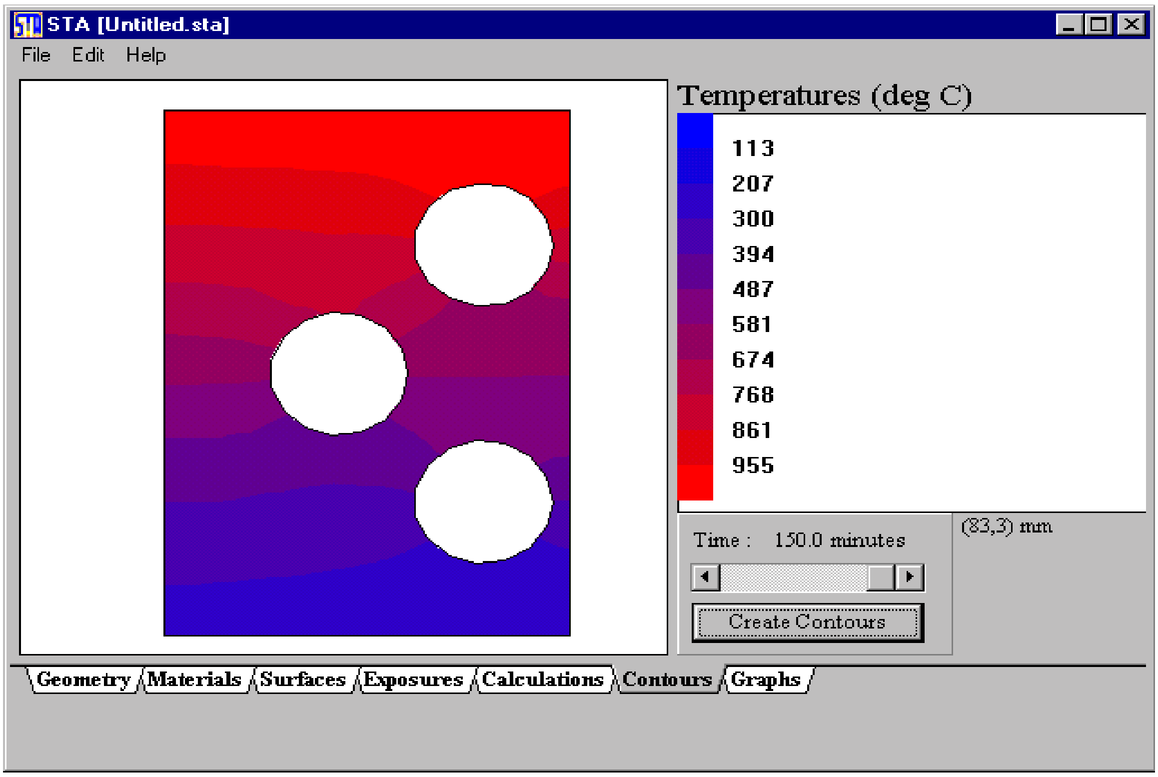

Figure C20 Predicted temperature distribution

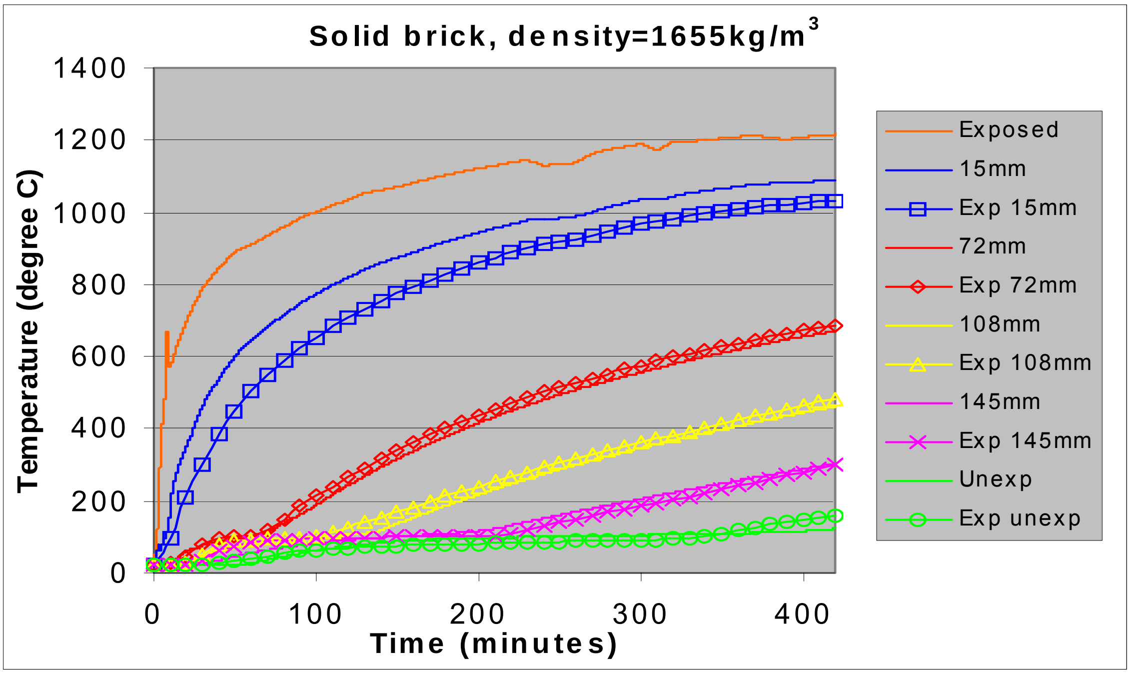

Figure C21 Comparison between measured and predicted temperatures masonry walls

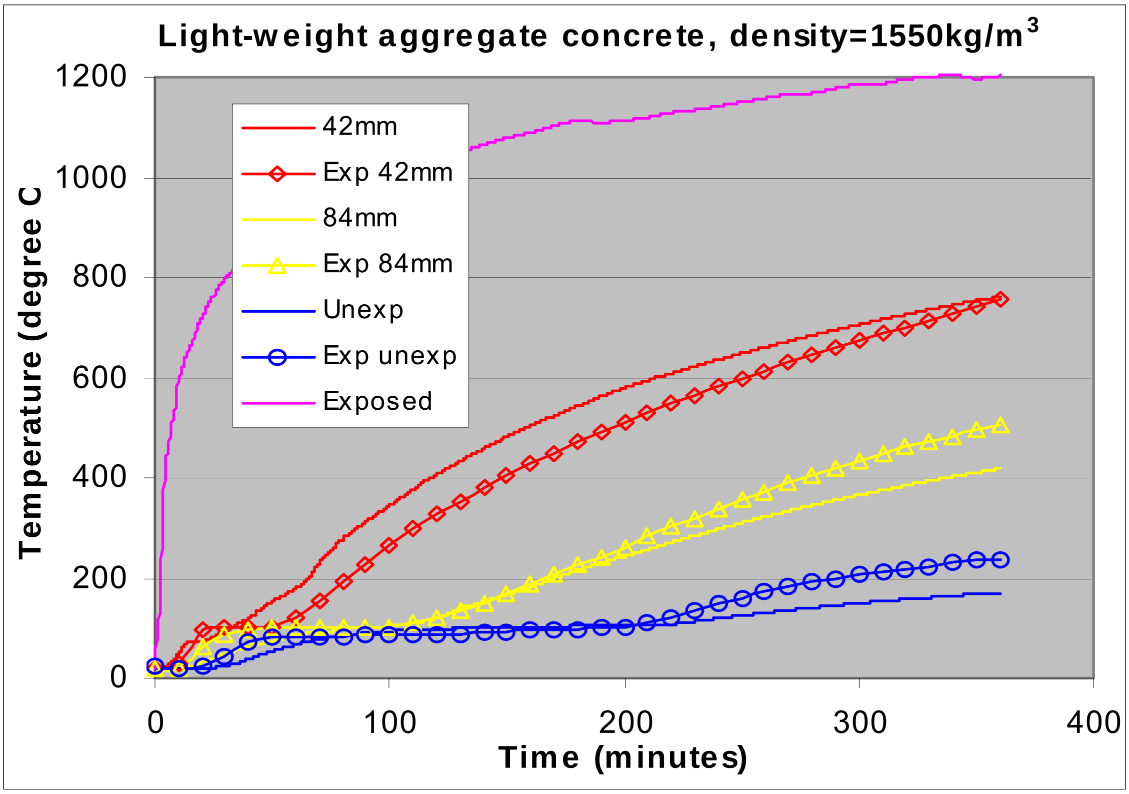

Figure C22 Comparison between measured and predicted values concrete wall

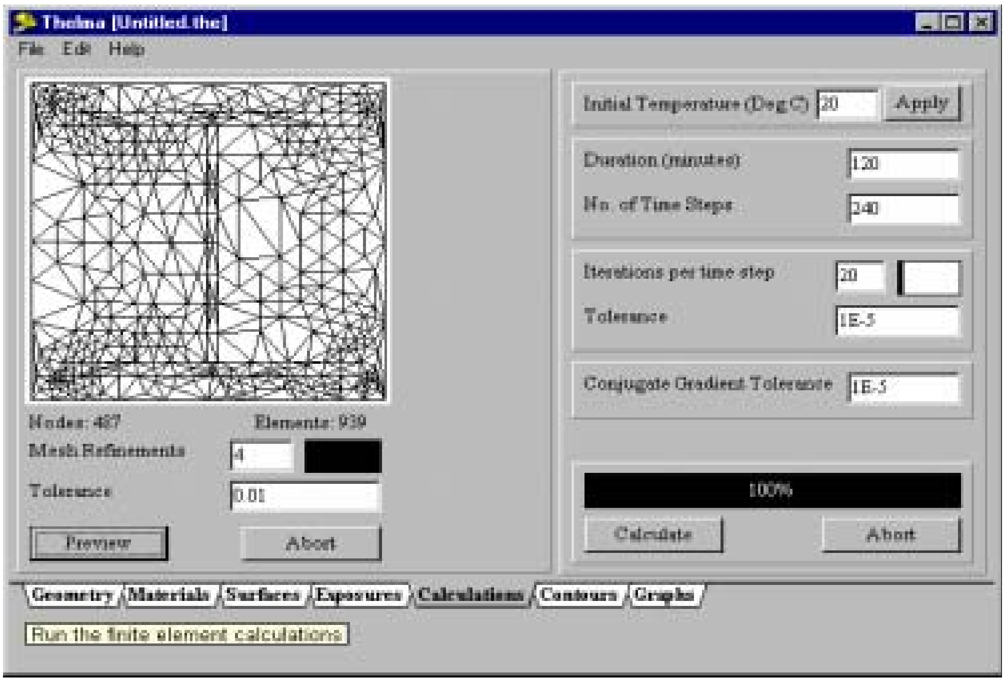

Figure C23 Computational mesh for protected steel section

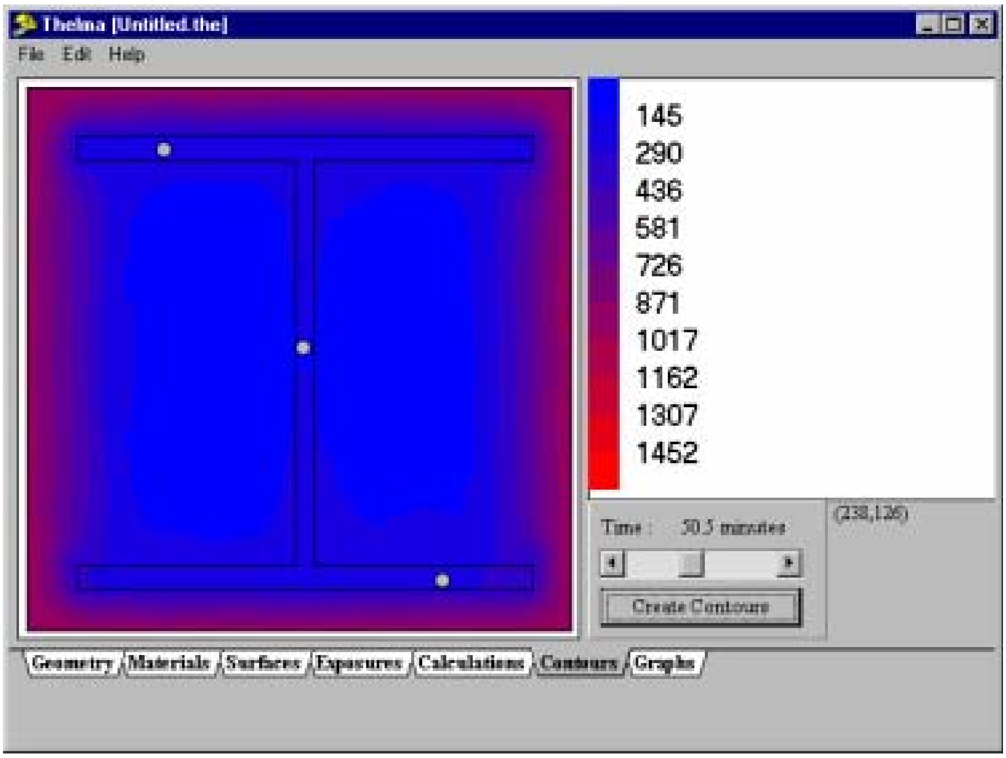

Figure C24 Predicted temperature distribution

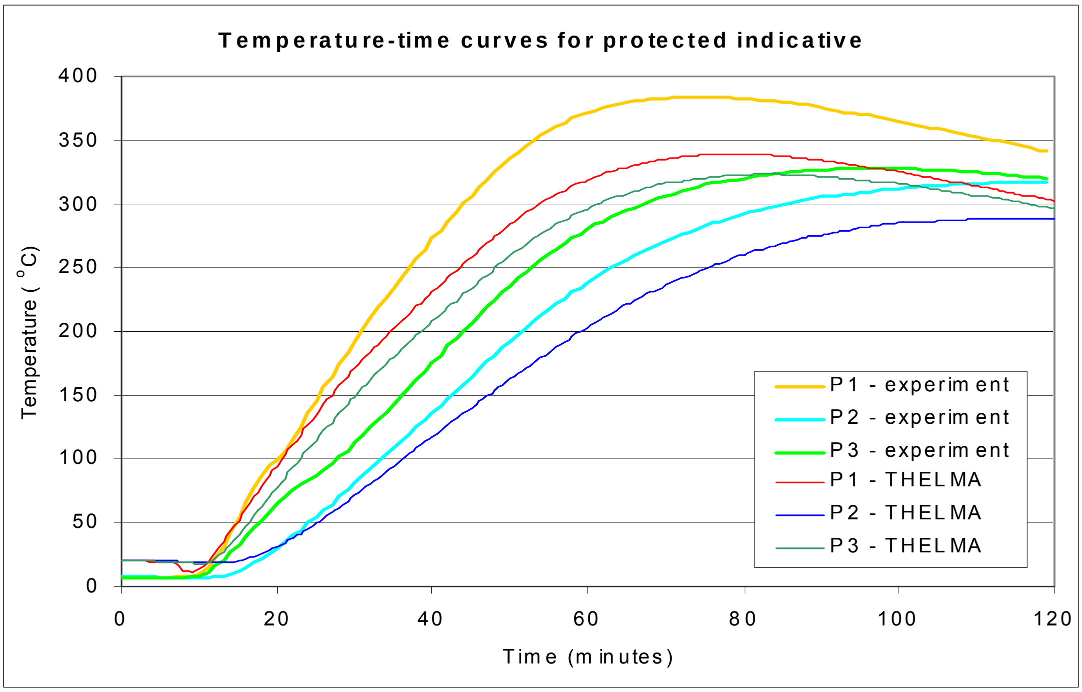

Figure C25 Predicted and measured values protected steel section

References for Appendix C

1. PD 7974-1:2003, Application of fire safety engineering principles to the design of buildings – Part 1: Initiation and development of fire within the enclosure of origin (Sub-system 1), British Standards Institution, London

2. Wainman D E and Martin D M, Preliminary assessment of the data arising from a standard fire resistance test performed on a Slimflor beam at the Warrington Fire research centre on 14th February 1996, Technical Note SL/HED/TN/S2440/4/96/D, British Steel Swinden Technology Centre, March 1996

3. Nadjai A, O'Garra M, Ali F A and Laverty D, A numerical model for the behaviour of masonry under elevated temperatures, Fire and Materials, 2003, 27: 163-182

4. Gnanakrishnan N, The effect of end restraint on the stability of masonry walls exposed to fire, National Building Technology Centre, Australia

5. Laverty D, Nadjai A, O'Connor D J, Modelling of thermo-structural response of concrete masonry walls subjected to fire, Journal of Applied Science, 2001, 10, pp 3-19

Appendix D The use of existing data for subsequent analysis

Availability and utilisation of full scale test data

Although there is a great deal of full-scale test data in the public domain (see Appendix B of this report) much of this information has been extensively analysed and disseminated and has already been used to provide validation (see Appendix C of this report) for the structural model used in this project.

The last full-scale fire test carried out on the steel framed building at Cardington took place in January 2003. This test was carried out with the support of the European Community and the active participation of a number of European partners. The funding obtained was sufficient to carry out the full-scale test but did not include any allowance for data analysis and interpretation. The results from this large scale fire test were recently made available for the first time and were able to be used in support of this work.

The use of the results from the Cardington fire test provided a number of advantages over the original proposal to include an experimental study.

- Reduced cost to ODPM and better value for money.
- The use of the results from this test will provide a more effective means of meeting the project objectives in providing a quantitative assessment of the results from the numerical studies.
- The data is extensive and comprehensive relating to the performance of a full-scale building rather than a small compartment (as originally proposed) and therefore the results incorporate realistic levels of both loading and restraint.
- The test was undertaken on a modern steel framed building with composite floors typical of the form of construction to which innovative fire engineering design methods apply.
- The test incorporated both protected and unprotected members.
- The instrumentation was extensive and included vertical displacement and lateral movement of the floor slab, the thermal profile through the depth of the slab and longitudinal and cross-sectional thermal distributions through the steel members.
- The data has not been included in previous validation of numerical models and therefore the simulations will not incorporate assumptions based on a prior knowledge of the results.

Description of the test

The test was carried out as part of a European collaborative research project "tensile membrane action and robustness of structural steel joints under natural fire" (EC FP5 HPRI – CV5535). The objective of the project was to investigate the global structural integrity of a realistic fire compartment within a real building subject to realistic levels of imposed load and a natural fire. Specific objectives were to determine the temperature distribution in the structural elements and connections, the internal forces in the connections and the transfer of forces through the composite slab.

The detailed construction of the 8 storey steel framed building at Cardington is very familiar to those responsible for subsequent analysis and has been the subject of a number of other papers[1,2]. It is therefore not discussed in this report.

Test Compartment

The fire test was undertaken on the 4th floor of the building (fire load on the third floor) in an area measuring 11m by 7m in plan. The location of the compartment on the building is illustrated in figure D1 below.

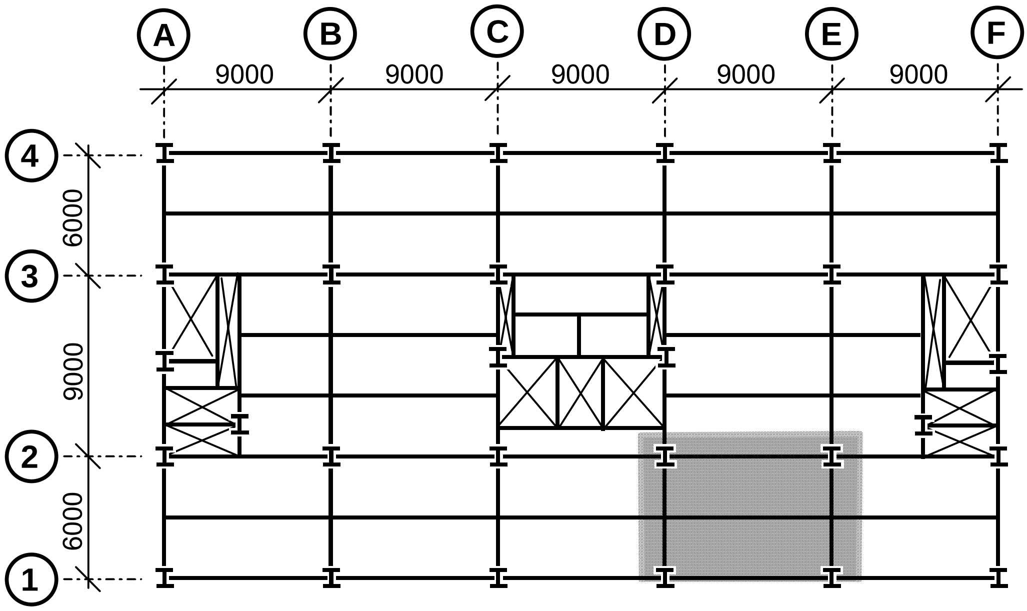

Figure D1 Location of test compartment

The compartment was formed using three layers of plasterboard (15mm+12.5mm+15mm) with a thermal conductivity of between 0.19 and 0.24 W/mK on three sides of the test area. Over the existing window opening a single layer of full height (2.4m) was fixed to the existing 0.9m high dado wall to contain the fire within the test area. An allowance of approximately 500mm was made for vertical deformation of the floor slab above the compartment walls. The gap between the top of the compartment wall and the underside of the floor slab was sealed using ceramic fibre blanket which prevented the escape of flames and hot gases whilst allowing unrestricted vertical deflection of the floor slab. The situation is illustrated in figure D2 and D3 below.

Figure D2 Compartment wall parallel to gridline E – external and internal view

Figure D3 Fireline plasterboard over window opening

Mechanical Load

The imposed load was simulated using sandbags each weighing 110kN applied over an area of 18m by 10.5m on the 5th floor. The location and distribution of sandbags on the fifth floor is illustrated in figure D4 below. Together the self load of the structure and the sandbags represent 100% of the permanent actions (dead load), 100% of the variable permanent actions (partitions and services) and 56% of the live load. This is considerably higher than the value of load adopted in the previous full-scale fire tests undertaken on this structure.

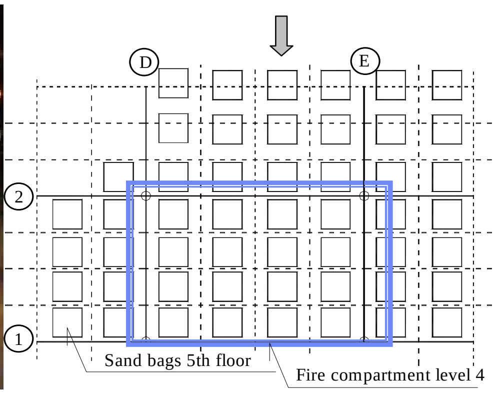

Figure D4 Sandbag layout on 5th floor

Fire Load

The fire load was provided by 40 kg of wood per m^2 of floor area in the form of wooden cribs (average moisture content < 14 %) placed in a uniform manner within the test area. The ventilation area consisted of a single opening 1.27 m high and 9 m in length. The original open area was reduced to give rise to a fire of sufficient duration and temperature to provide the required thermal input to the structural members. The fire design parameters include the predicted time-temperature response according to the latest version of the fire part of the Eurocode for Actions[3]. The ventilation opening and the wooden cribs are shown in figure D5 below.

Figure D5 Restricted ventilation and fire load

Instrumentation locations and channel allocation

In order to carry out the subsequent analysis and correlation with the measured data it is necessary for the modellers to be aware of the nature and location of the measurement positions. Approximately 300 individual instruments were used to record the thermal and structural response of the building throughout the test and for a considerable period following the test. In order to evaluate and analyse the data it is necessary to uniquely locate each instrument and to refer the location back to the channel allocation in the data files. A series of drawings have been produced to identify the positions of the individual instruments within the building (both in plan and, where appropriate, on the cross-section). The channel allocations are classified according to the type of response being measured i.e. strain, displacement and temperature and refer to the figures for reference. In this way it should be possible for researchers to identify both the location of the measuring device and the type of instrument referred to in order to interrogate the data files.

Table D1 below shows which drawings relate to the measurement of strain, displacement and temperature respectively.

Type of measurement	Drawing reference
Strain	6,7,8,9,11,14,15
Displacement	16,17
Temperature	6,7,8,9,10,12,13,18

Table D1 Relationship between drawings and type of measurement

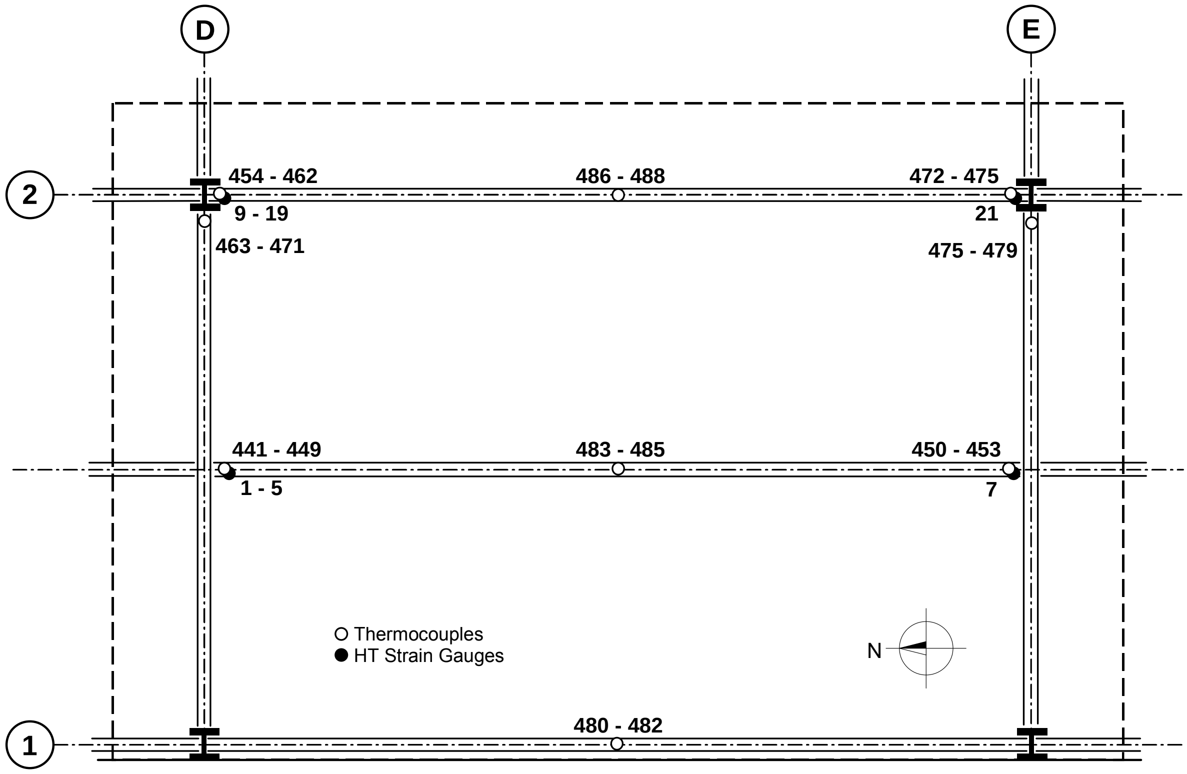

Figure D6 instrument locations beams and connection details general view on third floor

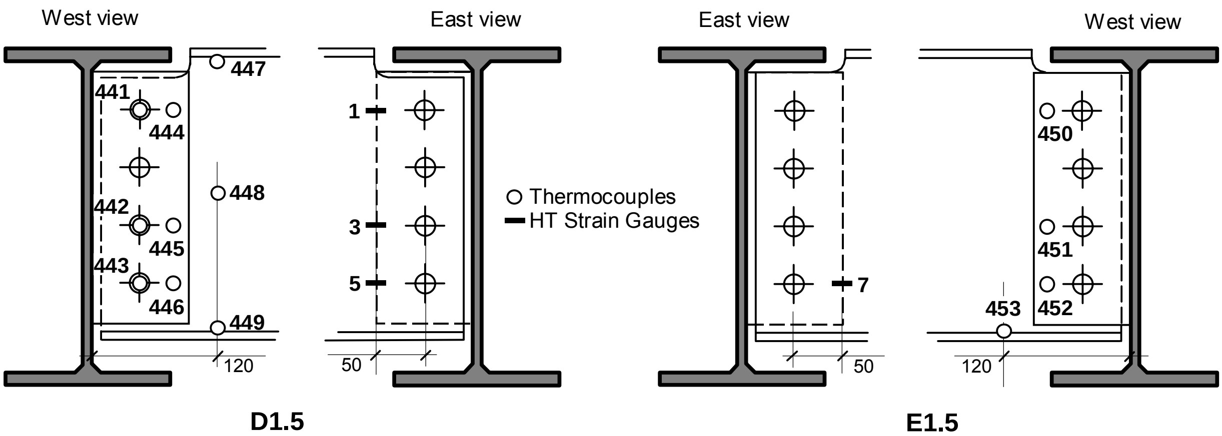

Figure D7 instrument locations fin plate connections

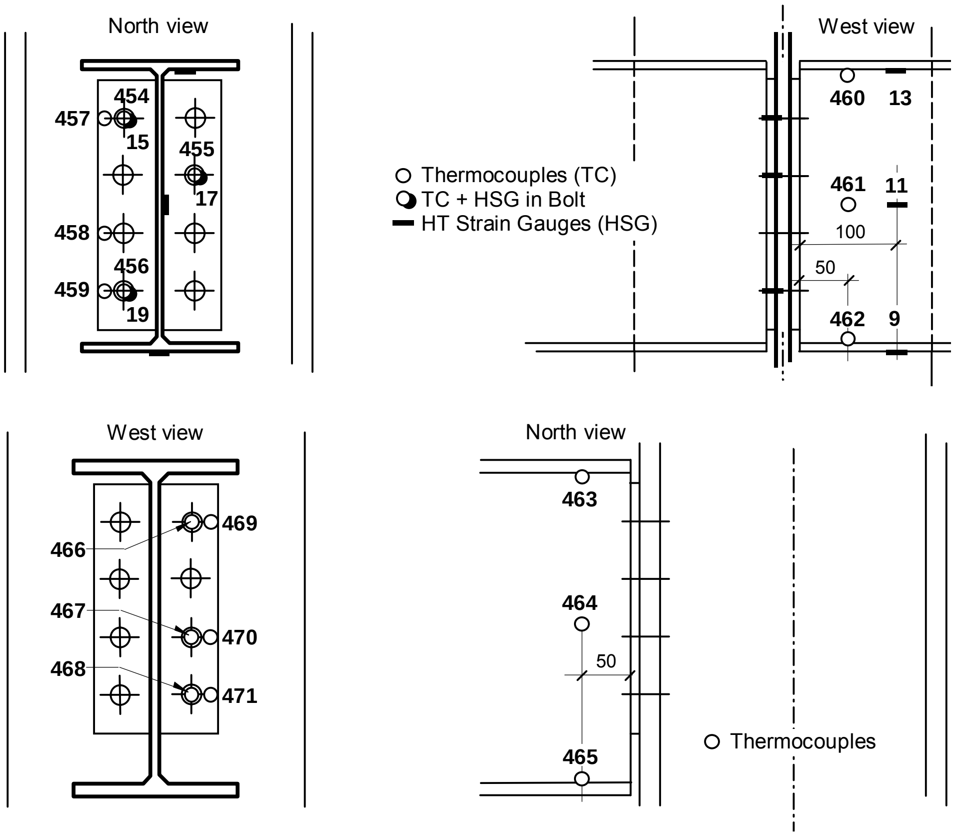

Figure D8 Partial depth end plate connections

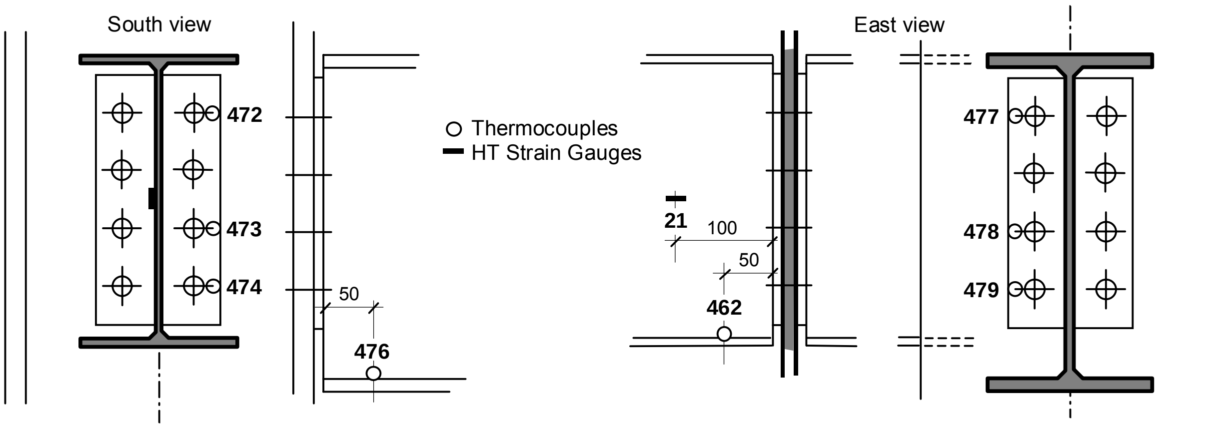

Figure D9 Partial depth end plate connections

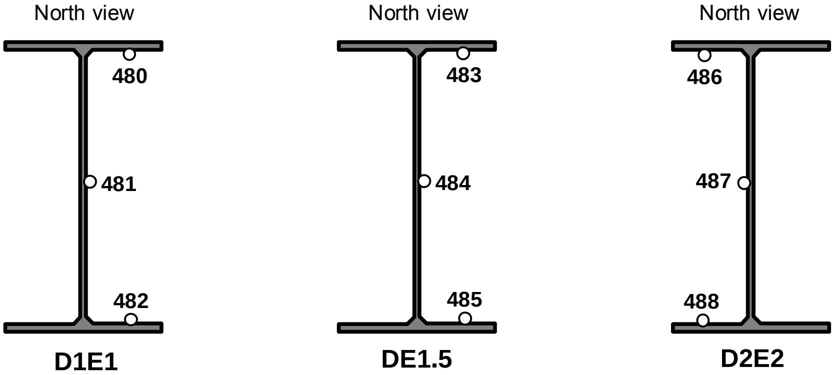

Figure D10 instrument locations – mid-span beam thermocouples (D1E1;DE1.5;D2E2)

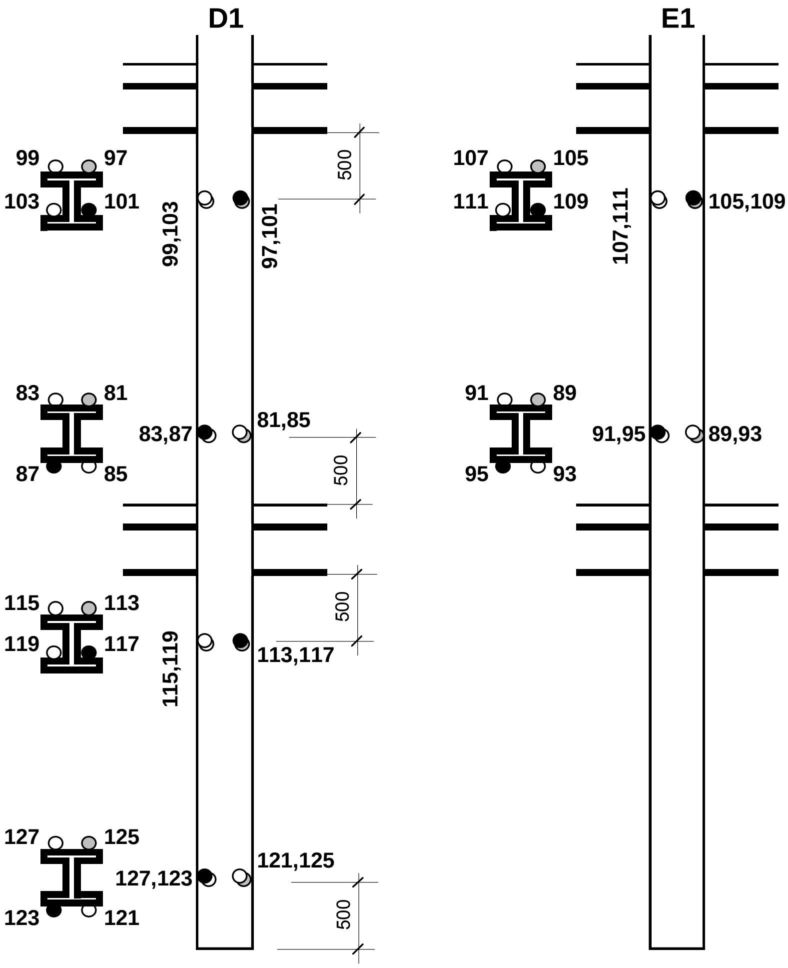

Figure D11 instrument locations – strain gauges in columns

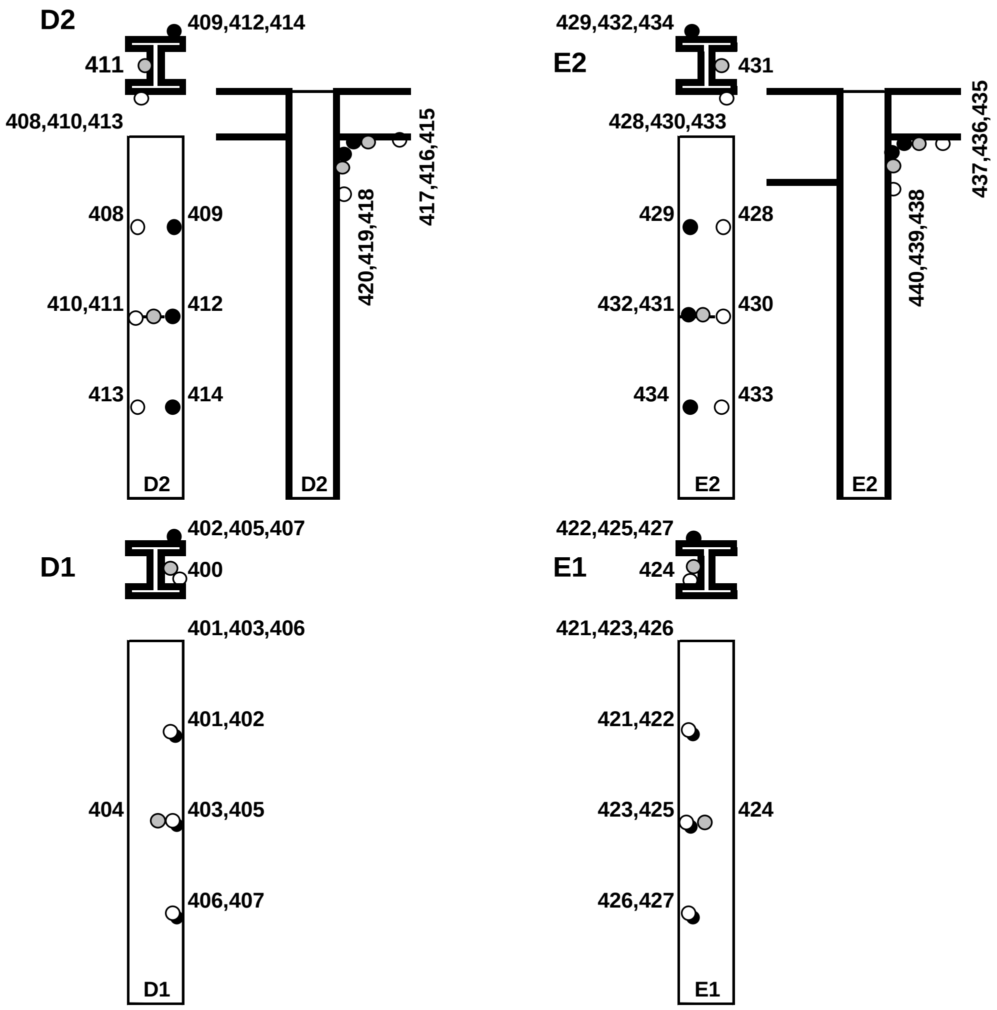

Figure D12 Location of thermocouples in columns

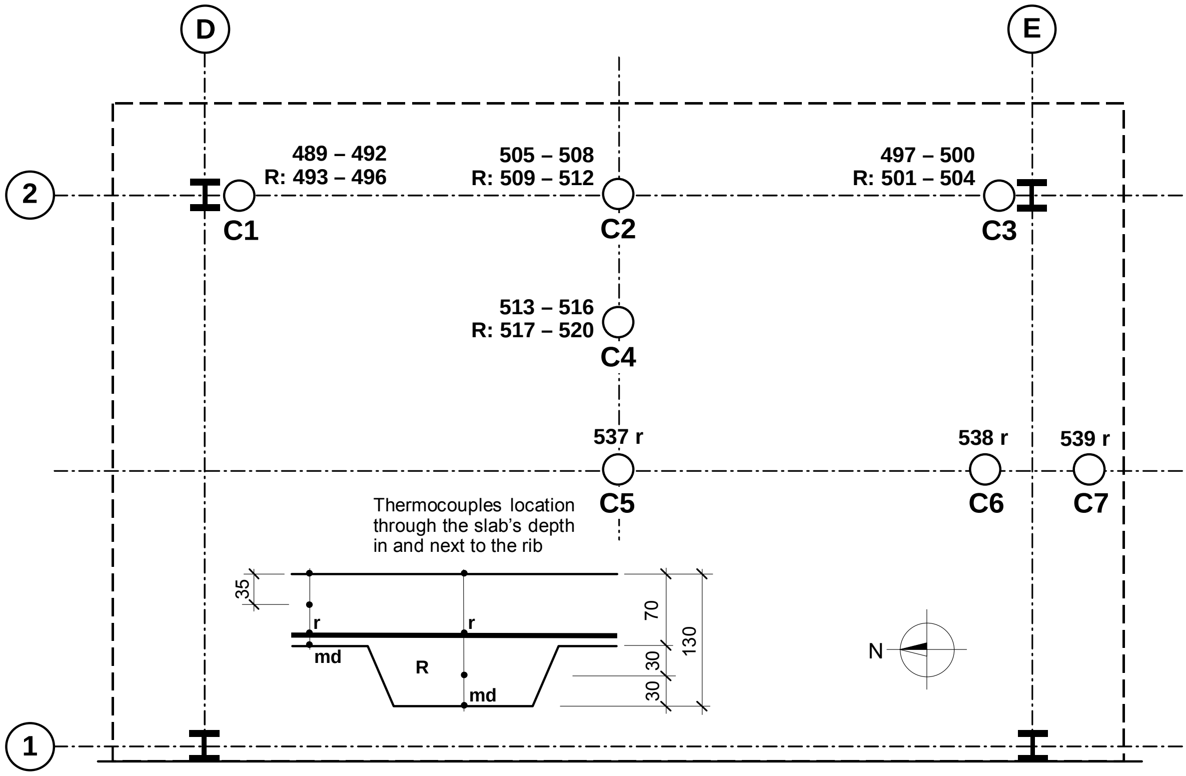

Figure D13 Location of thermocouples in slab 4th floor

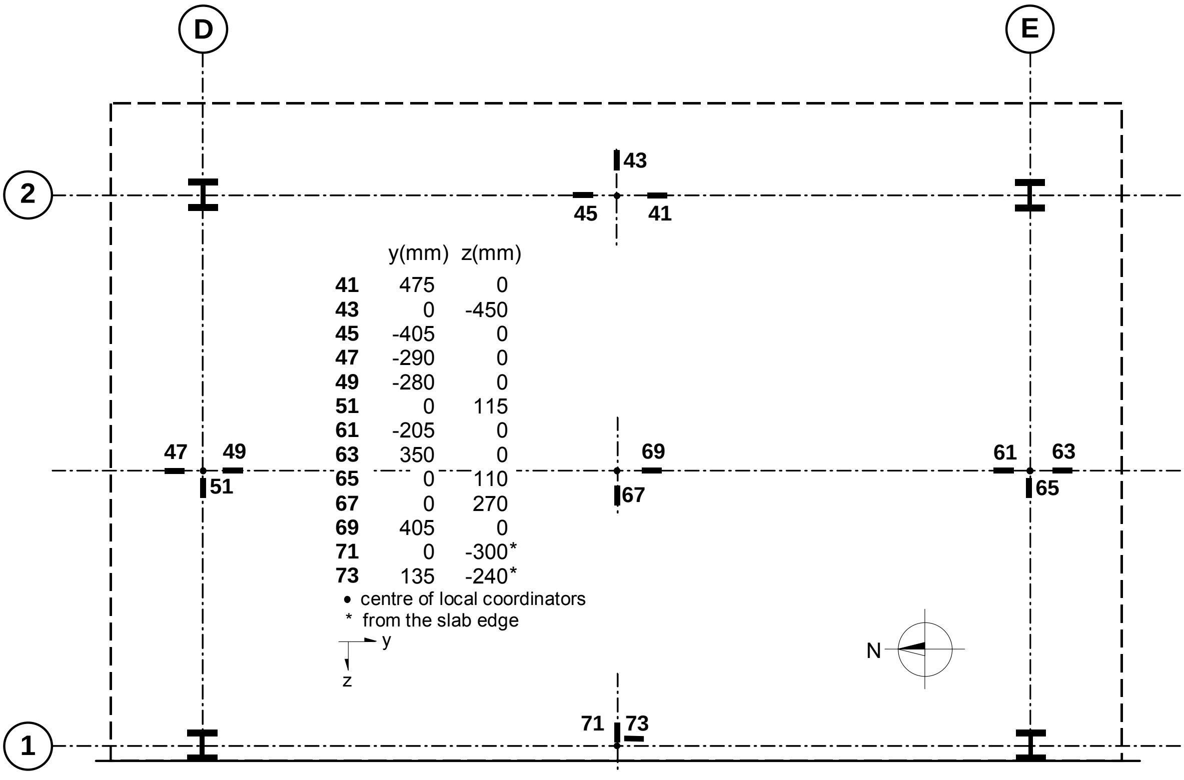

Figure D14 Location of strain gauges in slab 4th floor

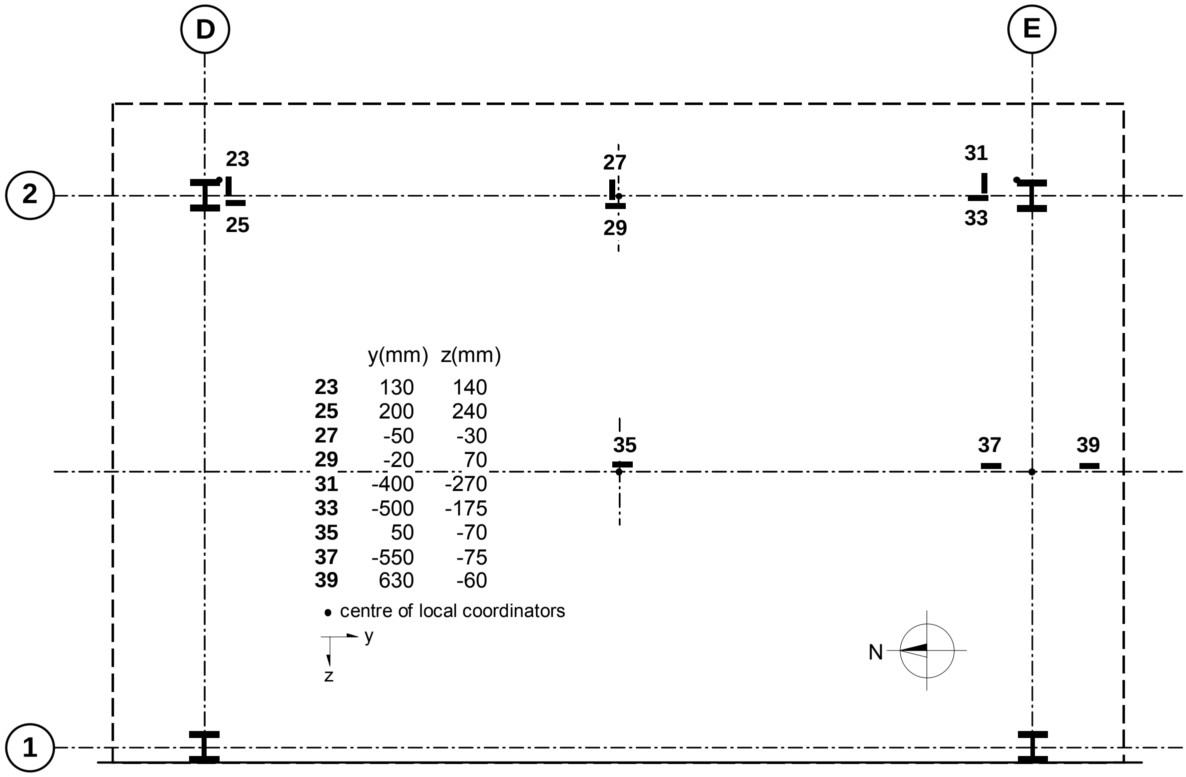

Figure D15 Location of strain gauges in reinforcing mesh 4th floor

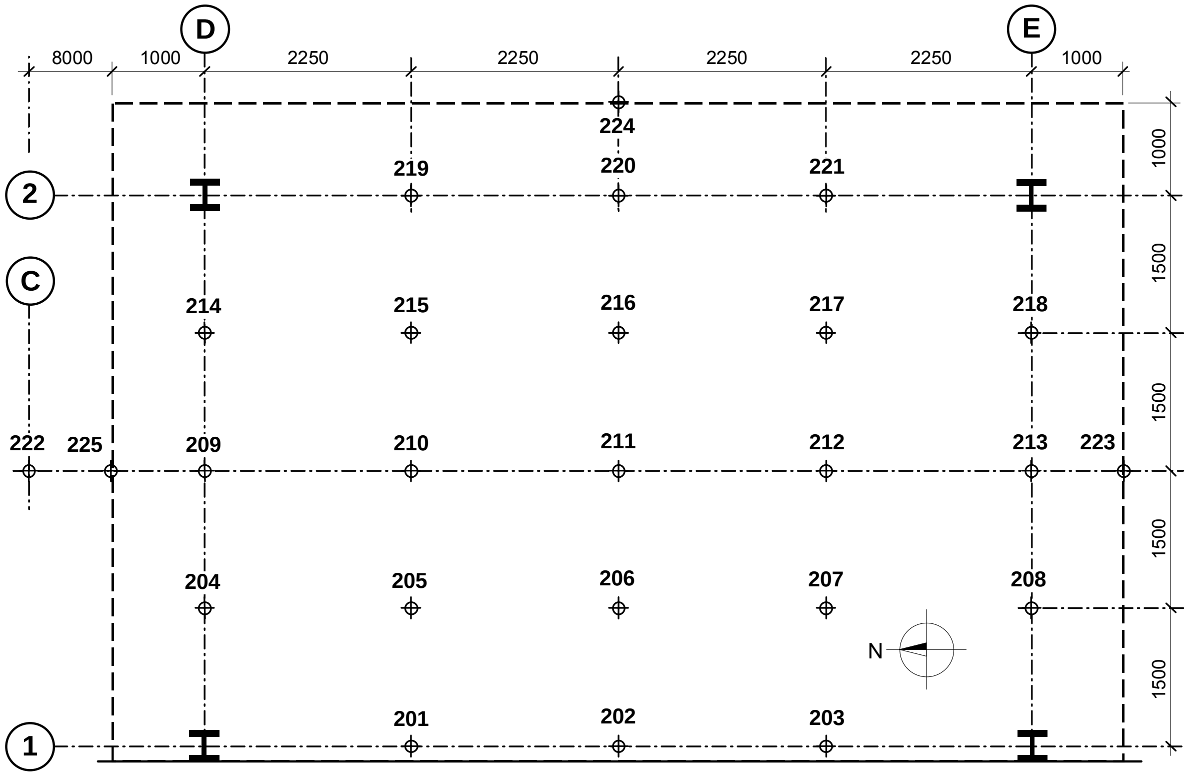

Figure D16 Location of vertical displacements 4th floor slab

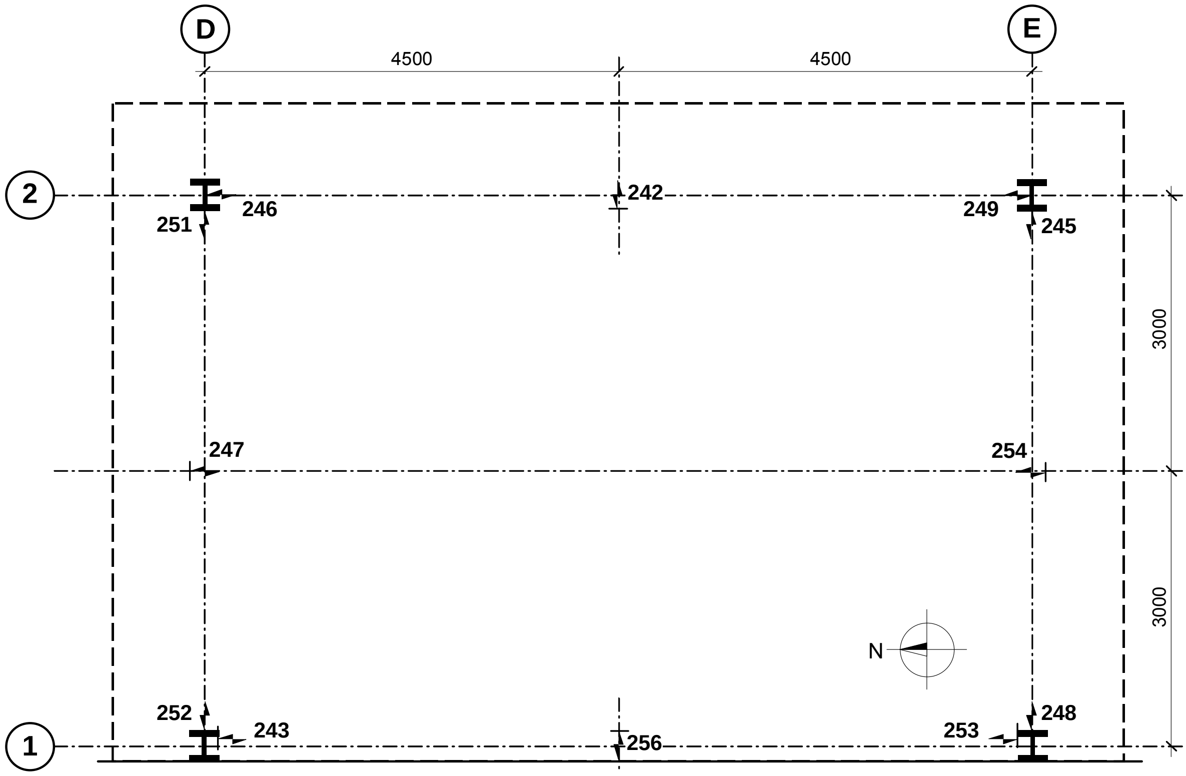

Figure D17 Location of horizontal displacements – 4th floor slab

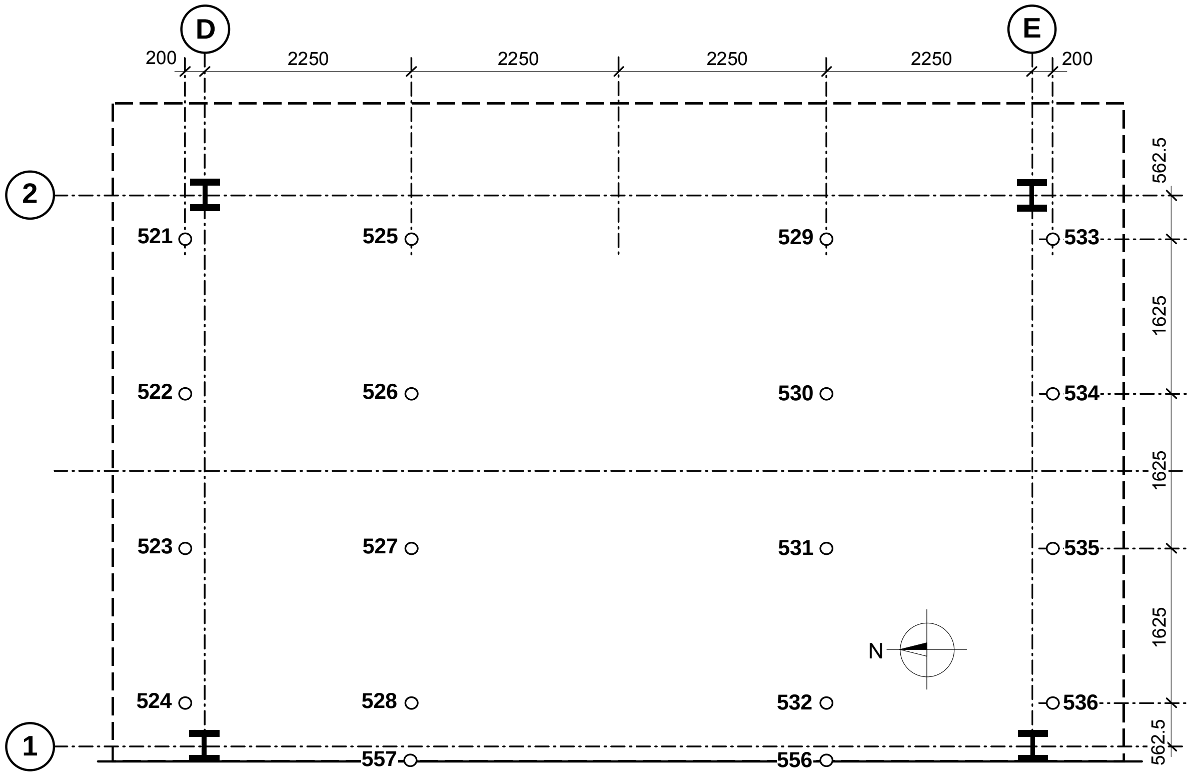

Figure D18 Location of atmosphere thermocouples in compartment 300mm below ceiling

The channel allocations contain all the information required (used together with the drawings above) to interrogate the data files. For each of the data files the data has been investigated to identify missing/erroneous data. In the final column of the channel allocation an X relates to data that is either not present or is clearly not reading from the outset of the test. A ? identifies a possible problem with the data but this may have been a problem which occurred during the test (instrument over range, cables burnt through) but does not necessarily invalidate the readings for the entire period of the test. It can clearly be seen that the vast majority of instruments are providing reliable results for the duration of the test.

Logger Channel	Card Channel	Cable Number	Drawing Ref.	Location Key	Gauge Factor	User Dummy	Comments	OK
1	1	1	fig 6,7	D1.5	1.36		Fin plate, SE side aligned with the 1st bolt row	
3	3	3	fig 6,7	D1.5	1.36		Fin plate, SE side aligned with the 3rd bolt row	
5	5	5	fig 6	D1.5	1.36		Fin plate, SE side aligned with the 4th bolt row	
~~7~~	~~7~~	~~7~~	~~fig 6~~	~~E1.5~~	~~1.36~~		~~Fin plate, NE side aligned with the 4th bolt row~~	X
9	9	9	fig 6,8	Beam D2-E2	1.36		Center of bottom flange 100 mm from D2	
11	11	11	fig 6,8	Beam D2-E2	1.36		E side of web centre 100 mm from D2	
~~13~~	~~13~~	~~13~~	~~fig 6,8~~	~~Beam D2-E2~~	~~1.36~~		~~E upper flange 100 mm from D2~~	X
15	15	15	fig 6,8	D2	1.36		W bolt of 1st bolt row	
17	17	17	fig 6,8	D3	1.36		E bolt of 2nd bolt row	
19	19	19	fig 6,8	D4	1.36		W bolt of 4th bolt row	

Table D/CA1 Gauges

Logger Channel	Card Channel	Drawing Ref.	Gauge Resistance	Location Key	Gauge Factor	User Dummy	Comments	OK
21	1	fig 6,9		Beam D2-E2	1.36		E middle of web 100 mm from E2	
23	3	fig 15	120	Cavity C1	2.1		Slab reinforcement WE direction	
25	5	fig 15	120	Cavity C1	2.1		Slab reinforcement NS direction	
27	7	fig 15	120	Cavity C2	2.1		Slab reinforcement WE direction	
29	9	fig 15	120	Cavity C2	2.1		Slab reinforcement NS direction	
31	11	fig 15	120	Cavity C3	2.1		Slab reinforcement WE direction	
33	13	fig 15	120	Cavity C3	2.1		Slab reinforcement NS direction	
35	15	fig 15	120	Cavity C5	2.1		Slab reinforcement NS direction	
37	17	fig 15	120	Cavity C6	2.1		Slab reinforcement NS direction	
39	19	fig 15	120	Cavity C7	2.1		Slab reinforcement NS direction	

Table D/CA2 Strain Gauges

bre

Logger Channel	Card Channel	Drawing Ref.	Gauge Resistance	Location Key	Gauge Factor	User Dummy	Comments	OK
41	1	fig 14	120	DE2 slab	2.1		NS direction S of axis, 60 mm gauge	
43	3	fig 14	120	DE2 slab	2.1		WE direction E of axis, 60 mm gauge	
45	5	fig 14	120	DE2 slab	2.1		NS direction N of axis, 60 mm gauge	
47	7	fig 14	120	D12 slab	2.1		NS direction N of axis, 70 mm gauge	
49	9	fig 14	120	D12 slab	2.1		NS direction S of axis, 70 mm gauge	
51	11	fig 14	120	D12 slab	2.1		WE direction W of axis, 70 mm gauge	
53	13							
55	15							
57	17							
59	19							

Table D/CA3 Strain gauges

Logger Channel	Card Channel	Drawing Ref.	Gauge Resistance	Location Key	Gauge Factor	User Dummy	Comments	OK
61	1	fig 14	120	E12 slab	2.1		NS direction N of axis, 70 mm gauge	
63	3	fig 14	120	E12 slab	2.1		NS direction S of axis, 70 mm gauge	?
65	5	fig 14	120	E12 slab	2.1		WE direction W of axis, 70 mm gauge	
67	7	fig 14	120	DE1.5 slab	2.1		WE direction W of axis, 70 mm gauge	X
69	9	fig 14	120	DE1.5 slab	2.1		NS direction S of axis, 70 mm gauge	
71	11	fig 14	120	DE1 slab	2.1		WE direction E of axis, 70 mm gauge	
73	13	fig 14	120	DE1 slab	2.1		NS direction S of axis, 70 mm gauge	X
75	15							
77	17							
79	19							

Table D/CA4 Strain gauges

Logger Channel	Card Channel	Drawing Ref.	Gauge Resistance	Location Key	Gauge Factor	User Dummy	Comments	OK
81	1	fig 11	120	D1	2.1		Unprotected column on 4th floor, SE flange 500 mm above the floor	
83	3	fig 11	120	D1	2.1		Unprotected column on 4th floor, NE flange 500 mm above the floor	
85	5	fig 11	120	D1	2.1		Unprotected column on 4th floor, SW flange 500 mm above the floor	
87	7	fig 11	120	D1	2.1		Unprotected column on 4th floor, NW flange 500 mm above the floor	
89	9	fig 11	120	E1	2.1		Unprotected column on 4th floor, SE flange 500 mm above the floor	
91	11	fig 11	120	E1	2.1		Unprotected column on 4th floor,NE flange 500 mm above the floor	
93	13	fig 11	120	E1	2.1		Unprotected column on 4th floor, SW flange 500 mm above the floor	
95	15	fig 11	120	E1	2.1		Unprotected column on 4th floor, NW flange 500 mm above the floor	
97	17	fig 11	120	D1	2.1		Unprotected column on 4th floor, SE flange 500 mm below the beam	
99	19	fig 11	120	D1	2.1		Unprotected column on 4th floor, NE flange 500 mm below the beam	

Table D/CA5 Strain gauges

Logger Channel	Card Channel	Drawing Ref.	Gauge Resistance	Location Key	Gauge Factor	User Dummy	Comments	OK
101	1	fig 11	120	D1	2.1		Unprotected column on 4th floor, SW flange 500 mm below the beam	
103	3	fig 11	120	D1	2.1		Unprotected column on 4th floor, NW flange 500 mm below the bean	
105	5	fig 11	120	E1	2.1		Unprotected column on 4th floor, SE flange 500 mm below the beam	
107	7	fig 11	120	E1	2.1		Unprotected column on 4th floor, NE flange 500 mm below the beam	
109	9	fig 11	120	E1	2.1		Unprotected column on 4th floor, SW flange 500 mm below the beam	
111	11	fig 11	120	E1	2.1		Unprotected column on 4th floor, NW flange 500 mm below the bean	
113	13	fig 11	120	D1	2.1		Protected column SW flange 500 mm below the beam	
115	15	fig 11	120	D1	2.1		Protected column NW flange 500 mm below the beam	
117	17	fig 11	120	D1	2.1		Protected column SE flange 500 mm below the beam	
119	19	fig 11	120	D1	2.1		Protected column NE flange 500 mm below the beam	

Table D/CA6 Strain gauges

Logger Channel	Card Channel	Drawing Ref.	Gauge Resistance	Location Key	Gauge Factor	User Dummy	Comments	OK
121	1	fig 11	120	D1	2.1		Protected column SE flange 500 mm above the floor	
123	3	fig 11	120	D1	2.1		Protected column NE flange 500 mm above the floor	
125	5	fig 11	120	D1	2.1		Protected column SW flange 500 mm above the floor	
127	7	fig 11	120	D1	2.1		Protected column NW flange 500 mm above the floor	
129	9							
131	11							
133	13							
135	15							
137	17							
139	19							

Table D/CA7 Strain gauges

bre

Logger Channel	Card Channel	Drawing Ref.	Instrument Type	Location Key	Convers Factor	Offset	Comments	OK
201	1	Fig 16	ASM 10	Gridline 1	100	64.55	1/4 span D-E	
202	2	Fig 16	ASM 27	Gridline 1	100	52.357	Midspan D-E	
203	3	Fig 16	ASM 33	Gridline 1	100	56.189	3/4 span D-E	
204	4	Fig 16	ASM 35	Line 1/4 span D1-D2	100	73.777	Gridline D	?
205	5	Fig 16	ASM 37	Line 1/4 span D1-D2	100	87.427	1/4 span D-E	
206	6	Fig 16	ASM 47	Line 1/4 span D1-D2	100	66.514	Midspan D-E	
207	7	Fig 16	ASM 52	Line 1/4 span D1-D2	100	28.073	3/4 span D-E	
208	8	Fig 16	ASM 55	Line 1/4 span D1-D2	100	34.994	Gridline E	
209	9	Fig 16	ASM 59	Gridline 1.5	100	73.659	Gridline D	
210	10	Fig 16	ASM 60	Gridline 1.5	100	63.065	1/4 span D-E	
211	11	Fig 16	ASM 63	Gridline 1.5	100	75.368	Midspan D-E	
212	12	Fig 16	ASM 66	Gridline 1.5	100	55.632	3/4 span D-E	
213	13	Fig 16	ASM 67	Gridline 1.5	100	70.886	Gridline E	
214	14	Fig 16	ASM 68	Line 3/4 span D1-D2	100	4.6606	Gridline D	
215	15	Fig 16	ASM 69	Line 3/4 span D1-D2	100	69.48	1/4 span D-E	
216	16	Fig 16	ASM 71	Line 3/4 span D1-D2	100	34.102	Midspan D-E	
217	17	Fig 16	ASM 73	Line 3/4 span D1-D2	100	78.496	3/4 span D-E	
218	18	Fig 16	ASM 74	Line 3/4 span D1-D2	100	43.284	Gridline E	
219	19	Fig 16	ASM 75	Gridline 2	100	53.536	1/4 span D-E	
220	20	Fig 16	ASM 77	Gridline 2	100	25.554	Midspan D-E	

Table D/CA8 Displacements

bre

Logger Channel	Card Channel	Drawing Ref,	Instrument Type	Location Key	Convers Factor	Offset	Comments	OK
221	1	fig 16	ASM 78	Gridline 2	100	65.145	1/4 span D-E	
222	2	fig 16	ASM 79	Gridline C	100	25.315	Midspan	
223	3	fig 16	ASM 83	S comprt. wall	100	18.533	Midspan	
224	4	fig 16	ASM 84	W comprt. wall	100	74.957	Midspan	
225	5	fig 16	ASM 87	N comprt. wall	100	23.444	Midspan	
226	6							
227	7							
228	8							
229	9							
230	10							
231	11							
232	12							
233	13							
234	14							
235	15							
236	16							
237	17							
238	18							
239	19							
240	20							

Table D/CA9 Displacements

Logger Channel	Card Channel	Drawing Ref.	Instrument Type	Location Key	Convers Factor	Offset	Comments	OK
~~241~~	~~1~~		~~SAKI,1~~					
242	2	fig 17	SAKI,2	Gridline DE	10	-48.989	Midspan D2-E2	
243	3	fig 17	SAKI,3	D1	10	-63.46	S column web	
~~244~~	4		~~SAKI,4~~					
245	5	fig 17	SAKI,5	E2	10	-52.585	W column flange	
246	6	fig 17	SAKI,6	D2	10	-39.93	S column web	
247	7	fig 17	SAKI,7	Gridline 1.5	10	-43.301	Gridline D	
248	8	fig 17	SAKI,8	E1	10	-32.078	E column flange	
249	9	fig 17	SAKI,9	E2	10	-60.013	N column web	
~~250~~	~~10~~		~~SAKI,10~~					
251	11	fig 17	SAKI,11	D2	10	-56.365	W column flange	
252	12	fig 17	SAKI,12	D1	10	-31.69	E column flange	
253	13	fig 17	SAKI,13	E1	10	-42.815	N column web	
254	14	fig 17	SAKI,14	Gridline 1.5	10	-45.837	Gridline E	
~~255~~	~~15~~		~~SAKI,15~~					
256	16	fig 17	SAKI,16	Gridline DE	10	-39.07	Midspan D1-E1	
257	17							
258	18							
259	19							
260	20							

Table D/CA10 Displacements

Logger Channel	Card Channel	Drawing Ref.	TC Type	Location Key	Comments	OK
401	1	fig 12	K,1	D1,BREdwg1	Protected Column 3/4 height SW flange	
402	2	fig 12	K,2	D1,BREdwg1	Protected Column 3/4 height SE flange	
403	3	fig 12	K,3	D1,BREdwg1	Protected Column 1/2 height SW flange	
404	4	fig 12	K,4	D1,BREdwg1	Protected Column 1/2 height S Web	
405	5	fig 12	K,5	D1,BREdwg1	Protected Column 1/2 height SE flange	
406	6	fig 12	K,6	D1,BREdwg1	Protected Column 1/4 height SW flange	
407	7	fig 12	K,7	D1,BREdwg1	Protected Column 1/4 height SE flange	
408	8	fig 12	K,8	D2,BREdwg1	Protected Column 3/4 height SW flange	
409	9	fig 12	K,9	D2,BREdwg1	Protected Column 3/4 height SE flange	
410	10	fig 12	K,10	D2,BREdwg1	Protected Column 1/2 height NW flange	
411	11	fig 12	K,11	D2,BREdwg1	Protected Column 1/2 height N Web	
412	12	fig 12	K,12	D2,BREdwg1	Protected Column 1/2 height SE flange	
413	13	fig 12	K,13	D2,BREdwg1	Protected Column 1/4 height NW flange	
414	14	fig 12	K,14	D2,BREdwg1	Protected Column 1/4 height SE flange	
415	15	fig 12	K,29	Beam D1-D2	Bottom of N flange 200 mm from D2	
416	16	fig 12	K,30	Beam D1-D2	Bottom of N flange 100 mm from D2	X
417	17	fig 12	K,31	Beam D1-D2	Bottom of N flange 50 mm from D2	
418	18	fig 12	K,32	D2,BREdwg1	NW flange 200 mm below Beam D!-D2	
419	19	fig 12	K,33	D2,BREdwg1	NW flange 200 mm below Beam D!-D2	
420	20	fig 12	K,34	D2,BREdwg1	NW flange 200 mm below Beam D!-D2	

Table D/CA11 Thermocouples

bre

Logger Channel	Card Channel	Drawing Ref.	TC Type	Location Key	Comments	OK
421	1	fig 12	K,15	E1,BREdwg1	Protected Column 3/4 height NW flange	
422	2	fig 12	K,16	E1,BREdwg1	Protected Column 3/4 height NE flange	
423	3	fig 12	K,17	E1,BREdwg1	Protected Column 1/2 height NW flange	
424	4	fig 12	K,18	E1,BREdwg1	Protected Column 1/2 height N Web	
425	5	fig 12	K,19	E1,BREdwg1	Protected Column 1/2 height NE flange	
426	6	fig 12	K,20	E1,BREdwg1	Protected Column 1/4 height NW flange	
427	7	fig 12	K,21	E1,BREdwg1	Protected Column 1/4 height NE flange	
428	8	fig 12	K,22	E2,BREdwg1	Protected Column 3/4 height SW flange	
429	9	fig 12	K,23	E2,BREdwg1	Protected Column 3/4 height NE flange	
430	10	fig 12	K,24	E2,BREdwg1	Protected Column 1/2 height SW flange	
431	11	fig 12	K,25	E2,BREdwg1	Protected Column 1/2 height S Web	
432	12	fig 12	K,26	E2,BREdwg1	Protected Column 1/2 height NE flange	
433	13	fig 12	K,27	E2,BREdwg1	Protected Column 1/4 height SW flange	
434	14	fig 12	K,28	E2,BREdwg1	Protected Column 1/4 height NE flange	
435	15	fig 12	K,35	Beam E1-E2	Bottom of S flange 200 mm from D2	X
436	16	fig 12	K,36	Beam E1-E2	Bottom of S flange 100 mm from D2	
437	17	fig 12	K,37	Beam E1-E2	Bottom of S flange 50 mm from D2	
438	18	fig 12	K,38	E2,BREdwg1	SW flange 200 mm below Beam D1-D2	
439	19	fig 12	K,39	E2,BREdwg1	SW flange 200 mm below Beam D1-D2	
440	20	fig 12	K,40	E2,BREdwg1	SW flange 200 mm below Beam D1-D2	

Table D/CA12 Thermocouples

Logger Channel	Card Channel	Drwawing Ref.	TC Type	Location Key	Comments	OK
441	1	fig 6	K,41	D1.5	1st bolt	
442	2	fig 6	K,42	D1.5	3rd bolt	
443	3	fig 6	K,43	D1.5	4th bolt	
444	4	fig 6	K,44	D1.5	SW Fin Plate aligned with the 1st bolt row	
445	5	fig 6	K,45	D1.5	SW Fin Plate aligned with the 3rd bolt row	X
446	6	fig 6	K,46	D1.5	SW Fin Plate aligned with the 4th bolt row	
447	7	fig 6	K,47	Beam DE1.5	Bottom of W top flange 120 mm from D1.5	
448	8	fig 6,7	K,48	Beam DE1.5	Middle of W web 120 mm from D1.5	
449	9	fig 6,7	K,49	Beam DE1.5	Bottom of W flange 120 mm from D1.5	
450	10	fig 6,7	K,50	E1.5	NW Fin Plate aligned with the 1st bolt row	
451	11	fig 6,7	K,51	E1.5	NW Fin Plate aligned with the 3rd bolt row	
452	12	fig 6,7	K,52	E1.5	NW Fin Plate aligned with the 4th bolt row	
453	13	fig 6,7	K,53	Beam DE1.5	Bottom of W flange 120 mm from E1.5	
454	14	fig 6,8	K,54	D2	W 1st bolt, S minor axis connection	
455	15	fig 6,8	K,55	D2	E 2nd bolt, S minor axis connectionn	
456	16	fig 6,8	K,56	D2	W 4th bolt, S minor axis connection	
457	17	fig 6,8	K,57	D2	SW End plate aligned with 1st bolt, minor axis	
458	18	fig 6,8	K,58	D2	SW End plate aligned with 3rd bolt, minor axis	
459	19	fig 6,8	K,59	D2	SW End plate aligned with 4th bolt, minor axis	
460	20	fig 6,8	K,60	Beam D2-E2	Top flange W bottom surface 50mm from D2	

Table D/CA13 Thermocouples

bre

Logger Channel	Card Channel	Drawing Ref.	TC Type	Location Key	Comments	OK
461	1	fig 6,8	K,61	Beam D2-E2	W web, middle heigth 50 mm from D2	
462	2	fig 6,8	K,62	Beam D2-E2	Bottom flange W upper surf. 50 mm from D2	
463	3	fig 6,8	K,63	Beam D1-D2	Top flange S bottom surface 50mm from D2	
464	4	fig 6,8	K,64	Beam D1-D2	S web, middle heigth 50 mm from D2	
~~465~~	~~5~~	~~fig 6,8~~	~~K,65~~	~~Beam D1-D2~~	~~Bottom flange S upper surf. 50 mm from D2~~	X
466	6	fig 6,8	K,66	D2	S 1st bolt, W major axis connection	
467	7	fig 6,8	K,67	D2	S 3rd bolt, W major axis connection	
468	8	fig 6,8	K,68	D2	S 4th bolt, W major axis connection	
469	9	fig 6,8	K,69	D2	WS End plate aligned with 1st bolt, major axis	
470	10	fig 6,8	K,70	D2	WS End plate aligned with 3rd bolt, major axis	
471	11	fig 6,8	K,71	D2	WS End plate aligned with 4th bolt, major axis	
472	12	fig 6,9	K,72	E2	NW End plate aligned with 1st bolt, minor axis	
473	13	fig 6,9	K,73	E2	NW End plate aligned with 3rd bolt, minor axis	
474	14	fig 6,9	K,74	E2	NW End plate aligned with 4th bolt, minor axis	
475	15	fig 6,9	K,75	Beam D2-E2	Bottom flange W upper surf. 50 mm from E2	
~~476~~	~~16~~	~~fig 6,9~~	~~K,76~~	~~Beam D1-D2~~	~~Bottom flange N upper surf. 50 mm from E2~~	X
477	17	fig 6,9	K,77	E2	WN End plate aligned with 1st bolt, major axis	
478	18	fig 6,9	K,78	E2	WN End plate aligned with 3rd bolt, major axis	
479	19	fig 6,9	K,79	E2	WN End plate aligned with 4th bolt, major axis	
480	20	fig 6,10	K,80	Beam D1-E1	Mid-span, E top flange	

Table D/CA14 Thermocouples

bre

Logger Channel	Card Channel	Drawing Ref.	TC Type	Location Key	Comments	OK
481	1	fig 6,10	K,81	Beam D1-E1	Mid-span, middle of the E web	
482	2	fig 6,10	K,82	Beam D1-E1	Mid-span, E bottom flange	
483	3	fig 6,10	K,83	Beam DE1.5	Mid-span, E top flange	
484	4	fig 6,10	K,84	Beam DE1.5	Mid-span, middle of the E web	
485	5	fig 6,10	K,85	Beam DE1.5	Mid-span, E bottom flange	
486	6	fig 6,10	K,86	Beam D2-E2	Mid-span, W top flange	
487	7	fig 6,10	K,87	Beam D2-E2	Mid-span, middle of the W web	
488	8	fig 6,10	K,88	Beam D2-E2	Mid-span, W bottom flange	
489	9	fig 9	K,89	Cavity C1	Next to rib, slab surface	
490	10	fig 9	K,90	Cavity C1	Next to rib 35 mm below the top surface	X
491	11	fig 9	K,91	Cavity C1	Reinforcement next to rib	?
492	12	fig 9	K,92	Cavity C1	Next to rib, steel decking	?
493	13	fig 9	K,93	Cavity C1	Rib, slab surface	
494	14	fig 9	K,94	Cavity C1	Reinforcement in the rib	?
495	15	fig 9	K,95	Cavity C1	Rib 100 mm below the top surface	
496	16	fig 9	K,96	Cavity C1	Rib, steel decking	X
497	17	fig 9	K,97	Cavity C3	Next to rib, slab surface	
498	18	fig 9	K,98	Cavity C3	Next to rib 35 mm below the top surface	
499	19	fig 9	K,99	Cavity C3	Reinforcement next to rib	
500	20	fig 9	K,100	Cavity C3	Next to rib, steel decking	?

Table D/CA15 Thermocouples

Logger Channel	Card Channel	Drawing Ref.	TC Type	Location Key	Comments	OK
501	1	fig 13	K,101	Cavity C3	Rib, slab surface	
502	2	fig 13	K,102	Cavity C3	Reinforcement in the rib	?
503	3	fig 13	K,103	Cavity C3	Rib 100 mm below the top surface	
504	4	fig 13	K,104	Cavity C3	Rib, steel decking	?
505	5	fig 13	K,105	Cavity C2	Next to rib, slab surface	
506	6	fig 13	K,106	Cavity C2	Next to rib 35 mm below the top surface	
507	7	fig 13	K,107	Cavity C2	Reinforcement next to rib	
508	8	fig 13	K,108	Cavity C2	Next to rib, steel decking	?
509	9	fig 13	K,109	Cavity C2	Rib, slab surface	
510	10	fig 13	K,110	Cavity C2	Reinforcement in the rib	
511	11	fig 13	K,111	Cavity C2	Rib 100 mm below the top surface	
512	12	fig 13	K,112	Cavity C2	Rib, steel decking	?
513	13	fig 13	K,113	Cavity C4	Next to rib, slab surface	
514	14	fig 13	K,114	Cavity C4	Next to rib 35 mm below the top surface	
515	15	fig 13	K,115	Cavity C4	Reinforcement next to rib	
516	16	fig 13	K,116	Cavity C4	Next to rib, steel decking	?
517	17	fig 13	K,117	Cavity C4	Rib, slab surface	
518	18	fig 13	K,118	Cavity C4	Reinforcement in the rib	
519	19	fig 13	K,119	Cavity C4	Rib 100 mm below the top surface	
520	20	fig 13	K,120	Cavity C4	Rib, steel decking	?

Table D/CA16 Thermocouples

Logger Channel	Card Channel	Drawing Ref.	TC Type	Location Key	Comments	OK
521	1	fig 18	K,121	gridline D	500 mm from D2	
522	2	fig 18	K,122	gridline D	2125 mm from D2	
523	3	fig 18	K,123	gridline D	2125 mm from D1	
524	4	fig 18	K,124	gridline D	500 mm from D1	
525	5	fig 18	K,125	2250 mm N from midspan	500 mm from gridline 2	
526	6	fig 18	K,126	2250 mm N from midspan	2125 mm from gridline 2	
527	7	fig 18	K,127	2250 mm N from midspan	2125 mm from gridline 1	
528	8	fig 18	K,128	2250 mm N from midspan	500 mm from gridline 1	
529	9	fig 18	K,129	2250 mm S from midspan	500 mm from gridline 2	
530	10	fig 18	K,130	2250 mm S from midspan	2125 mm from gridline 2	
531	11	fig 18	K,131	2250 mm S from midspan	2125 mm from gridline 1	
532	12	fig 18	K,132	2250 mm S from midspan	500 mm from gridline 1	
533	13	fig 18	K,133	gridline E	500 mm from E2	
534	14	fig 18	K,134	gridline E	2125 mm from E2	
535	15	fig 18	K,135	gridline E	2125 mm from E1	
536	16	fig 18	K,136	gridline E	500 mm from E1	
537	17	fig 13	K,137	Cavity C5	Reinforcement in the rib	
538	18	fig 13	K,138	Cavity C6	Reinforcement in the rib	?
539	19	fig 13	K,139	Cavity C7	Reinforcement in the rib	
540	20		K,140			

Table D/CA17 Thermocouples

Logger Channel	Card Channel	Drawing Ref.	TC Type	Location Key	Comments	OK
541	1	Red 1	K,141	Indicative 2	Thermocouple 1	
542	2	Red 2	K,142	Indicative 2	Thermocouple 2	
543	3	Red 3	K,143	Indicative 2	Thermocouple 3	
544	4	Red 4	K,144	Indicative 1	Thermocouple 1	
545	5	Red 5	K,145	Indicative 1	Thermocouple 2	
546	6	Red 6	K,146	Indicative 1	Thermocouple 3	X
547	7	Red 7	K,147	Indicative 3	Thermocouple 1	
548	8	Red 8	K,148	Indicative 3	Thermocouple 2	
549	9	Red 9	K,149	Indicative 3	Thermocouple 3	
550	10	Red 10	K,150	Indicative 4	Thermocouple 1	
551	11	Red 11	K,151	Indicative 4	Thermocouple 2	
552	12	Red 12	K,152	Indicative 4	Thermocouple 3	
553	13	Red 13	K,153	Indicative 5	Thermocouple 1	
554	14	Red 14	K,154	Indicative 5	Thermocouple 2	
555	15	Red 15	K,155	Indicative 5	Thermocouple 3	
556	16	Red 16	fig 18	Window	Close to gridline D	X
557	17	Red 17	fig 18	Window	Close to gridline E	
558	18					
559	19					
560	20					

Table D/CA18 Thermocouples

References for Appendix D

1. Newman G M, Robinson J T and Bailey C G, Fire Safe design: A New Approach to Multi-Storey Steel-Framed Buildings, SCI Publication P288, The Steel Construction Institute, Ascot, 2000
2. Moore D B and Lennon T, Fire engineering design of steel structures, Progress in Structural Engineering and Materials, Vol 1 No. 1, September 1997, pp 4-9
3. BS EN 1991-1-2:2002 Eurocode 1: Actions on structures – Part 1.2: General actions – Actions on structures exposed to fire, British Standards Institution, London

Appendix E Results from the parametric study

Comparison with full-scale test data

The full-scale fire test described in detail in the previous report produced under this contract (see Appendix D of this report) has been modelled using *Vulcan*. The intention was to predict the global structural behaviour in terms of overall deformation and compare the predicted response to the measured values from the test thereby providing additional validation for the *Vulcan* software.

The fire test was undertaken on the 4th floor of the building (fire load on the third floor) in an area measuring 11m by 7m in plan. The location of the compartment on the building is illustrated below.

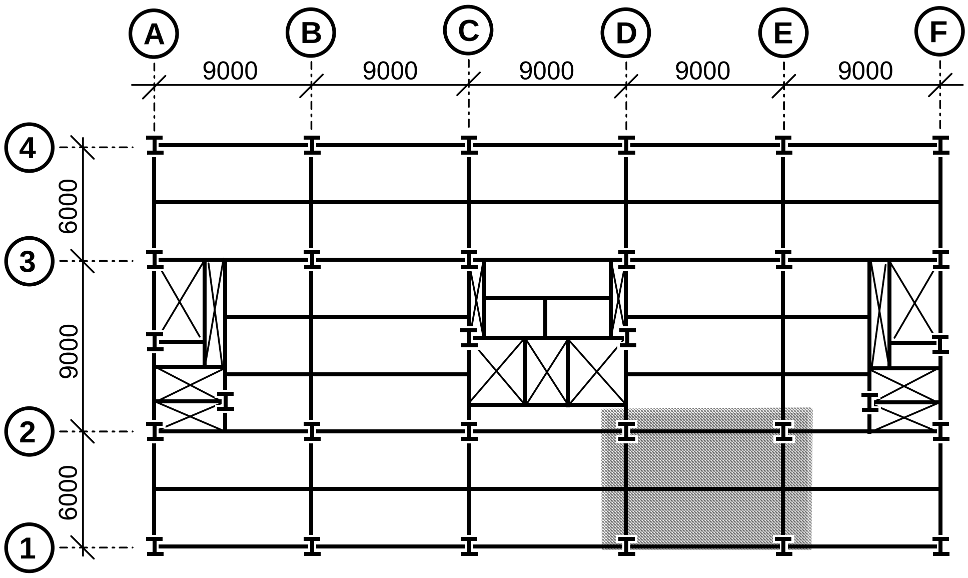

Figure E1: Location of test compartment

The analysis was carried out as a blind simulation for the structural response. Temperature data was taken from the test measurements. Those responsible for setting up the model and carrying out the analysis were not provided with the deflection measurements taken from the test.

Test Description

The fire compartment was located near to the central zone of the building and covered an area of 11m by 7m.The internal walls of the fire compartment were constructed using fire resistant board. The boards were not fixed to the composite floor at the top and allowed vertical movement from the floor above. The external edge of the compartment was left unglazed but two wind posts were left in place which provided some vertical restraint to the edge beam below (i.e. the fire effected beam was supported by the wind posts above). A uniform load of 3.19kN/m2 was simulated using sandbags. Each Sandbag weighed 1.1 ton and was applied over an area of 18 m by 10.5 m on the 4th floor. The imposed load was greater in magnitude than in previous fire tests conducted on the Cardington Frame.

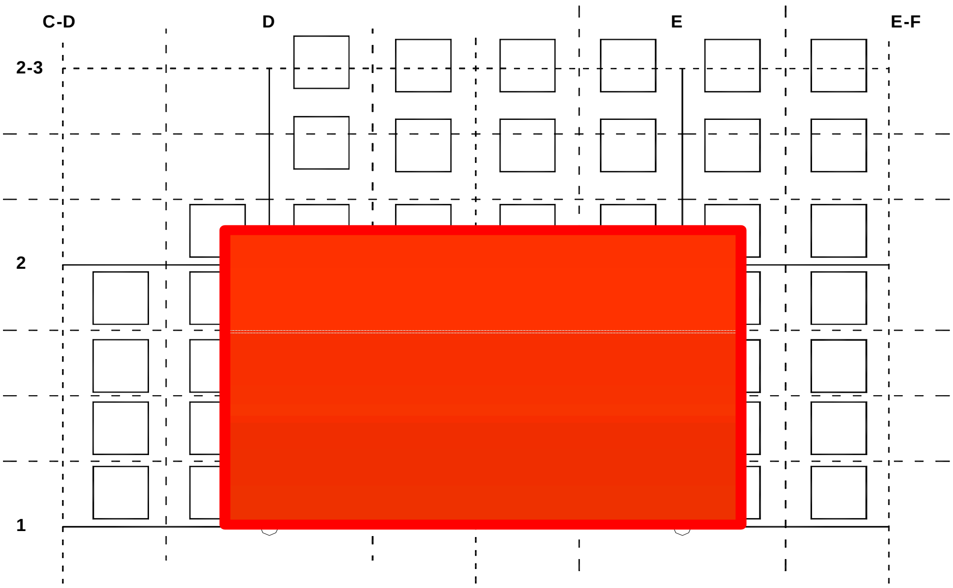

Figure E2: Positioning of sandbags

The fire load of 40 kg/m^2 was provided by wooden cribs distributed over the floor area. The compartment dimensions and material properties are contained in Table E1.

Compartment:	
Height H = 4 m Length L = 11 m Depth D = 7 m	**Floor area A_f = 77 m^2** **Total area of compartment A_t = 298 m^2**
Fire load:	
Wooden cribs 40 kg/m2	**Fire load density q_f = 720 MJ/m^2**
Openings:	
Height h_v = 1.27 m Length l_v = 9 m	**Opening factor O = 0.043**
Boundaries:	
Plasterboard b_p = 520 J/m^{2}s$^{1/2}$K LW concrete b_c = 1120 J/m^{2}s$^{1/2}$K	**Total b = 801 J/m^{2}s$^{1/2}$K**

Table E1: Compartment dimensions and material properties

bre

The primary and secondary beams within the fire compartment were left unprotected. All columns were protected. The displacements and temperatures were measured at the key locations shown in Figure E3 and Figure E4.

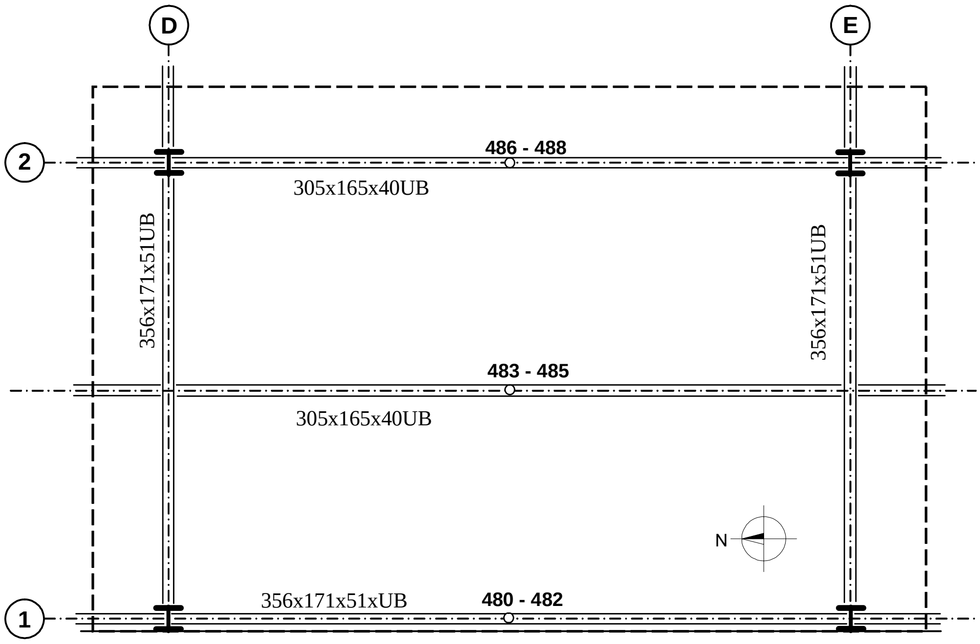

Figure E3: Arrangement of members and thermocouples

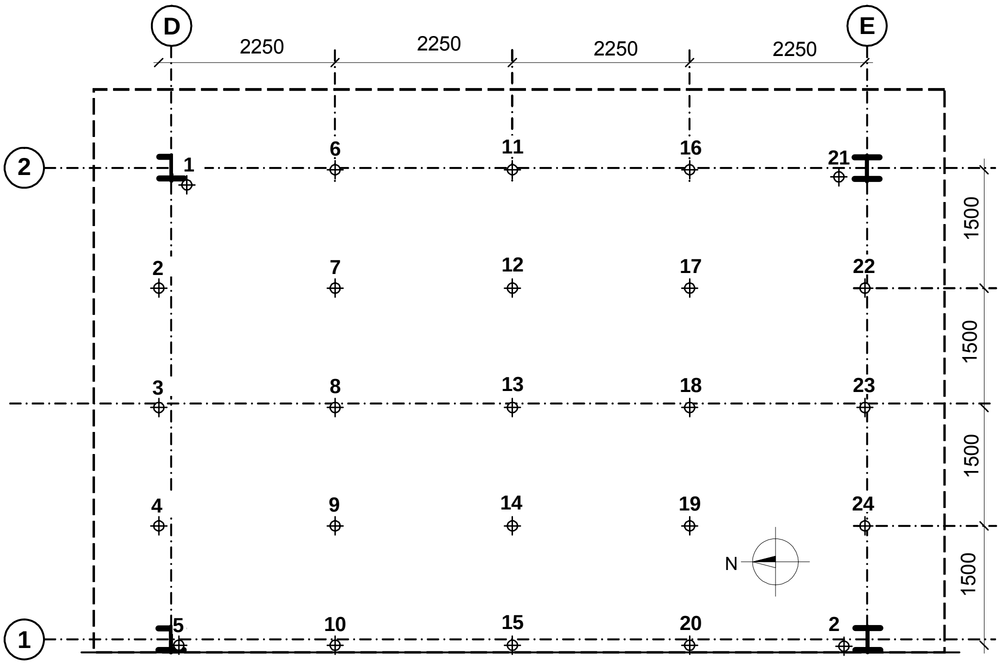

Figure E4: Position of displacement transducers

Thermal Modelling

The atmosphere temperatures measured within the fire compartment were used to carry out a 2-D thermal analysis of the composite slab. The thermal analysis was carried out using The University of Sheffield's in-house programme. The temperature distributions from the thermal model were validated against the measured temperature distributions from the experiment. Measurements of the temperatures through the slab were taken at the bottom, on the reinforcement, at the top of slab at and slab depths of 70 and 130mm. The features of the model are as follows:

- The compartment temperatures as measured in the test were used.
- The slab was assumed to have a 3% water content.
- The Eurocode 4 model for lightweight concrete was used.
- Only the top 70mm of the slab was modelled.

Figure E5 shows the results from the thermal analysis, the analysis was carried out over a period of 220 minutes and included the cooling phase. The results from the thermal analysis was compared with the measured Cardington temperatures, see Figure E6.

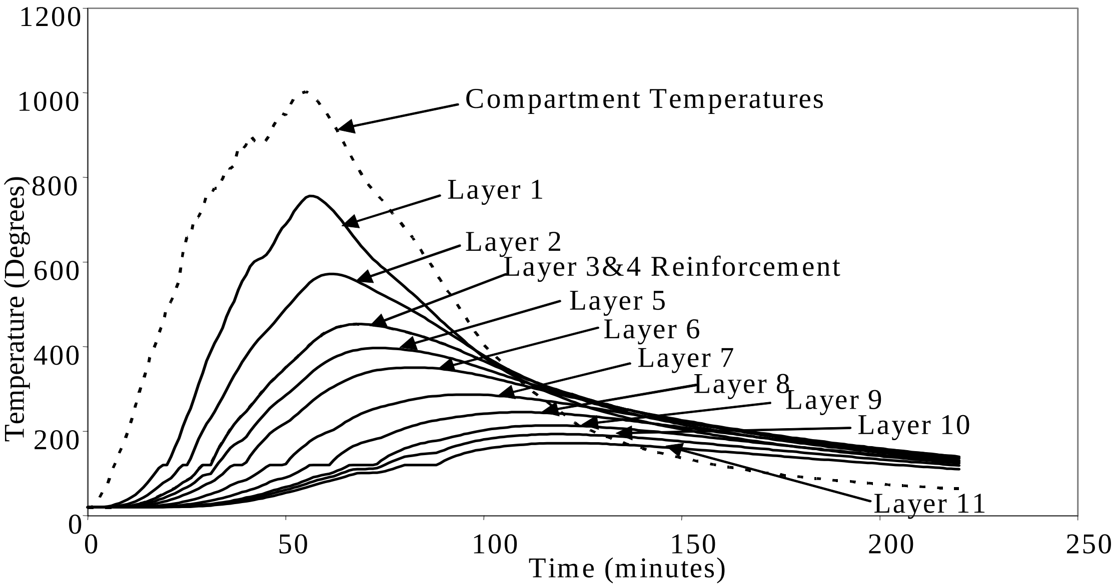

Figure E5: Calculated temperature distribution through depth of slab

The results from the thermal model compare well to the measured Cardington temperatures at 30 minutes.

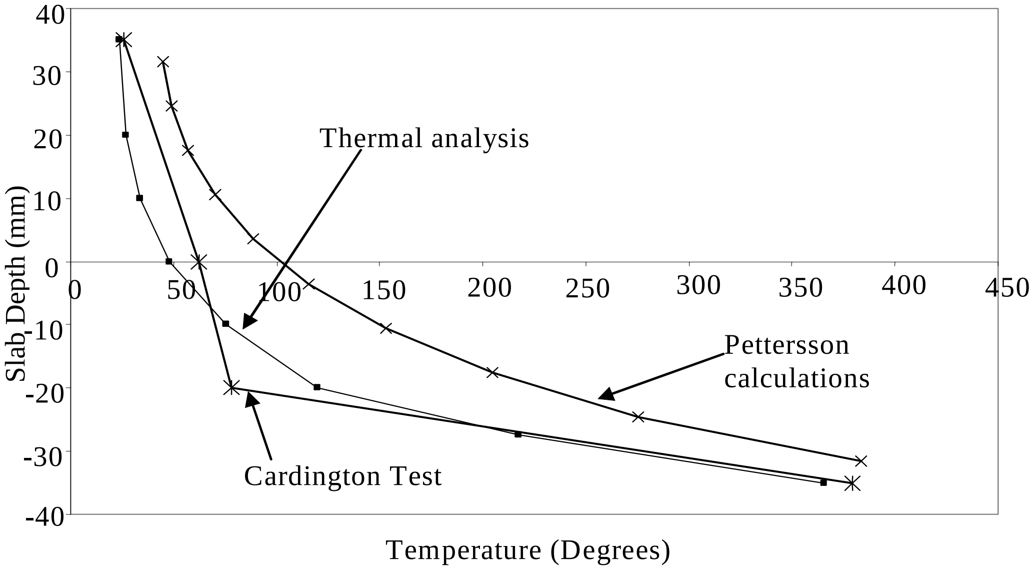

Figure E6: Comparison of calculated results with Cardington Test at 30 minutes

The measured temperatures for the columns are shown in Figure E7. Measurements were taken in the bottom flanges, in the web and in the upper flange. The maximum recorded steel temperature of 420°C occurred after 100 minutes of the fire in column D2. The recorded temperatures for the two edge columns show variation between the inner and outer flange.

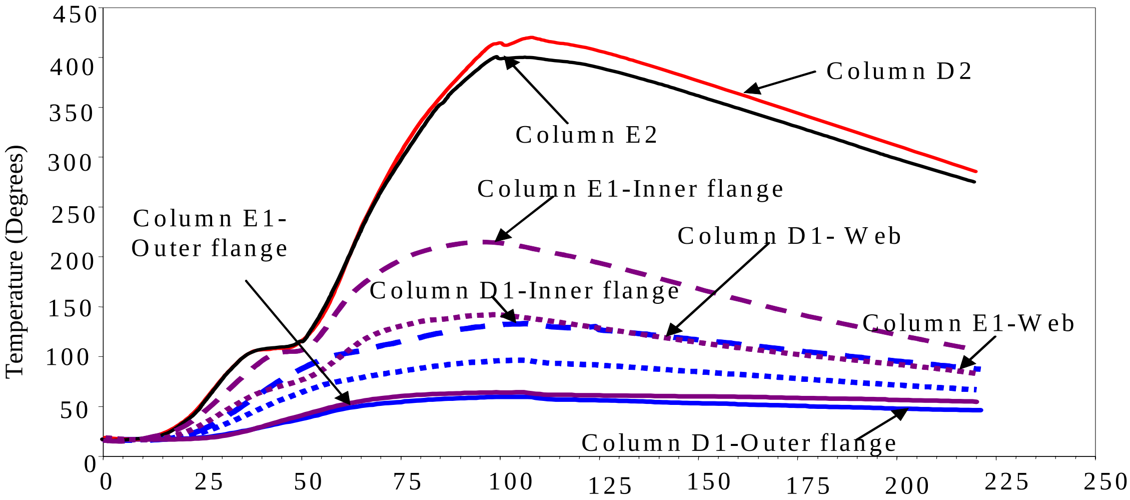

Figure E7: Measured temperature of columns in Cardington Test

Thermocouples were not placed on the 357x171x51UB beams. In this instance, temperatures were calculated using the procedure of heat transfer set out in Eurocode 3[1]. The temperature time curves of the unprotected 357x171x51UB beams are shown in Figure E8. The maximum temperature of 1000°C is attained at 75 minutes.

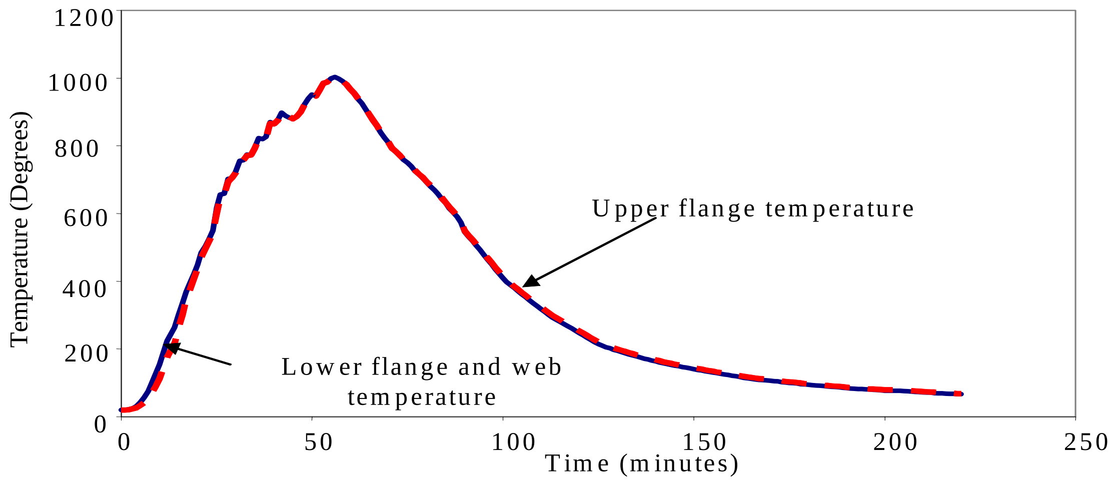

Figure E8: Temperature time curves for 357x171x51UB beams

Recorded temperatures in the mid-span beams were taken on the upper flange, web and bottom flange. The variation in the temperature distribution of the primary and edge beams is shown in Figure E9, the maximum recorded temperature of 1072°C was after 50 minutes on beam D2-E2.

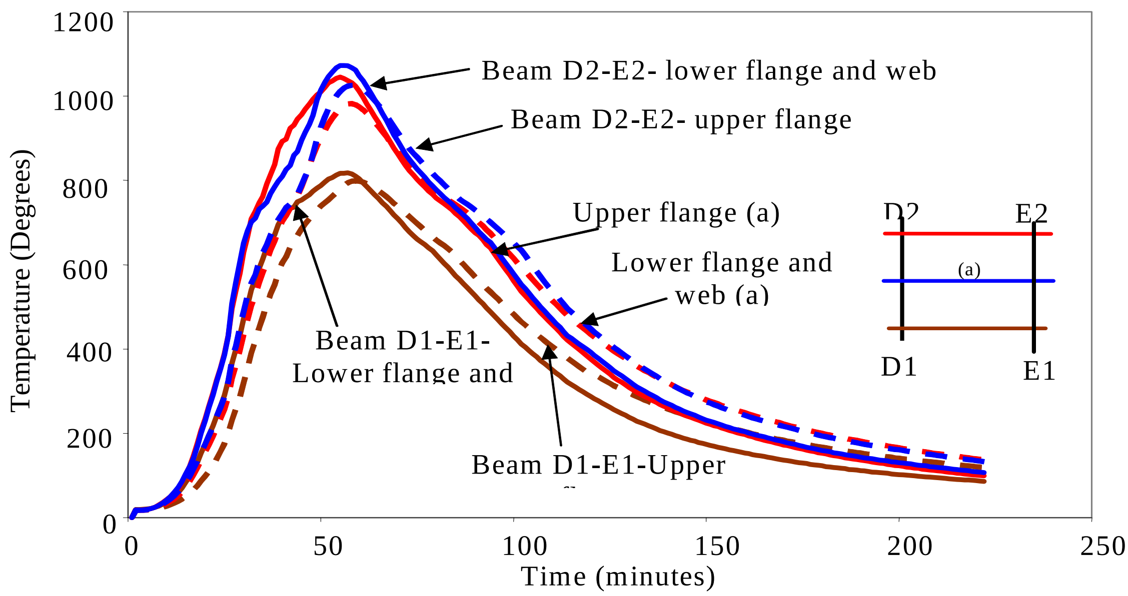

Figure E9: Measured temperature distribution for edge beam and primary beams

bre

Structural Modelling

The numerical modelling was undertaken using *Vulcan*. The extent of the model is shown in figures E10 and E11. Using the experience gained from the modelling of previous Cardington tests, the model was set up to include more of the structure than just the fire-effected zone. This reduces the impact of the assumed boundary conditions and helps to ensure that the fire-effected zone is modelled accurately. The model extended one structural bay either side of the fire compartment and included columns above and below the fire effected floor. A uniformly distributed load was applied to the floor structure to model the sandbags and vertical loads were applied to the tops of the columns to simulate the load generated by the upper floors.

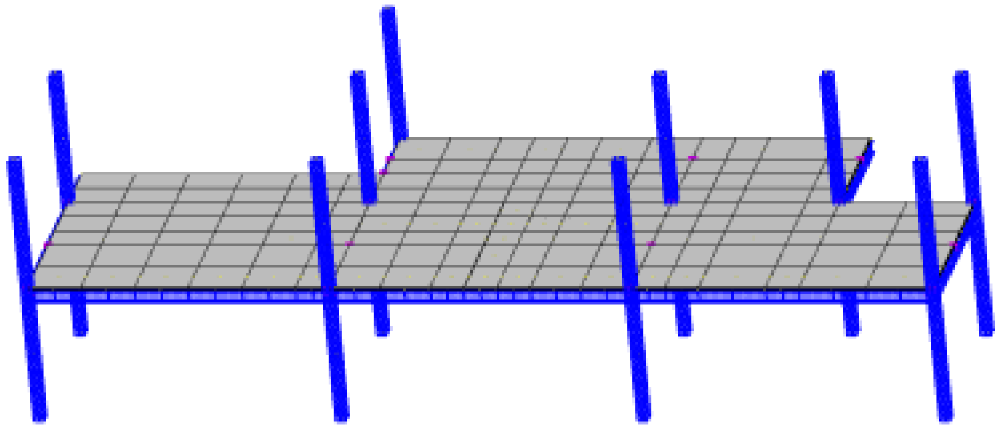

Figure E10: 3D representation of Vulcan model

The material strengths were the same as those specified for the test and the relationships contained within the Eurocodes were used for material properties such as stress-strain and thermal elongation, at elevated temperature.

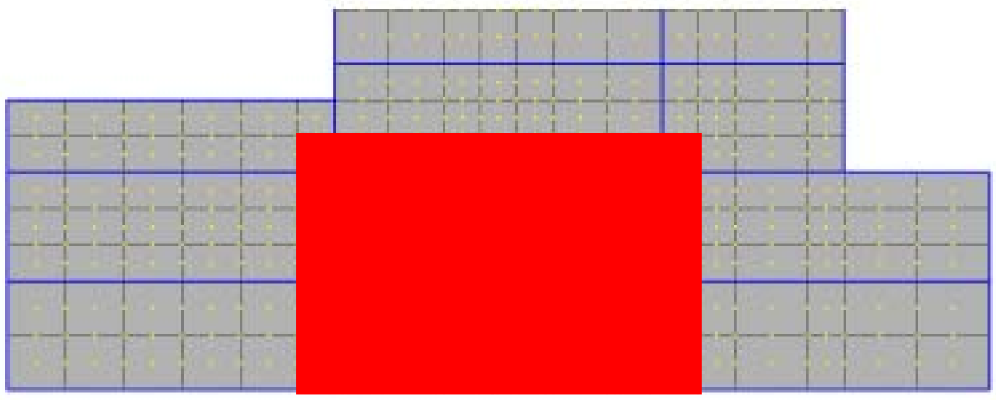

Figure E11: Plan showing extent of Vulcan model and heated zone

Results

Vulcan predicts deflections with respect to temperature and hence time. Figure E12 shows the deflected shape of the building at the end of the analysis.

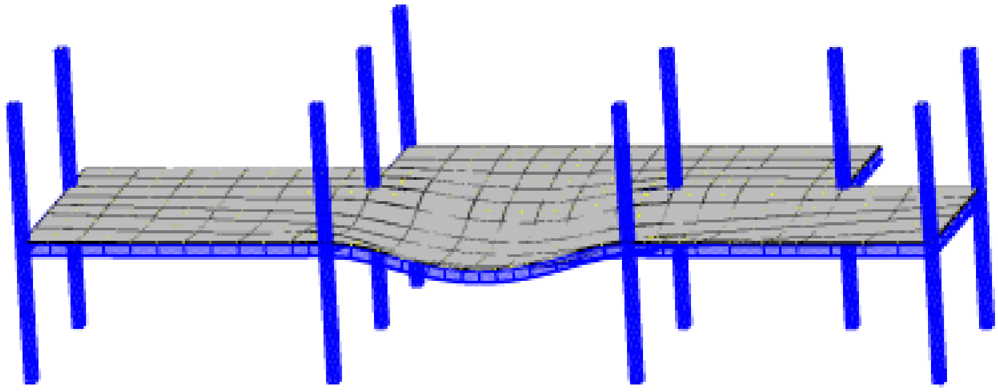

Figure E12: Deflected shape at end of analysis

In order to compare the Vulcan predictions with the test data, deflections with respect to time are plotted for locations indicated in Figures E13 and E14 and Table E2.

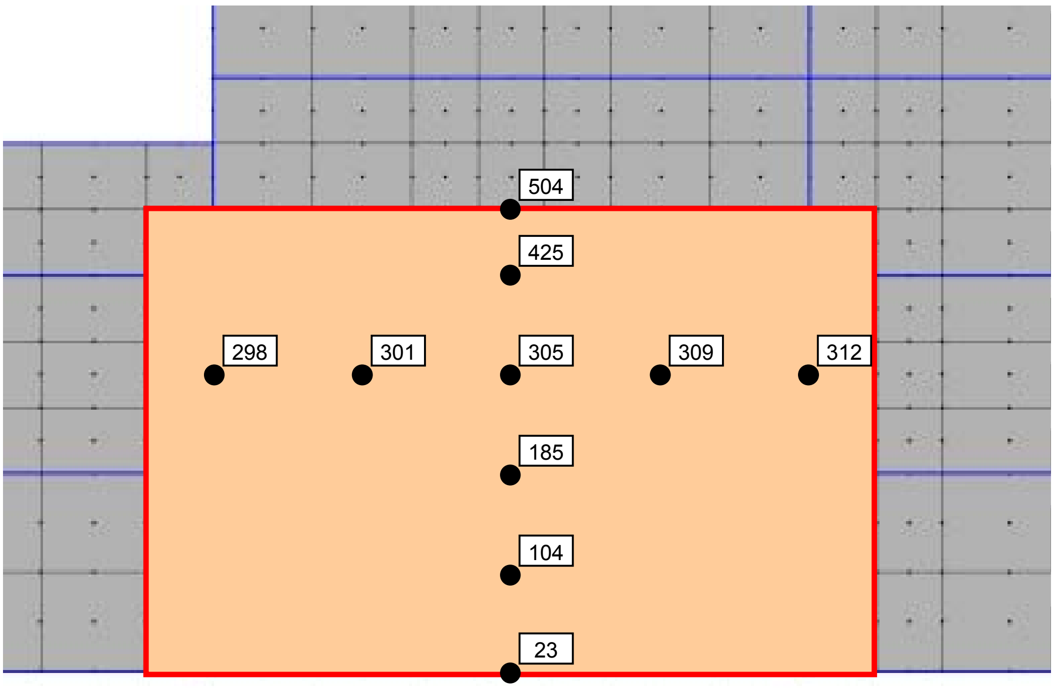

Figure E13: Location of output nodes

In the test itself, wind posts were included at the perimeter of the building. These were not modelled explicitly as it would over-complicate the model and insufficient data on their performance was available. Instead they were modelled by imposing boundary conditions on the beam nodes to which the wind posts are attached. In one set of analyses [1], the nodes were fixed in the vertical direction and in the other [2] they were fixed in the horizontal direction. Both sets of results are shown in the graphs below. As would be expected, fixing the nodes in the vertical direction gives the best representation of the test results. This is because the posts above the fire-effected floor; would remain relatively cool; and would have sufficient strength in tension to support the beams from above. However, fixing boundary conditions is an approximation and could explain why there are differences between the results of the analyses and the test measurements taken at the edge of the building. At all other locations, the agreement is excellent.

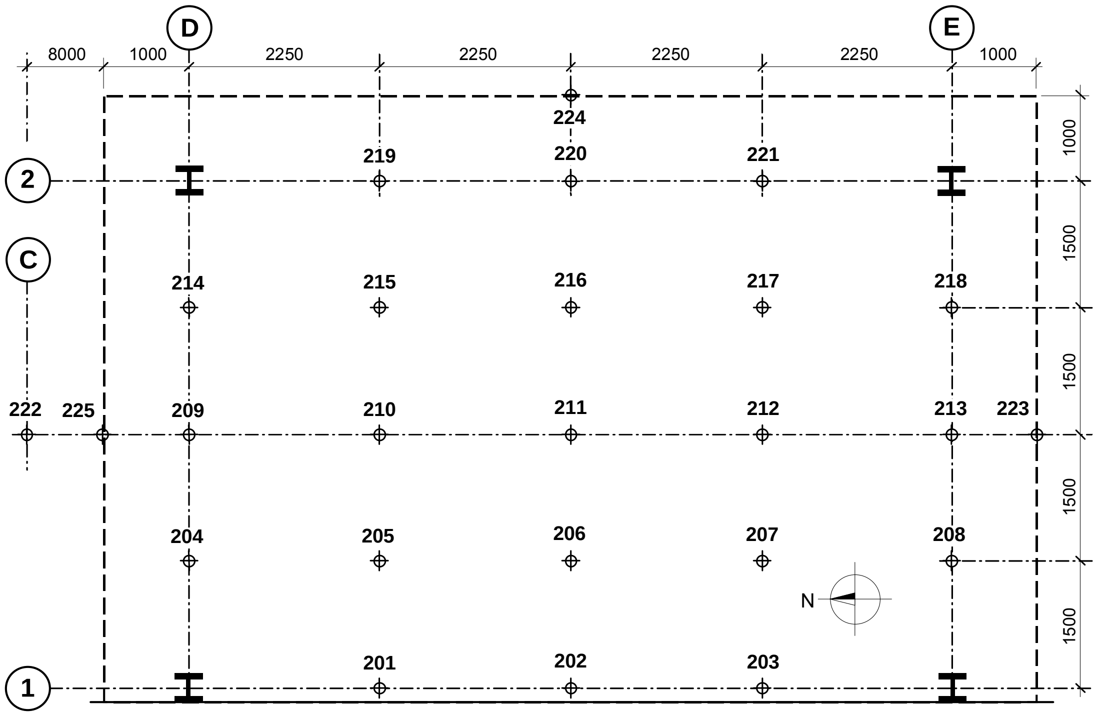

Figure E14: Location of vertical displacements

Displacement Transducers	202	206	211	214	215	216	217	218	220	224
Vulcan Nodes	23	104	185	298	301	305	309	312	425	504

Table E2 Relationship between measured displacements (Figure E14) and node points (Figure E13)

The comparisons are shown in Figures E15 to E26 for the individual node points.

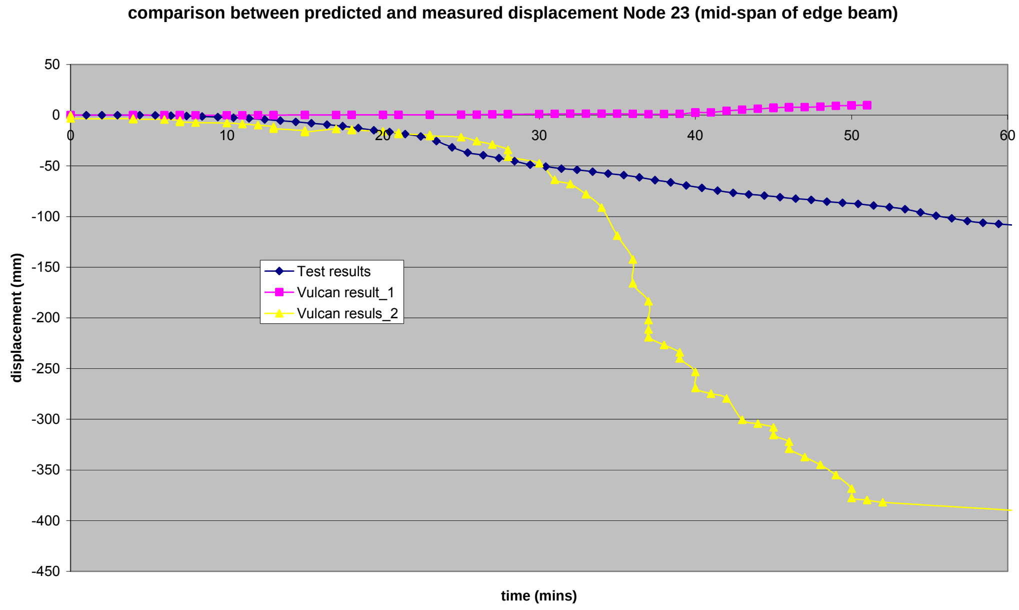

Figure E15: Comparison between predicted and measured displacement Node 23

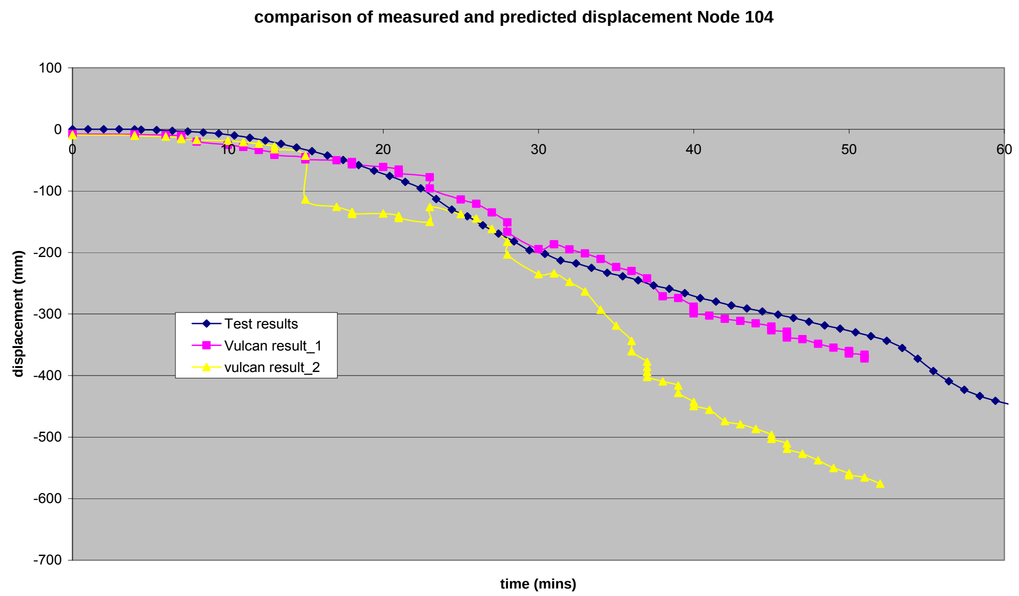

Figure E16: Comparison between predicted and measured displacement Node 104

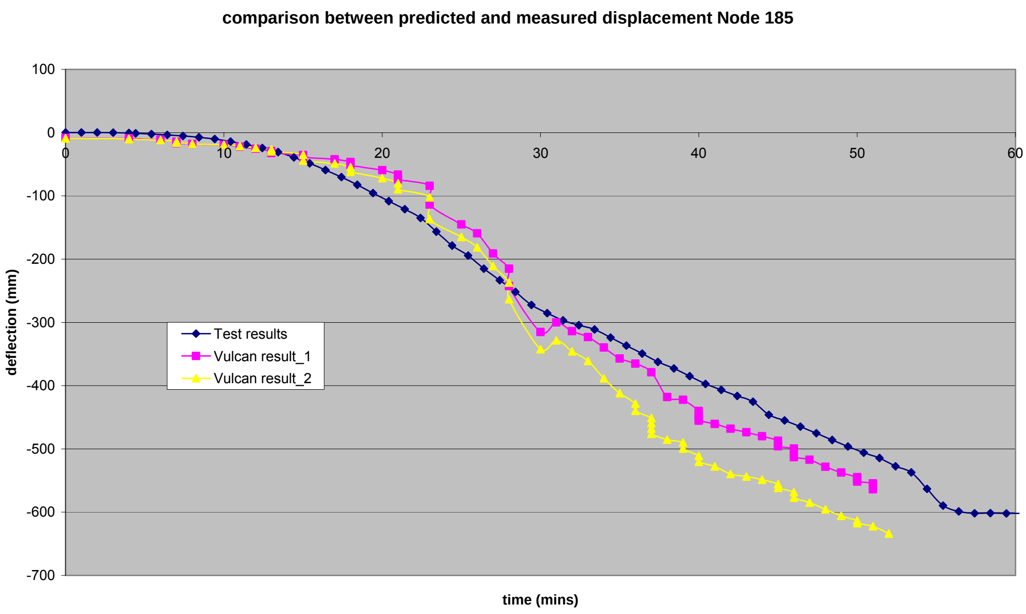

Figure E17: Comparison between predicted and measured displacement Node 185

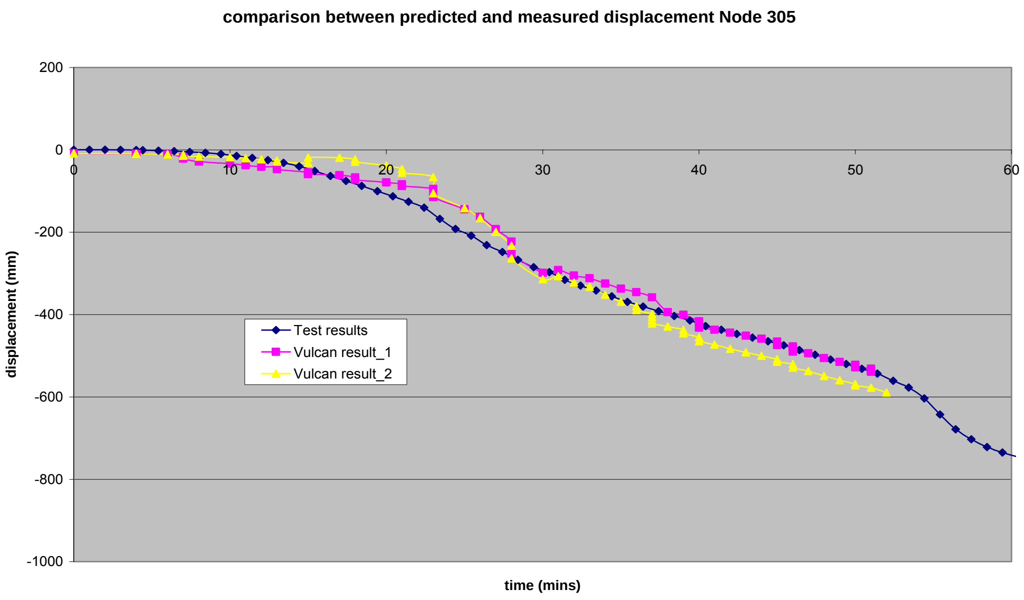

Figure E18: Comparison between predicted and measured displacement Node 305

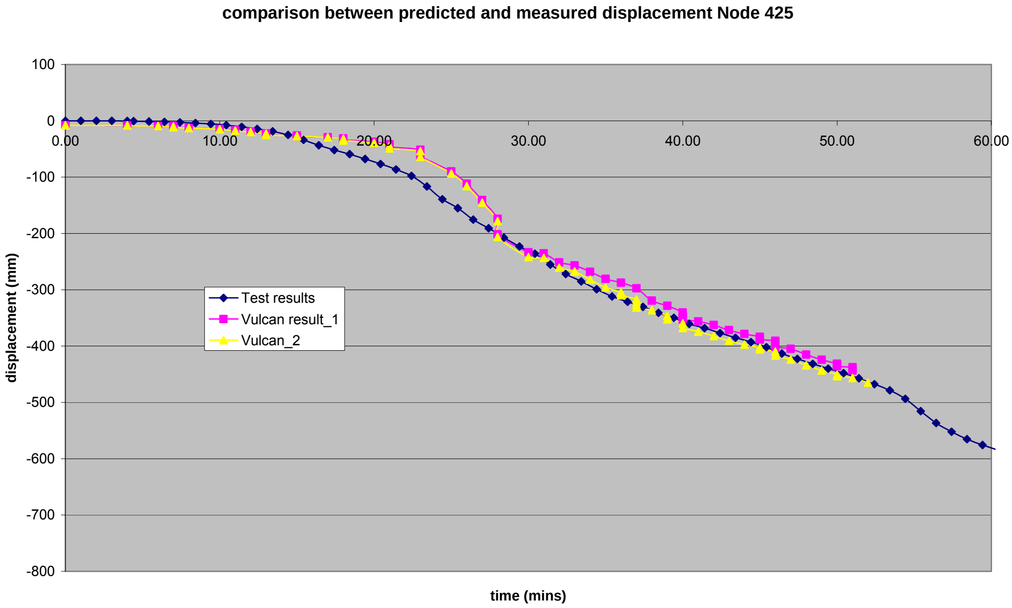

Figure E19: Comparison between predicted and measured displacement Node 425

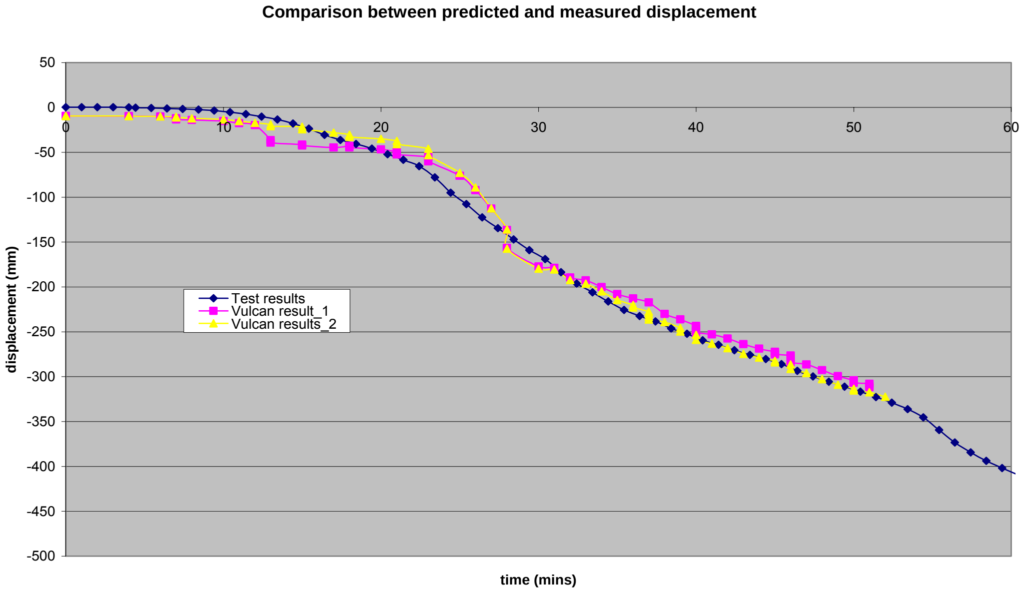

Figure E20: Comparison between predicted and measured displacement Node 504

What is clear from the above six graphs is that the accuracy of the predictions increases with distance away from the edge beam. This is clearly due to problems associated with modelling the behaviour of the wind posts in the area around the free edge. The restraint provided by the wind posts clearly lies somewhere between the two extremes of full vertical restraint and zero vertical restraint (full horizontal restraint). The influence of the assumption reduces with distance away from the edge of the building and in the areas where the location of the compartment wall may be critical (i.e. the centre of the slab) the model predicts the magnitude and nature of the displacement with great accuracy.

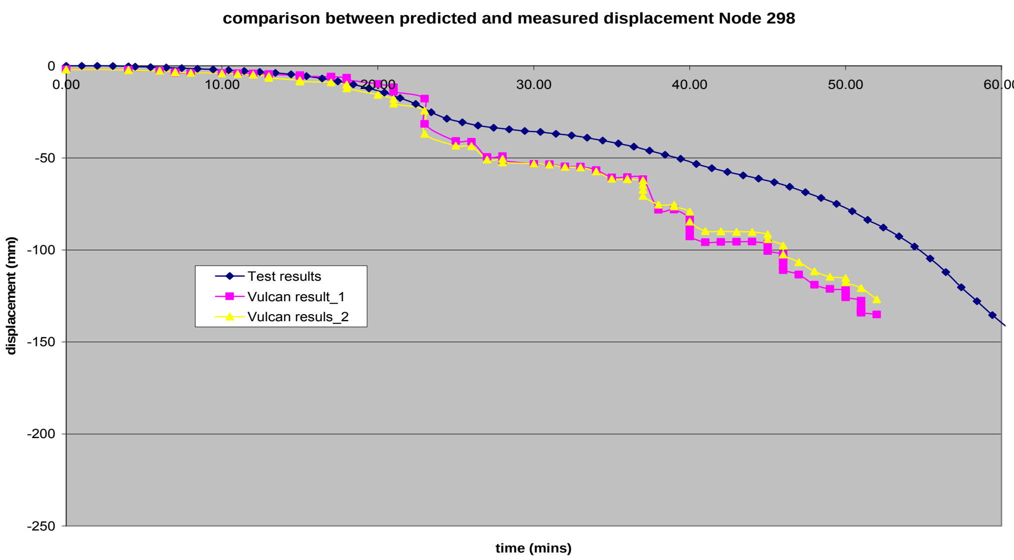

Figure E21: Comparison between predicted and measured displacement Node 298

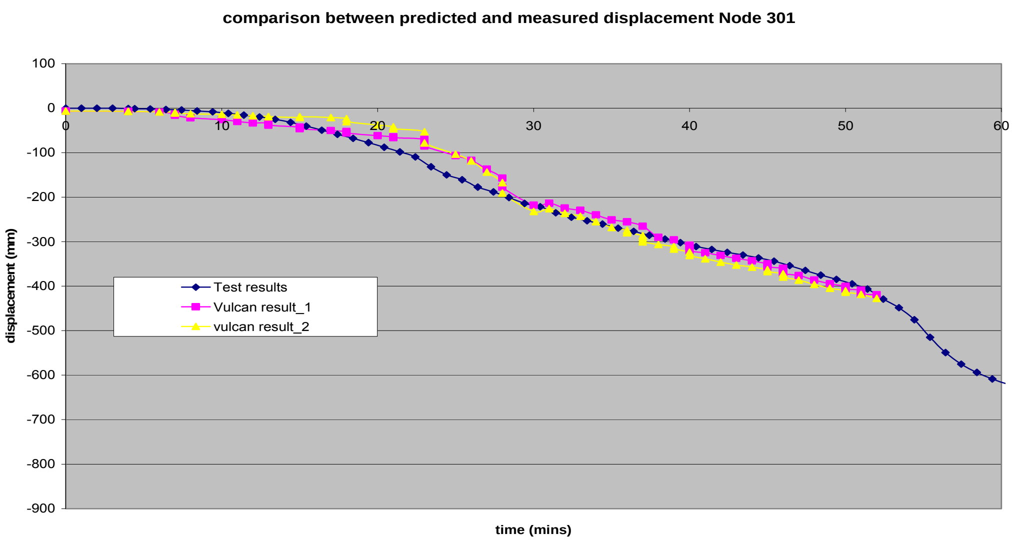

Figure E22: Comparison between predicted and measured displacement Node 301

Figure E23: Comparison between predicted and measured displacement Node 305

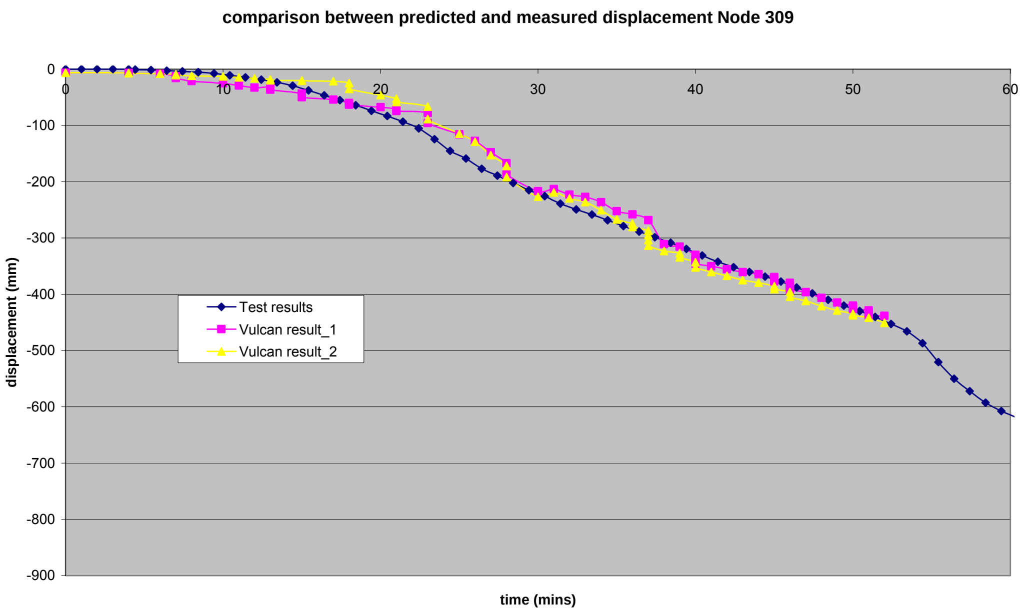

Figure E24: Comparison between predicted and measured displacement Node 309

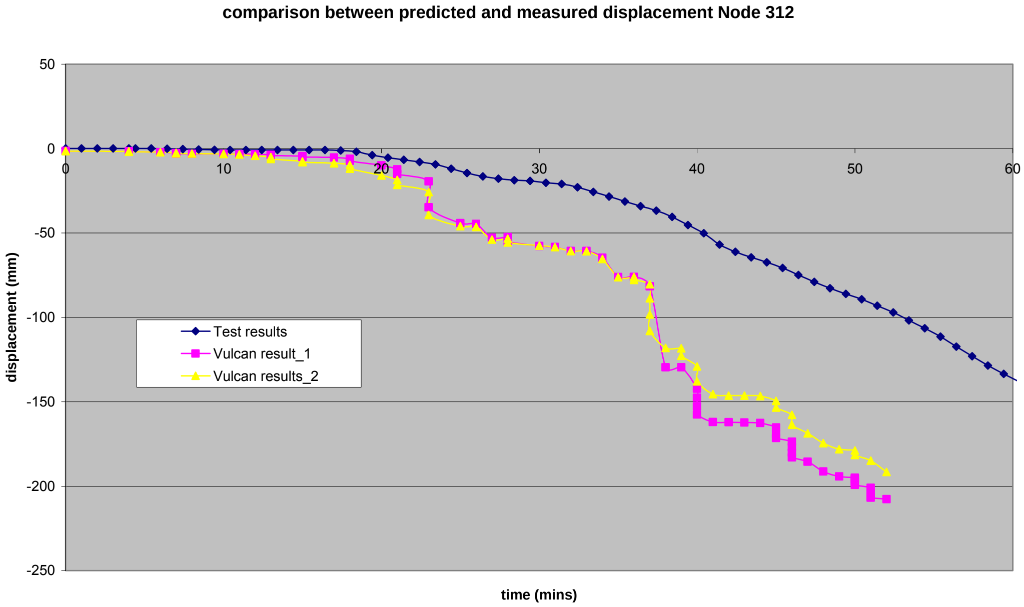

Figure E25: Comparison between predicted and measured displacement Node 312

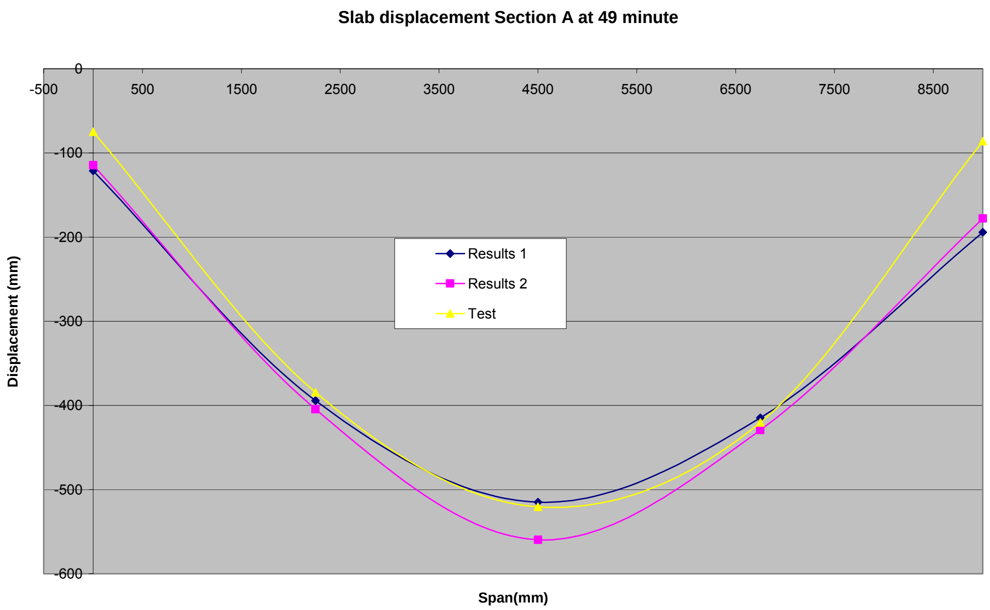

Figure E26: Slab displacement on section at 49 minutes

In the direction parallel to the edge beam the behaviour of the slab is accurately predicted in the area of the centre of the compartment (Nodes 301,305,309). At the edges (Nodes 298,312) the predicted response overestimates the measured deflection.

This is due to difficulties in accurately modelling the boundary conditions at the edges. However, this is not the critical area for the current study.

Parametric studies

An overview of the parameters to be included in the numerical studies is included as Appendix D to this report. The information is reproduced below (table E3) in order to aid the understanding of the results.

Analysis	Floor construction	Grid size (m)	Imposed load (kN/m²)	Fire exposure	Beam protection	Compartmentation (see figure 6)*
1A	Composite	9x9	4+1	60 mins	all	0
1B	Composite	9x9	4+1	60 mins	all	0
2	Composite	9x9	4+1	60 mins	all	1
3	Composite	9x9	4+1	60 mins	all	2
4	Composite	9x9	4+1	60 mins	all	3
5	Composite	9x9	4+1	60 mins	all	4
6	Composite	9x9	4+1	60 mins	partial	0
7	Composite	9x9	4+1	120 mins	all	0
8	Composite	9x9	4+1	Natural	all	0
9	Composite	9x9	2.5+1	60 mins	all	0
10	Composite	9x9	7.5+1	60 mins	all	0
11	Composite	9x6	4+1	60 mins	all	0
12	Composite	9x7.5	4+1	60 mins	all	0

* 0 corresponds to no compartment walls and represents a worst-case scenario.

Table E3 Summary of analyses undertaken

Compartment location

The layout of the compartment walls according to the scheme set out in table E3 is illustrated in Figure E27.

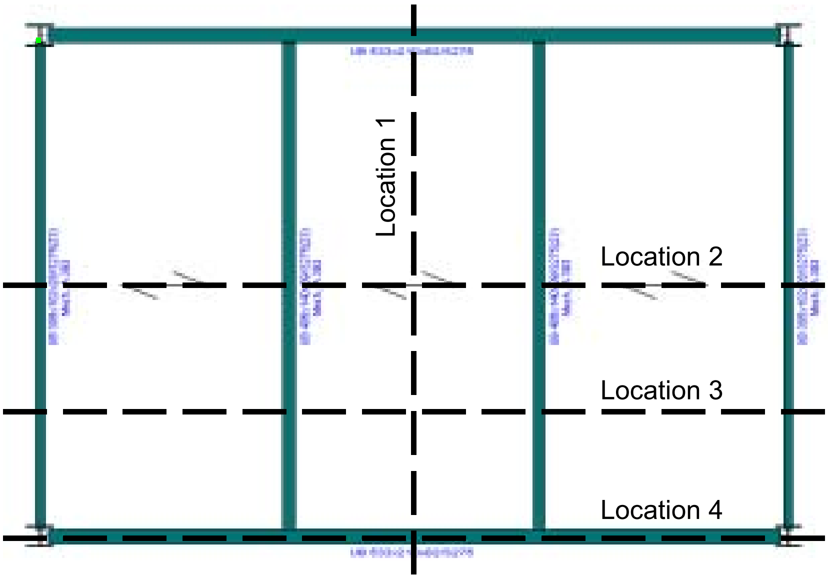

Figure E27: Location of compartmentation

Composite Design

Design loads

The loads used within the structure are the same as those which are commonly used in the design of office buildings and are as outlined in Table E4.

	Characteristic kN/m²	Fire Factor	Design Load kN/m²
Floor Slab	3.12	1.0	3.12
Finishes	1.70	1.0	1.70
Steelwork	0.50	1.0	0.50
Imposed Load	5.00	0.8	4.00
		Total	**9.32**

Table E4: Design loads

It should be noted that these values are for speculative office construction where the client is unsure if the end use at the time of construction. The design loads allow for flexibility and are therefore unlikely to be achieved for most office buildings.

The general layout for the model is illustrated in Figure E28.

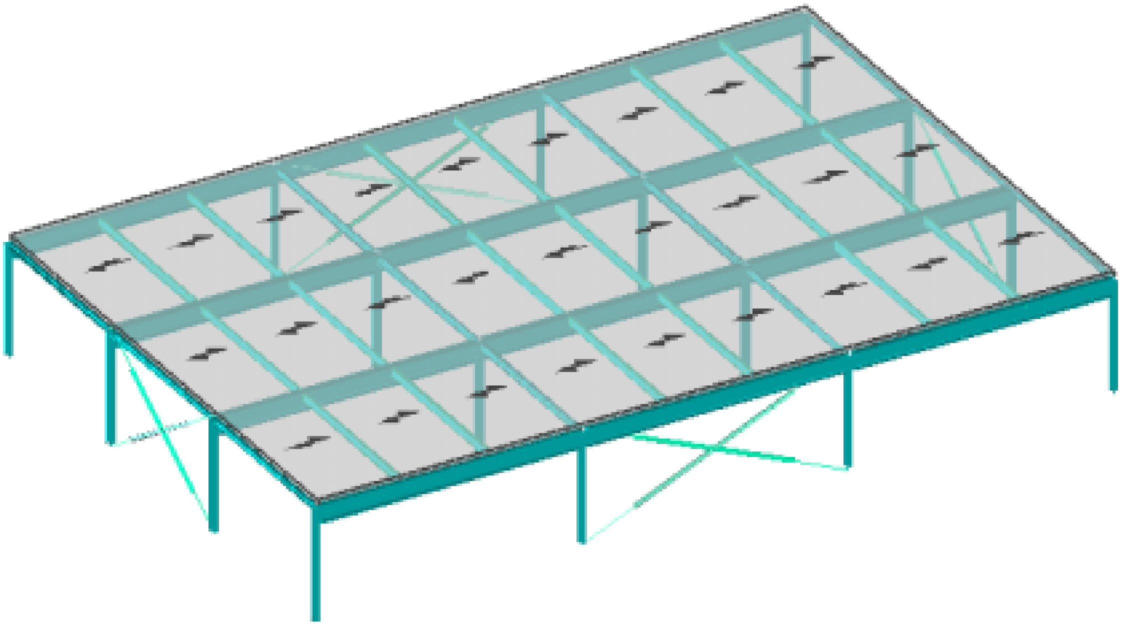

Figure E28: General arrangement for parametric studies

Slab design

The floor is 140mm composite slab using Wards Multideck trapezoidal decking 1.2mm thick. A single shear stud is provided in every trough. The slab is constructed using normal weight concrete with a cylinder compressive strength of 35N/mm^2. The floor slab is reinforced with a steel mesh (A393), which has a steel area of 393mm^2/m in both directions. The mesh is fabricated using 10mm bars at 200mm centres. The reinforcement has a yield strength 460N/mm^2 and a Young's Modulus 210000N/mm^2 at ambient temperature.

Steel design

All steel sections are assumed to be Grade S275 steel with a yield stress 275N/mm^2, Young's Modulus of 205000N/mm^2 and an ultimate tensile strain of 25%.

General arrangements

Figure E29 shows a corner bay for the 9m x 9m grid and Figure 30 shows a corner bay for the 9m x 7.5m and 9m x 6m grids. The member sizes for each of these grids are summarised in Table E5.

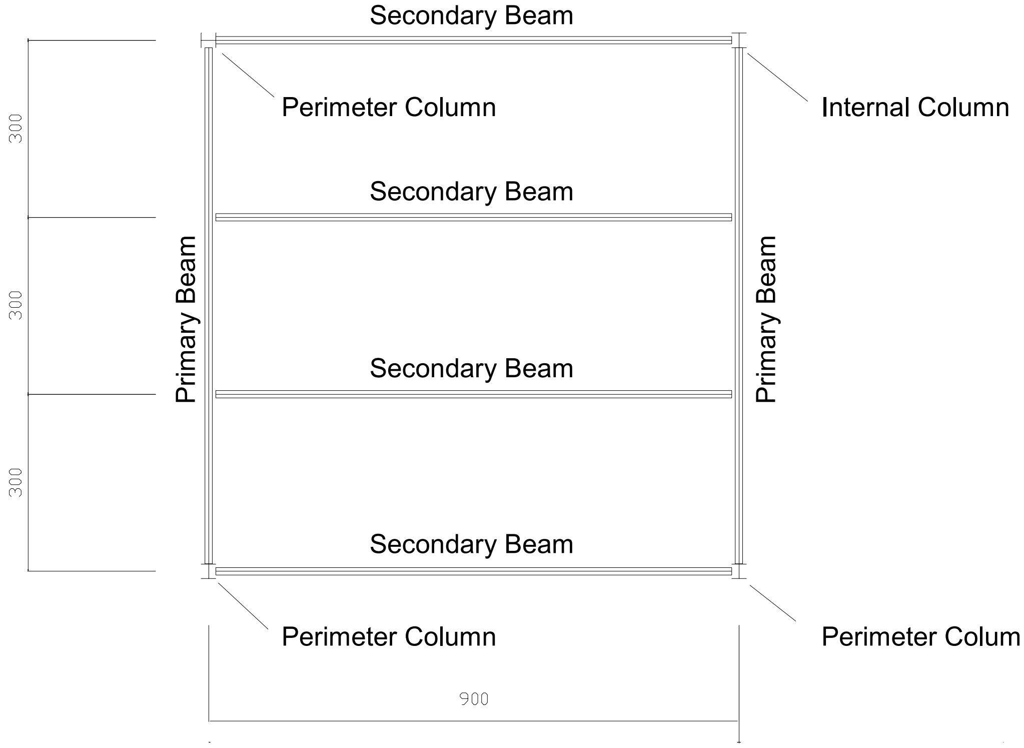

Figure E29: 9m x 9m corner bay

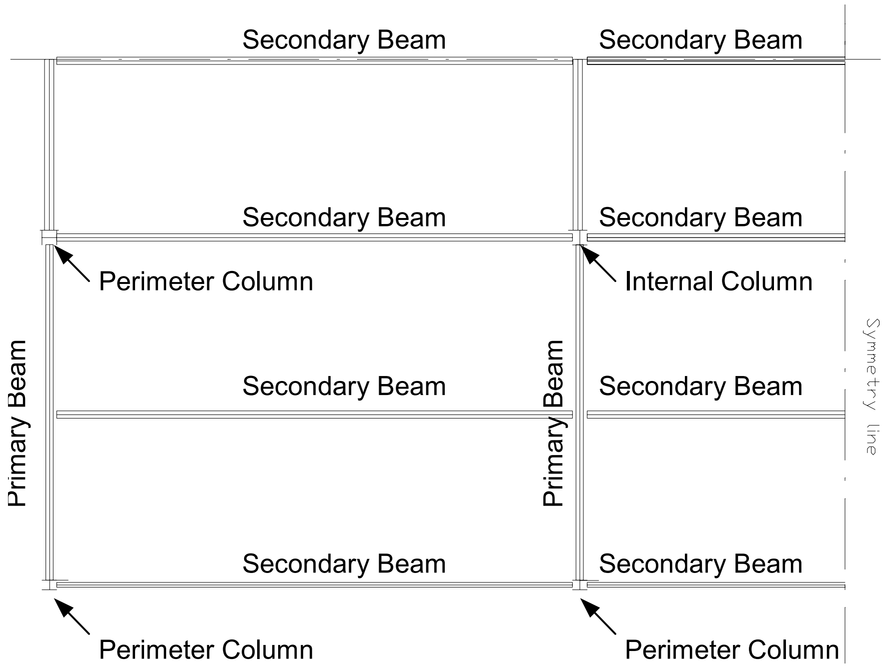

Figure E30: 9m x 7.5m and 9m x 6m corner bay

Bay Size (m)	Imposed Load (kN/m^2)	Primary Beams	Secondary Beams	Columns
9 x 9	4 + 1	610x229x113UB	356x171x57UB	254x254x73UC
9 x 9	2.5 + 1	610x229x101UB	356x171x51UB	254x254x73UC
9 x 9	7.5 + 1	762x267x134UB	457x191x67UB	254x254x73UC
9 x 7.5	4 + 1	610x229x113UB	305x165x40UB	254x254x73UC
9 x 6	4 + 1	533x210x82UB	305x102x28UB	254x254x73UC

Table E5: Member sizes – load ratios in parentheses

Load ratios are for comparative purposes and are based on axial loads only at Fire Limit State.

Model

The majority of Cases model the concrete slab using orthotropic slab elements 140mm thick. The software uses an effective stiffness model to account for the effect of the slab ribs on the relative stiffness of the slab in orthogonal directions. Temperatures were assessed based on the full depth of the slab. This method accurately represents the structural performance of the slab but does not account thermally for the effect of the slab troughs.

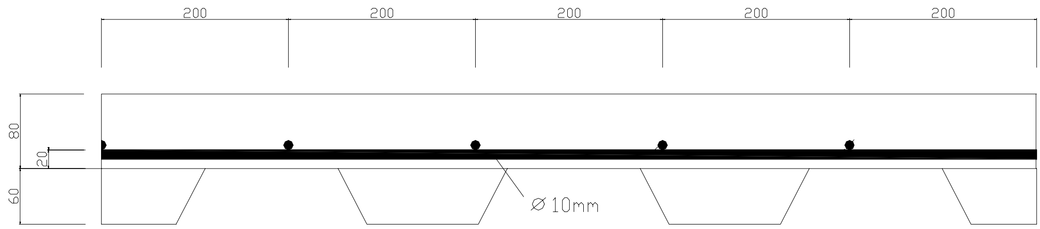

Figure E31: Cross section of the composite floor

Sensitivity studies were conducted using isotropic slab elements with a thickness of 80mm (see Cases 1B and 6B). This simulates the solid part of an orthotropic composite slab cast onto a trapezoidal metal deck. Slab temperature data was also calculated assuming an 80mm thick slab. Modelling the slab in this manner is conservative both structurally and thermally.

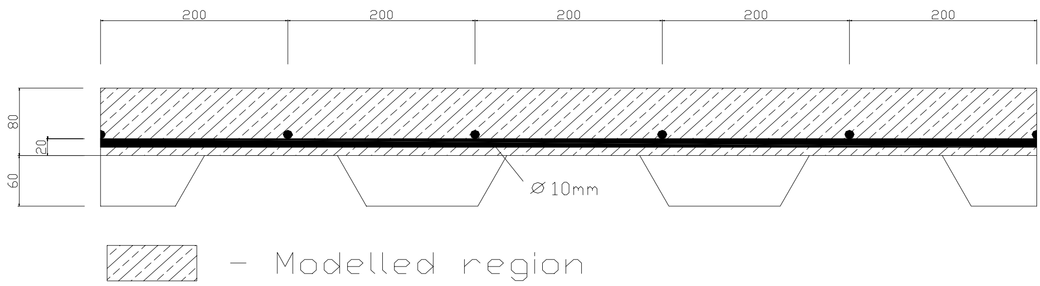

Figure E32: Cross section of the composite floor

In both cases, the centre line of the mesh is assumed to be located 20mm from the bottom of the slab. A cross section of the modelled concrete slab is shown in figure E31.

For all analyses, the material model for the concrete at ambient and elevated temperature has been adopted from EC4[2]. The elevated temperature behaviour for the reinforcement is taken from EC4. Full composite action is assumed between the steel beams and the floor slab.

All column bases are restrained vertically and horizontally and in rotation. This represents a fixed end condition and is an acceptable assumption for the purposes of this study since the primary focus of the study is the performance of the floor. The lateral restraint that would be provided by bracing has been modelled by fixing the lateral movement of the head of one of the corner columns in the direction parallel to the secondary beams and another corner column in the direction of the primary beams. All other nodes are free to translate and rotate.

Thermal analysis

Detailed thermal calculations were run for the floor system using a dedicated thermal analysis package known as THELMA.

The reason for using this code is to try to provide the most accurate information possible on temperature development. Previous studies have shown quite a high sensitivity of the structural calculations to the details of the thermal predictions[4]. In this regard, it is particularly important to account properly for the effects of moisture in inhibiting heat transfer. Data from real tests on composite floor systems normally shows a very extensive moisture plateau. Moisture is accommodated via the methodology described in references 4 and 5, cf Appendix C, which in summary is via modification of the specific heat term to include the effects of the latent heat, with an additional correction of the thermal conductivity in the temperature range up to the boiling point so as to accommodate moisture movement effects.

In any application of this sort of modelling procedure it is essential to tie the model back to validation with relevant test data. This is described in the following section.

<u>Validation</u>

The model was exercised in simulating the thermal response of the floor system in the natural fire test run in a 11m by 7m compartment on the fourth floor of the LBTF building at BRE Cardington on 11 January 2003. Through thickness thermocouples were installed in the composite floor at various locations in the ceiling slab. In particular, columns C1, C2 and C3 located at the rear of the compartment at the left-hand column, centreline and right-hand column respectively, included thermocouples 489-512 with four thermocouples at each rib and trough. In addition, column C4 on the compartment centreline was located about a metre further forward from the back row, with thermocouples 513 to 520.

THELMA simulations were run using temperature input from the nearest gas thermocouple, i.e. T 525. Details of the model inputs are summarised in Table E6. The value of the material thermal properties, i.e. the moisture content of the concrete, was carefully adjusted until a good match was achieved between prediction and experiment. Figures E33-E35 show the mesh and the computed temperature contours and time histories. Comparison with the test data is shown in Figure E36-E38.

Numerical timestep	1 minute
Convergence tolerance	0.001
Mesh refinements	4
Mesh refinement tolerance	0.005

Table E6: THELMA input details

The agreement between predictions and experiment is fair, with no systematic discrepancies in the results within the slab. The results for the surface temperatures are more variable, perhaps reflecting the difficulty of obtaining a good measure of this value experimentally.

Using the thermal properties calibrated in this manner, calculations were then run for the Wards MD60 flooring system. The true geometry was represented in the main simulations, and an additional simplified case was run where only an 80mm slab (i.e. the thickness at the troughs) was considered. Results for the former case are presented in Figures E33-41 below.

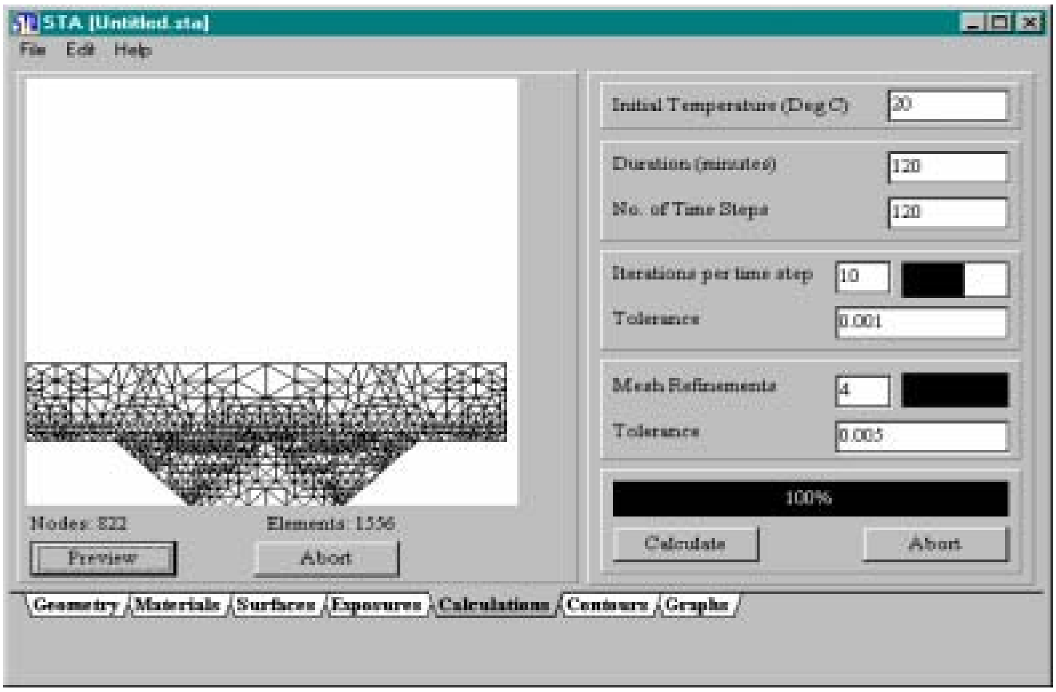

Figure E33: Computational mesh for PMF CF70 system

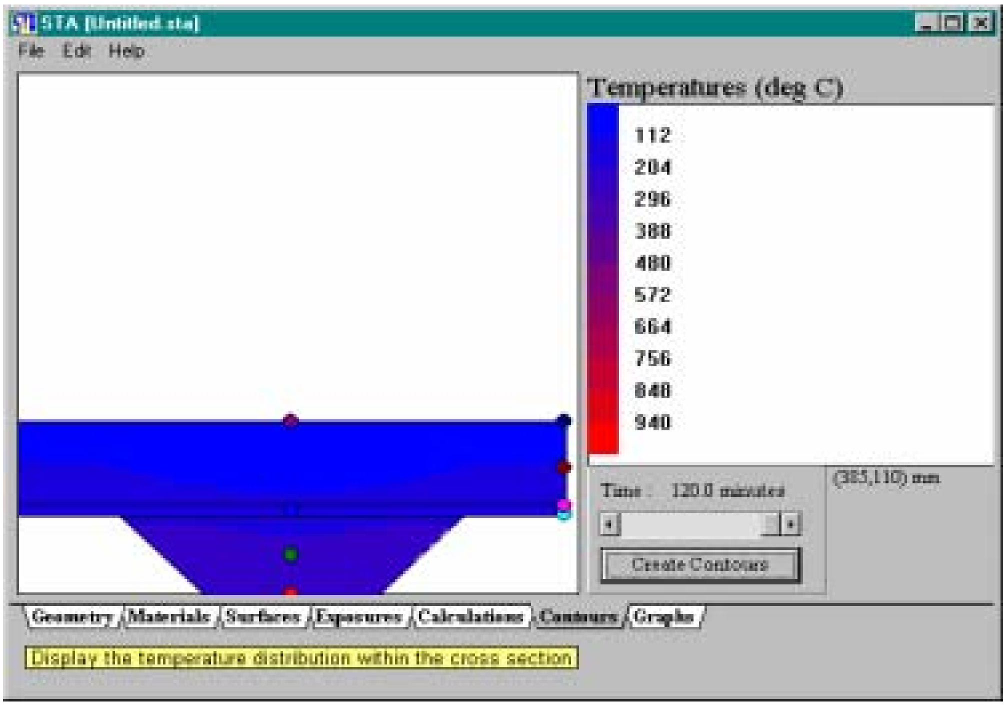

Figure E34: Computed temperature contours for PMF CF70 system

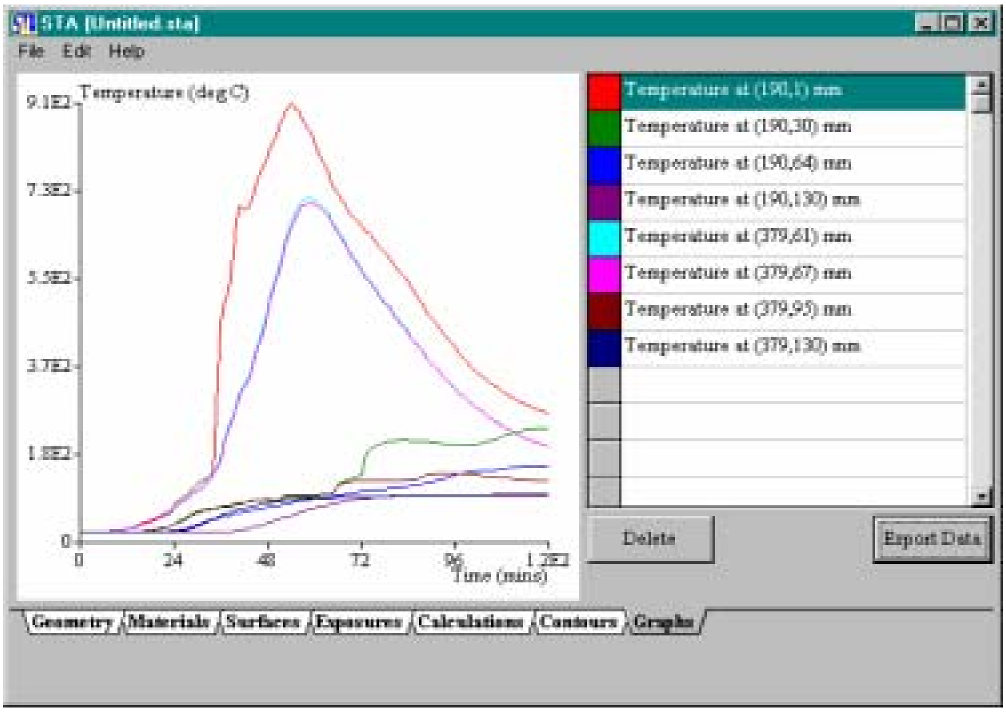

Figure E35: Comparison of slab temperature on unexposed faces for PMF CF70 system

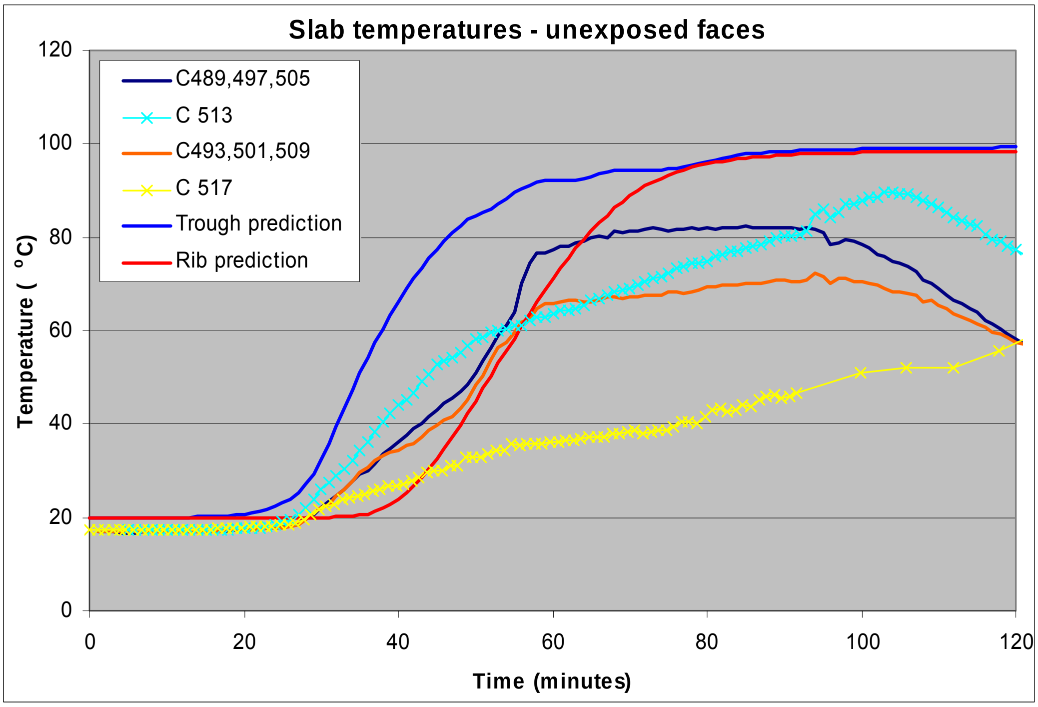

Figure E36: Comparison of slab temperature on unexposed faces for PMF CF70 system

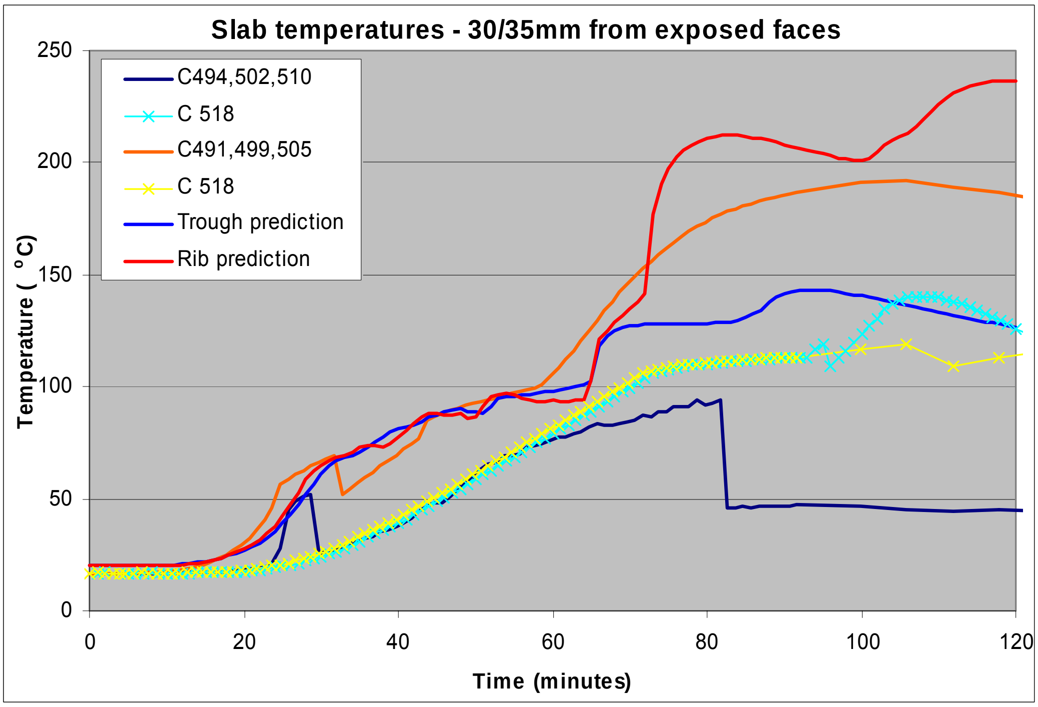

Figure E37: Comparison of slab temperature at locations 30/35mm from exposed faces for PMF CF70 system

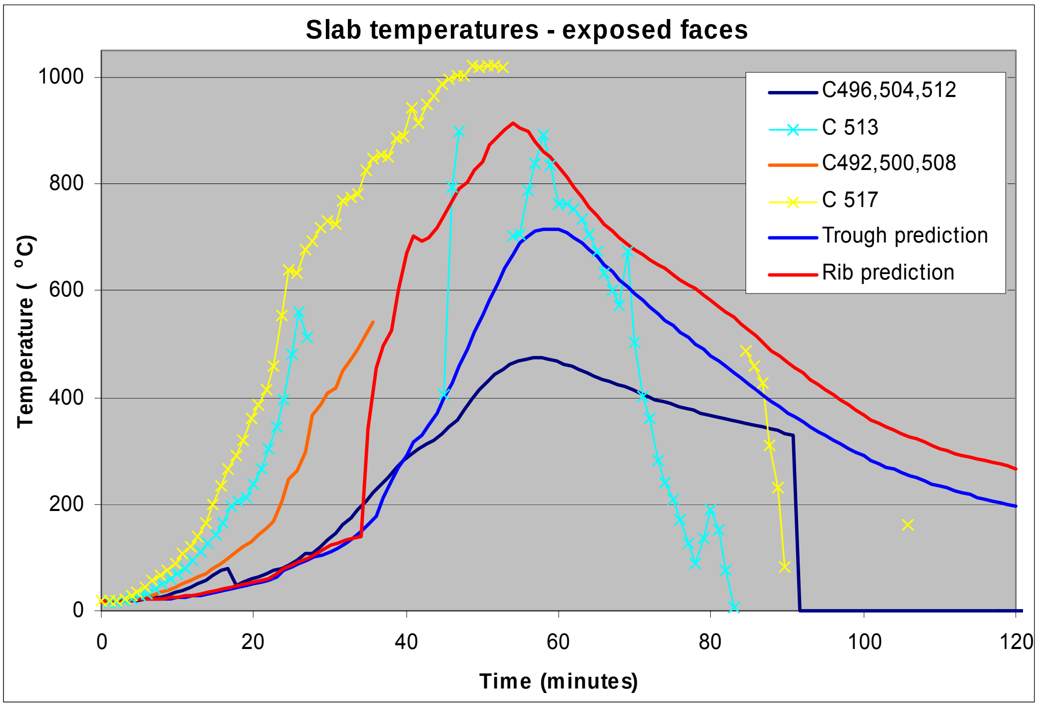

Figure E38: Comparison of slab temperature on exposed faces for PMF CF70 system

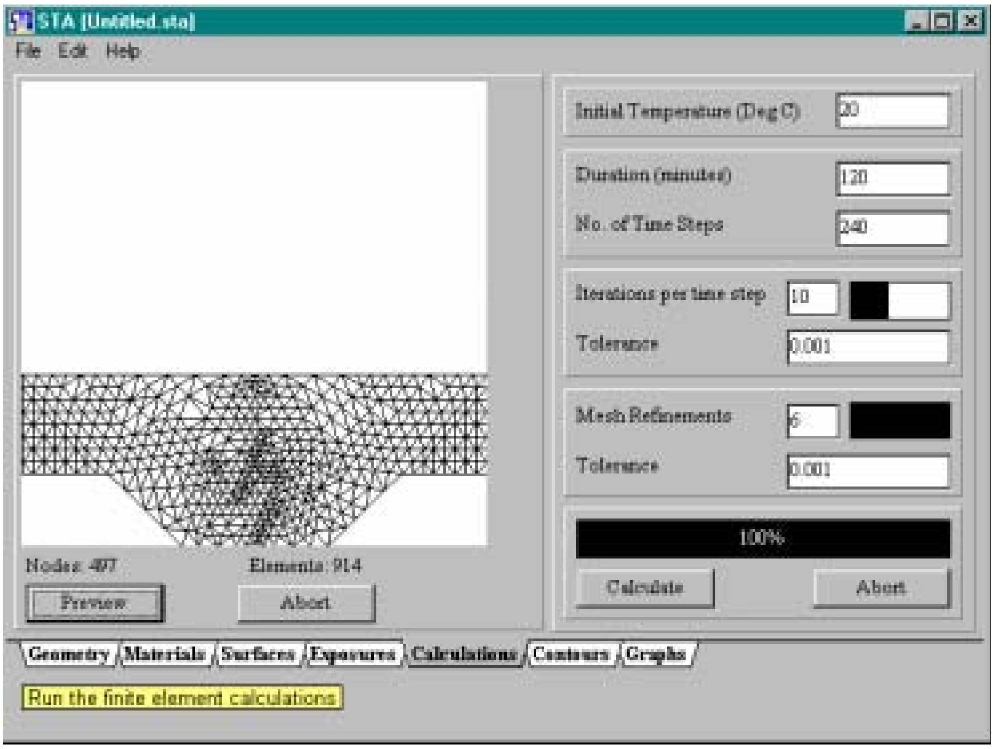

Figure E39: Computational mesh for Wards MD60 system

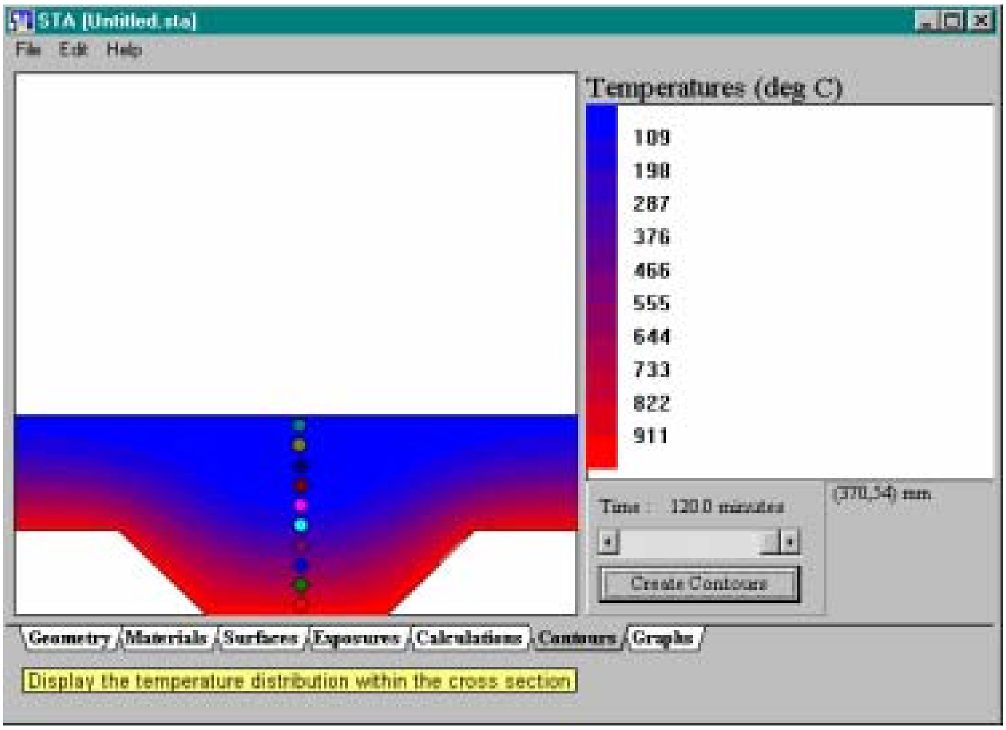

Figure E40: Computed temperature contours for Wards MD60 system

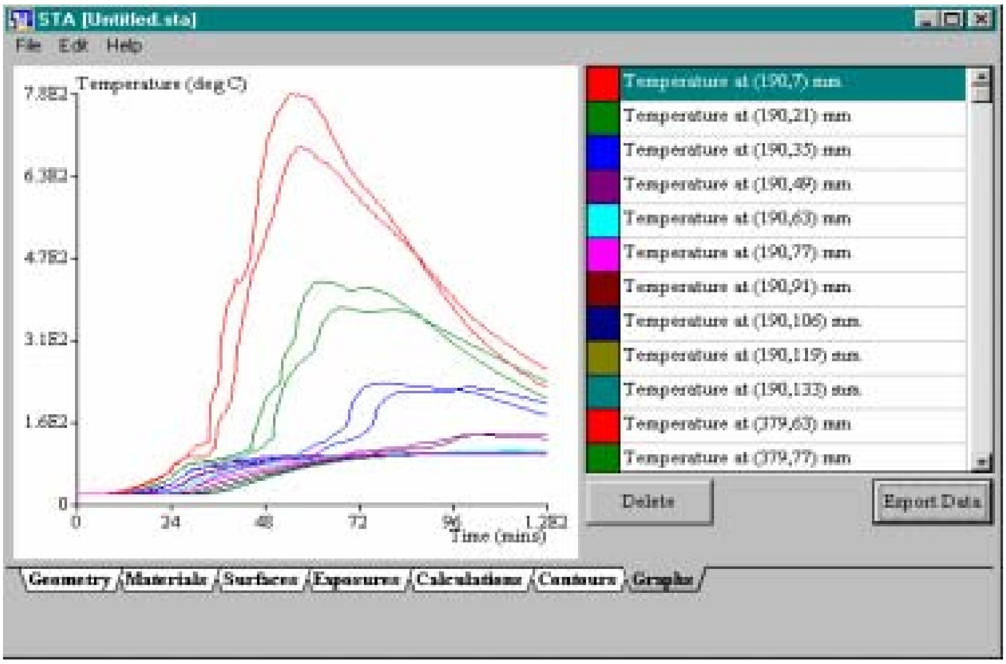

Figure E41: Comparison of slab temperature on unexposed faces for Wards MD60 system

Unprotected beam temperatures were calculated using the heat transfer method contained within Eurocode 3[1]. For protected beams, it was assumed that the maximum temperature of the beam reached 620°C at 60 minutes. This is in line with standard European testing procedures.

Results

The objective of the study is to investigate the likely deflection head requirements for compartment walls beneath fire effected slab. Therefore, predictions of deflection with respect to time have been produced for the point of maximum deflection and the point of maximum deflection directly above the compartment wall.

Base Design – Case 1A and 1B

Cases 1A and 1B represent a Base Design. This model is used to demonstrate that the *Vulcan* software is producing sensible results. It is also used as a reference case against which all other analyses can be compared.

Figure E42 shows the location of the bays for which output has been provided for all of the 9m x 9m grid analyses.

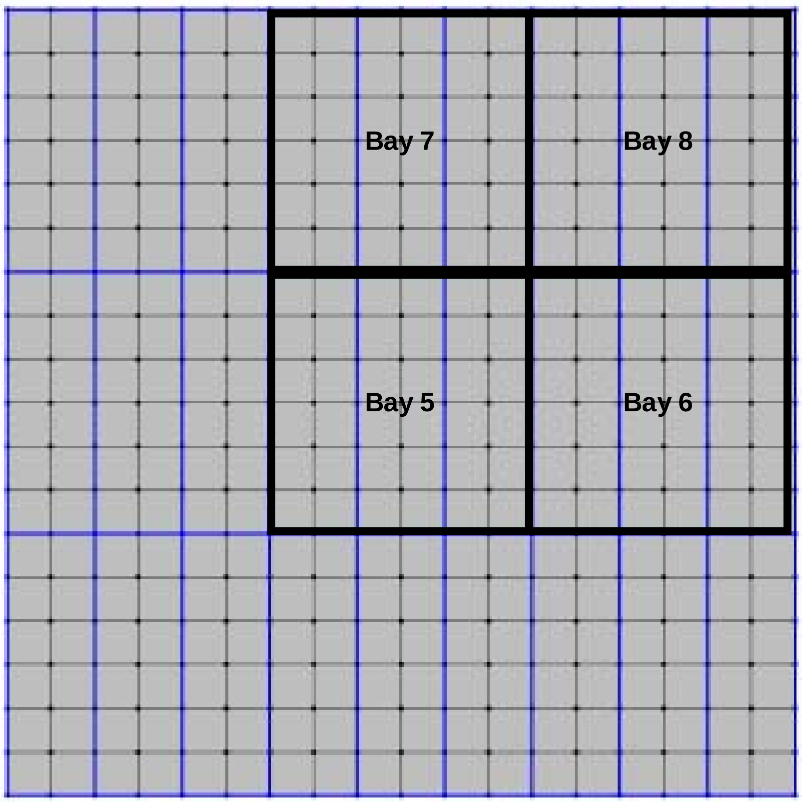

Figure E42: Bay locations and numbers

Figure E43 shows Bays 5, 6 8 and 9 and the node locations and numbers for which output has been provided for all of the 9m x 9m grids.

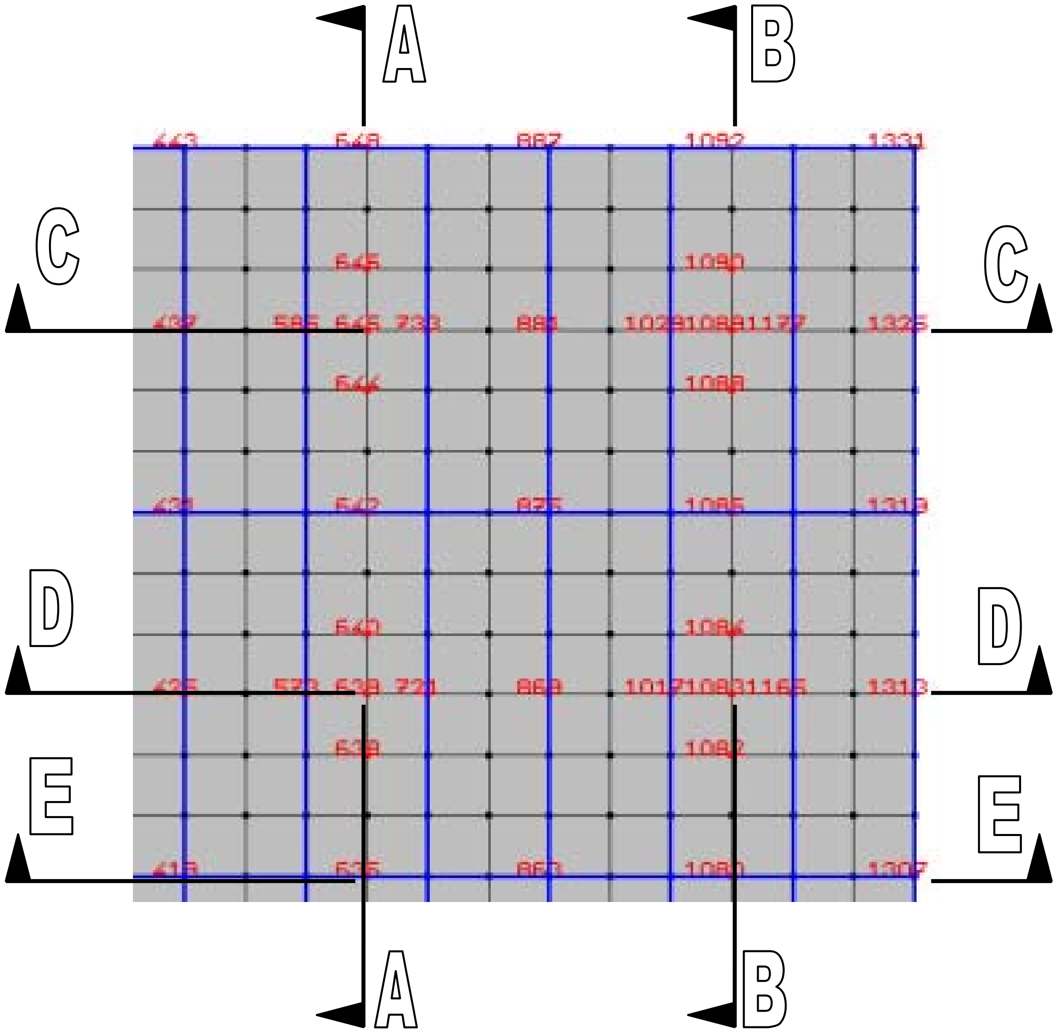

Figure E43: Location of data points

Figures E44 to E48 show slices of the deflected cross sections at 60 minutes along section lines A-A, B-B, C-C, D-D and E-E as indicated in Figure E43. The slices are taken from the centre lines of the slab (in plan) to the edge of the structure.

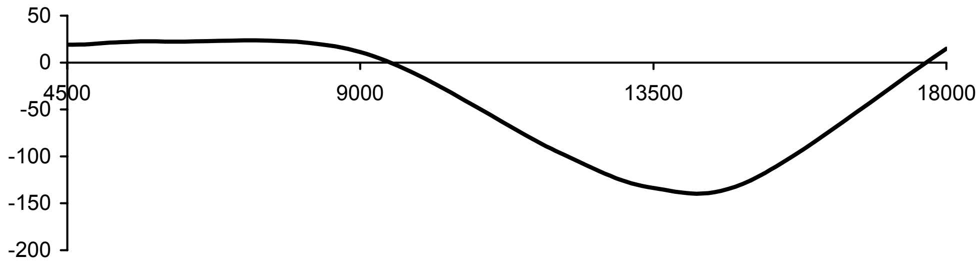

Figure E44: Deflected cross section slice A-A

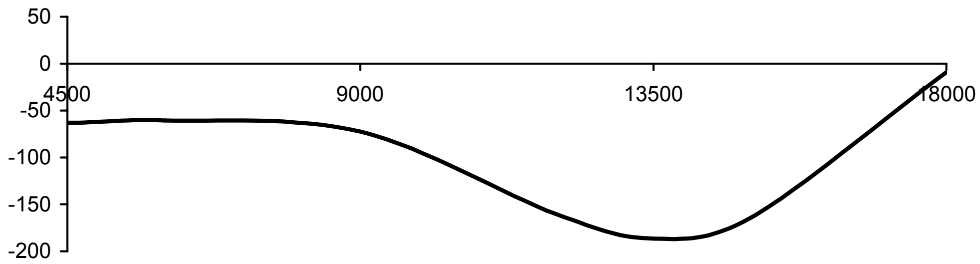

Figure E45: Deflected cross section slice B-B

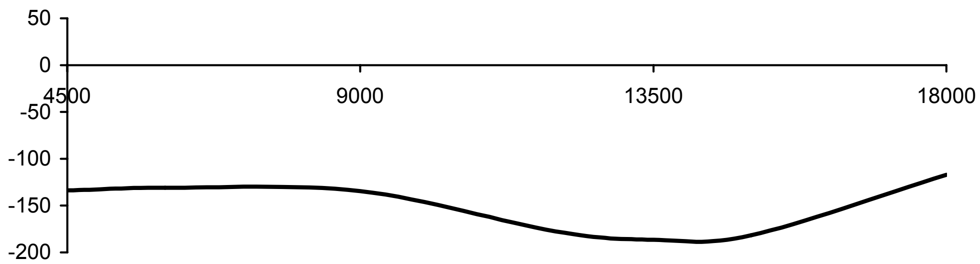

Figure E46: Deflected cross section slice C-C

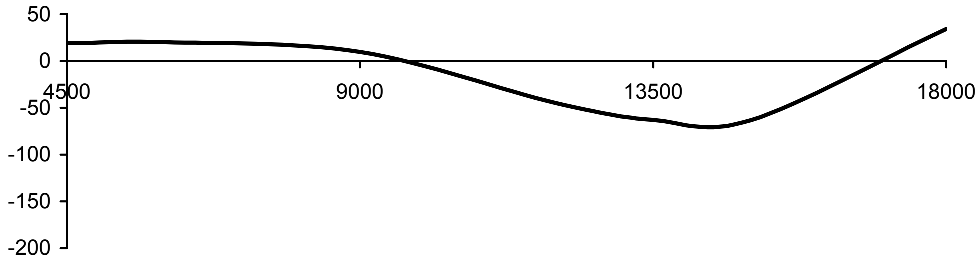

Figure E47: Deflected cross section slice D-D

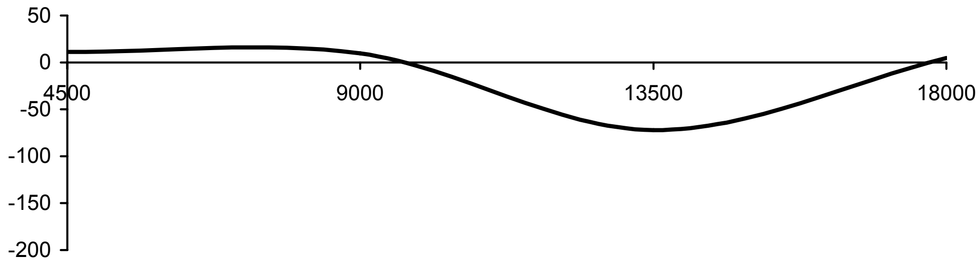

Figure E48: Deflected cross section slice E-E

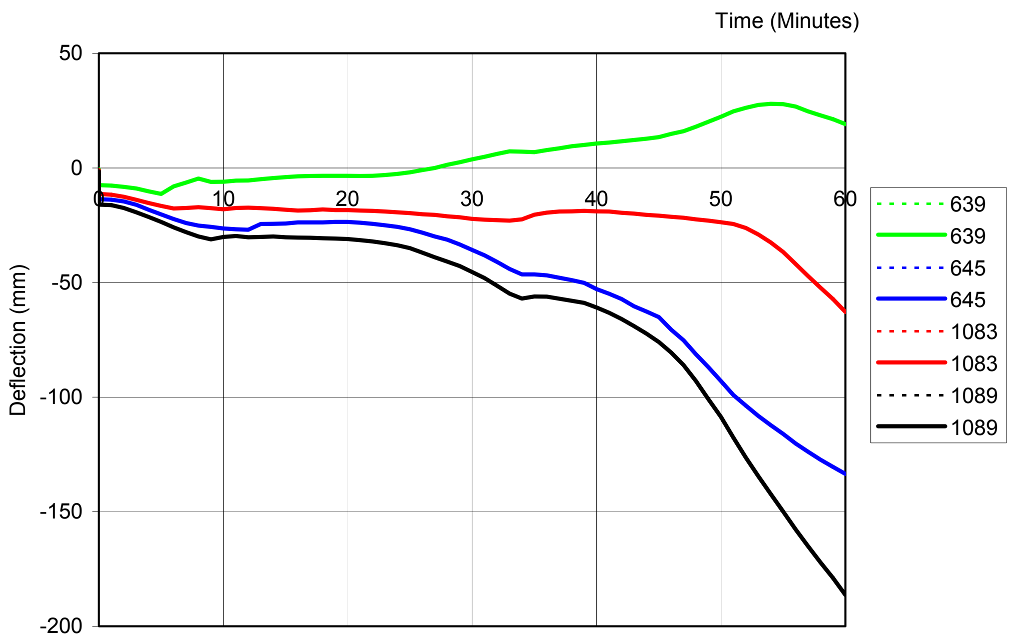

Figure E49: Deflections with respect to time

Figure E50 shows the deflected shape at elevated temperature. The vertical displacements have been magnified for visual purposes.

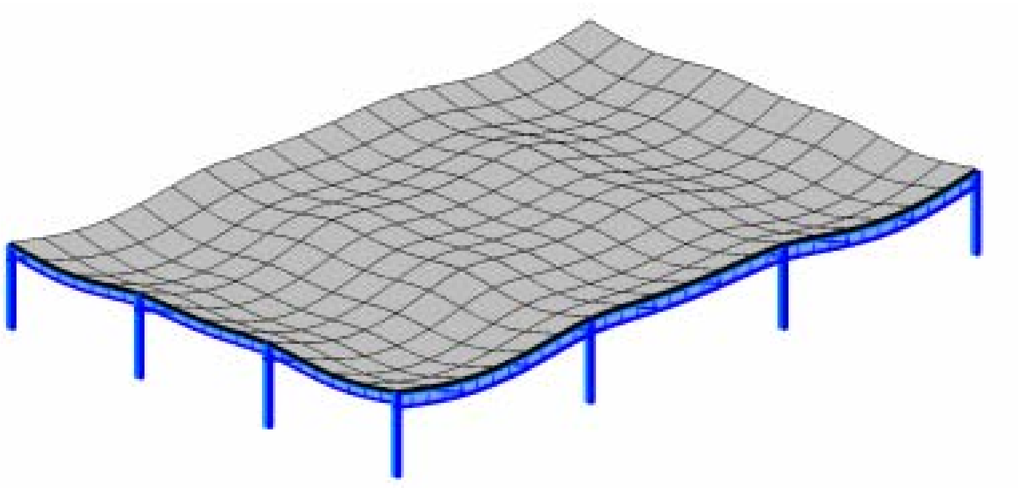

Figure E50: Deflected shape at elevated temperature

Inspection of the results from the figures above shows that the predicted behaviour is rational and the computer model is set up correctly. The vertical displacements of the slab show symmetrical behaviour about the centre line of the structure.

Figures E51 to E56 show comparisons between the results of the 140mm and 80mm slab thickness assumptions (dashed lines are for the 140mm slab base case). The results show a reasonable comparison between the two assumptions and in all cases the 140mm slab thickness gives conservative results. This demonstrates that it is acceptable that all remaining studies were conducted using the 140mm slab thickness assumption.

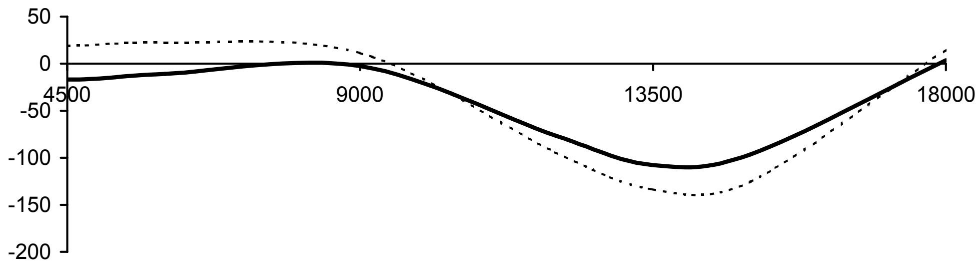

Figure E51: Deflected cross section slice A-A

bre

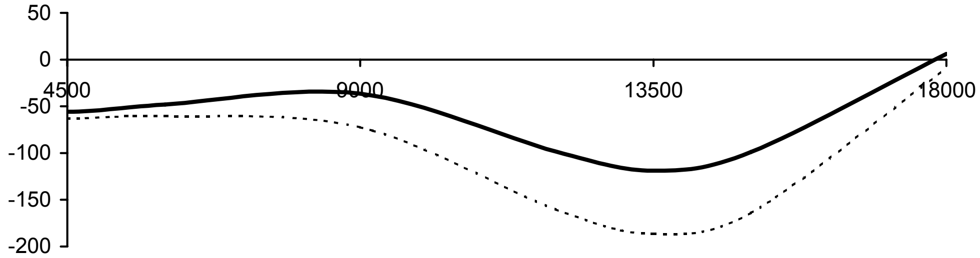

Figure E52: Deflected cross section slice B-B

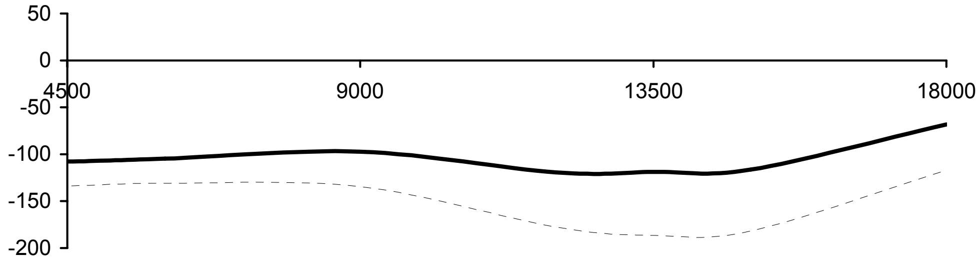

Figure E53: Deflected cross section slice C-C

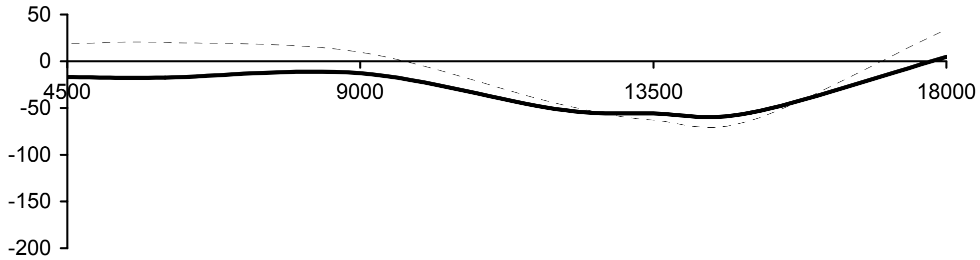

Figure E54: Deflected cross section slice D-D

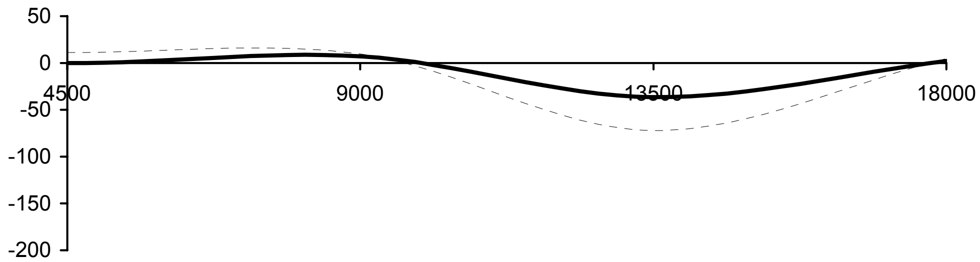

Figure E55: Deflected cross section slice E-E

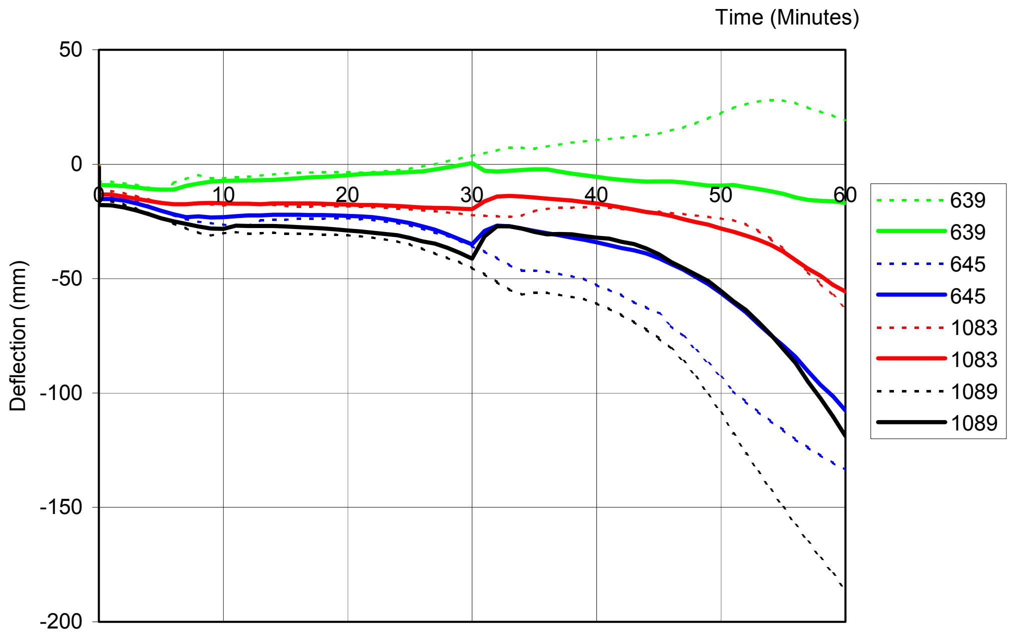

Figure E56: Deflections with respect to time

The results of the base case analyses are logical and can be explained. This provides confidence that the structural model is accurate and that the software is producing sensible results.

Compartment Location – Cases 2 to 5

Various compartment wall locations were considered. Figures E57 to E62 provide a comparison between the Base Design (no compartmentation) and Case 2, which has a compartment wall in the centre of the structure running parallel to the secondary beams (Position 1 in Figure E27). The solid lines are for the compartmented case.

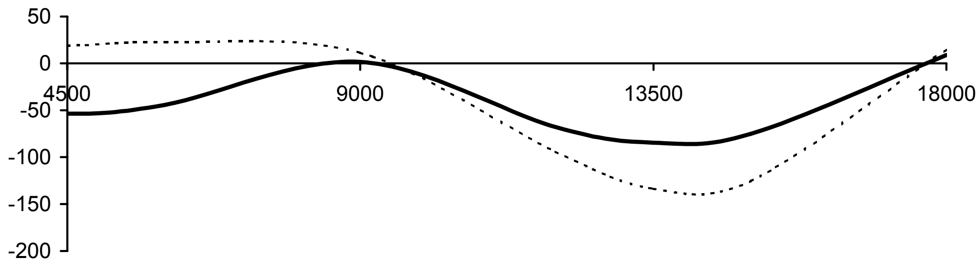

Figure E57: Deflected cross section slice A-A

Section A-A is along the line of the compartment wall. It clearly shows that the incorporation of the compartment wall reduced the deflections above the compartment wall itself. This would be expected as only the structure on one side of the compartment wall is heated. This is also particularly conservative as the analyses assume that the beam above the compartment wall is heated on both sides.

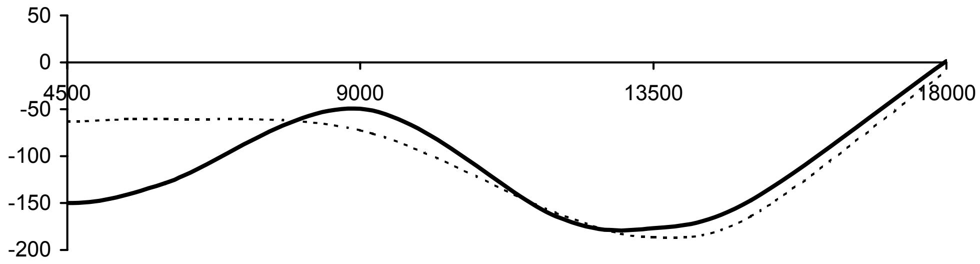

Figure E58: Deflected cross section slice B-B

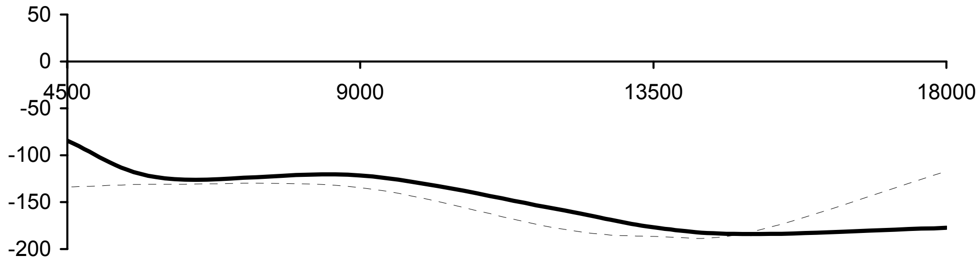

Figure E59: Deflected cross section slice C-C

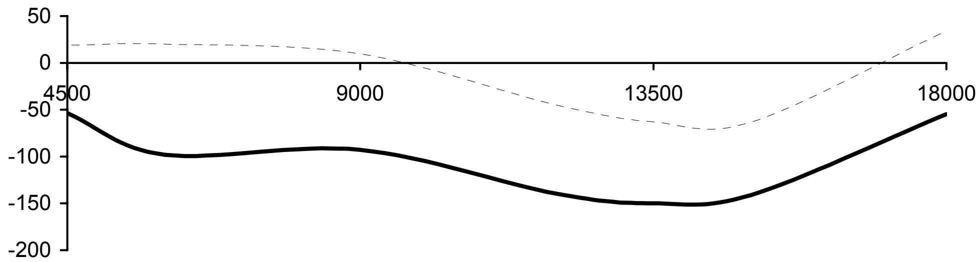

Figure E60: Deflected cross section slice D-D

Sections C-C and D-D clearly show how the slab deflection is reduced above the line of the compartment wall (x = 4500 on the graph marks the position of the compartment wall).

bre

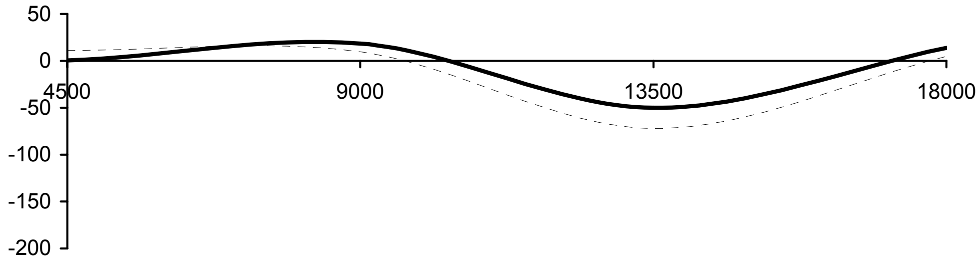

Figure E61: Deflected cross section slice E-E

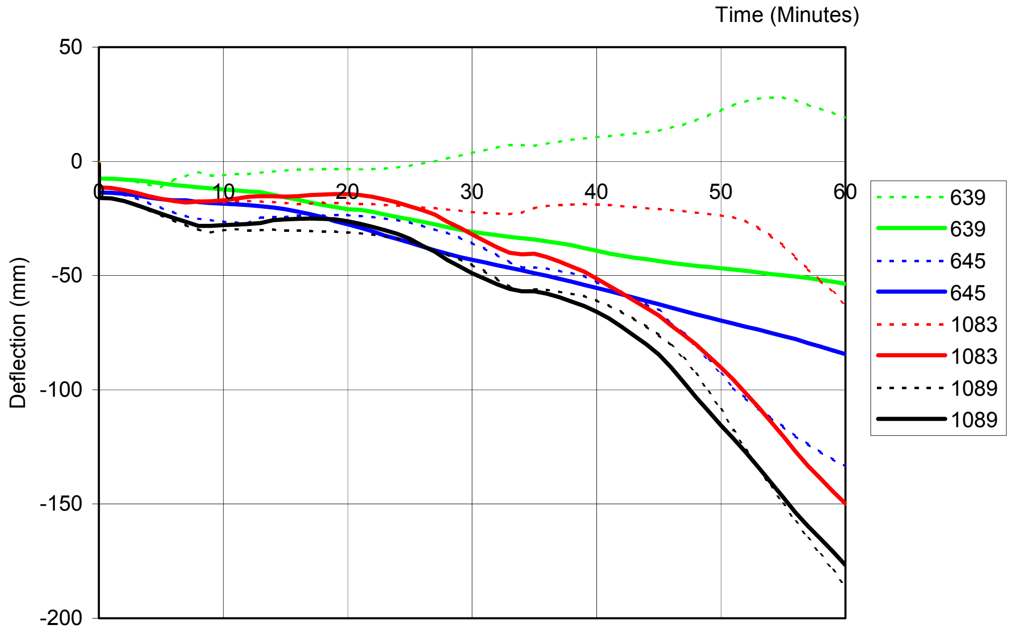

Figure E62: Deflections with respect to time

Figures E63 to E68 provide a comparison between the Base Design (no compartmentation) and Case 3, which has a compartment wall in the centre of the structure running perpendicular to the secondary beams (Position 2 in Figure E27). The solid lines are for the compartmented case.

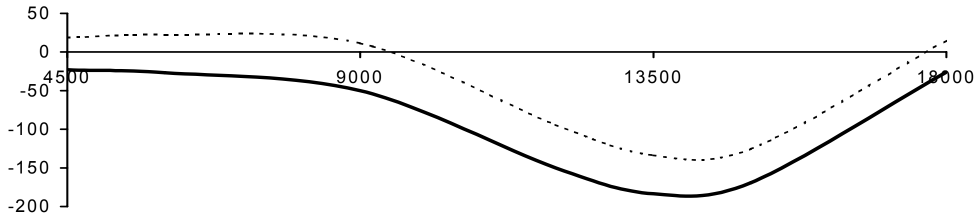

Figure E63: Deflected cross section slice A-A

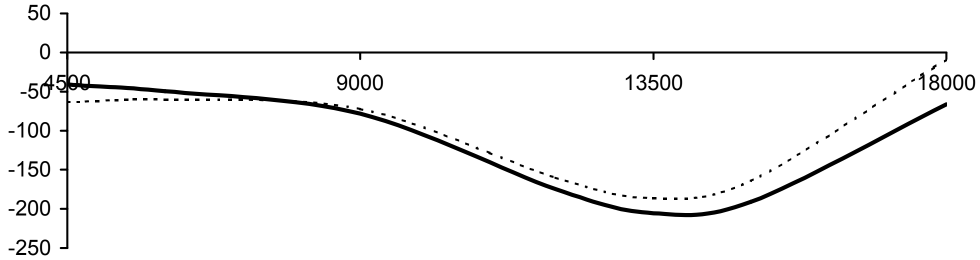

Figure E64: Deflected cross section slice B-B

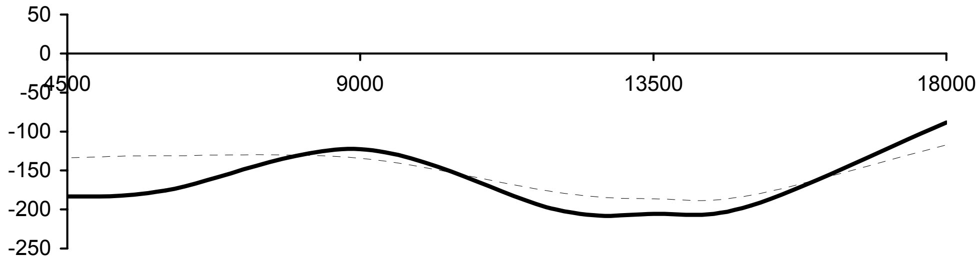

Figure E65: Deflected cross section slice C-C

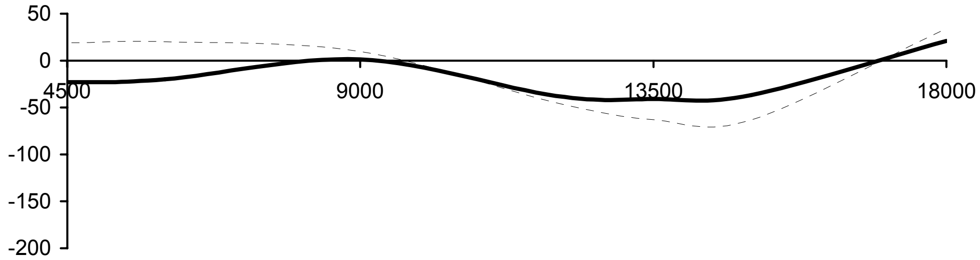

Figure E66: Deflected cross section slice D-D

Section D-D is along the line of the compartment wall. It shows that the incorporation of the compartment wall reduced the deflections above the compartment wall itself, but only slightly. This is different from the case where the compartment wall ran parallel to the secondary beams (see Figure E27). The reason behind this is that when the comparrtmentation ran parallel to the beam, it was directly under the beam for the full length of the beam. This is in contrast to this case where the compartmentation is perpendicular to the secondary beams and has heated beams passing through the compartment wall.

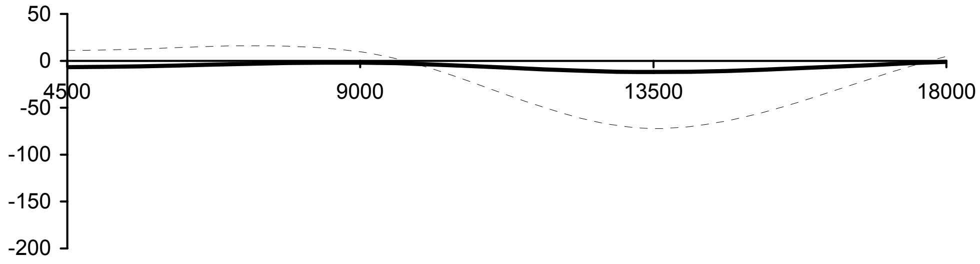

Figure E67: Deflected cross section slice E-E

Section E-E is taken on the cold side of the compartment wall. As would be expected, there is minimal deflection as all of the structure in the vicinity of Section E-E is cold.

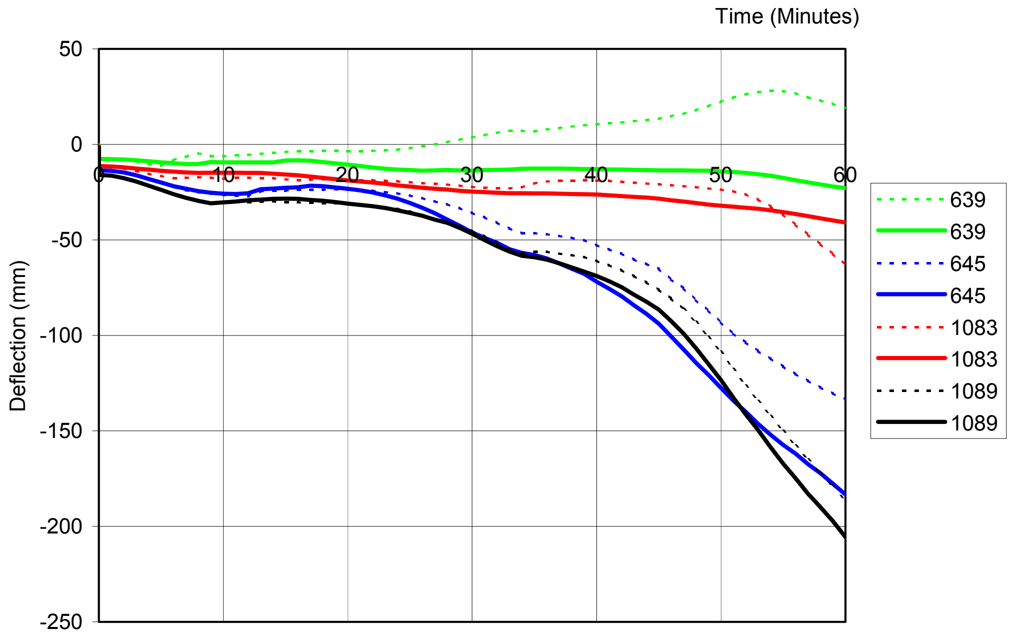

Figure E68: Deflections with respect to time

Figures E69 to E74 provide a comparison between the Base Design (no compartmentation) and Case 4, which has a compartment wall off-centre running perpendicular to the secondary beams (Position 3 in Figure E27). The solid lines are for the compartmented case.

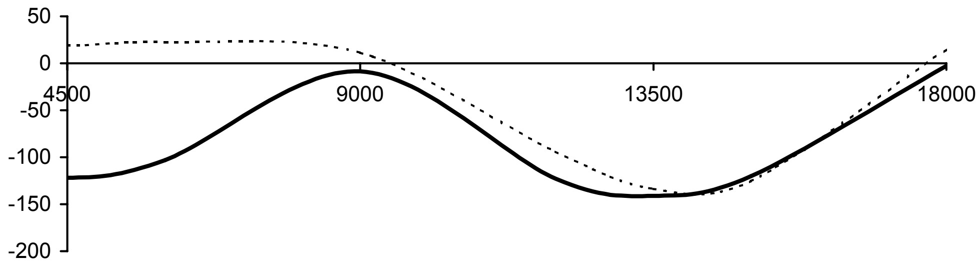

Figure E69: Deflected cross section slice A-A

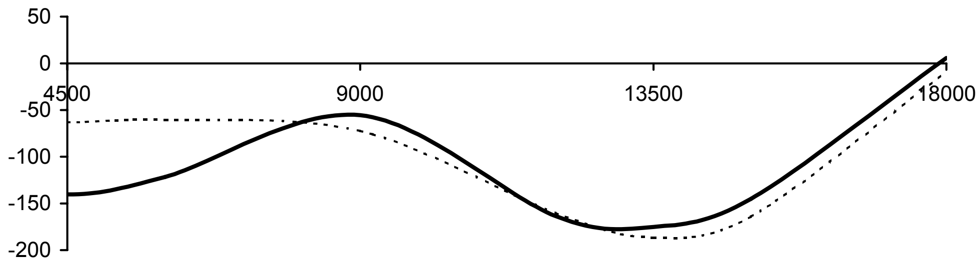

Figure E70: Deflected cross section slice B-B

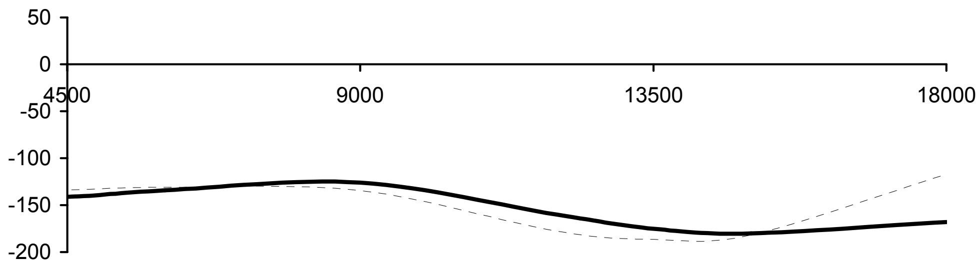

Figure E71 Deflected cross section slice C-C

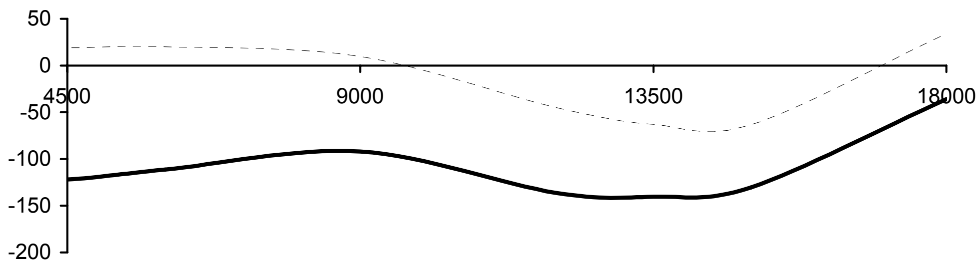

Figure E72 Deflected cross section slice D-D

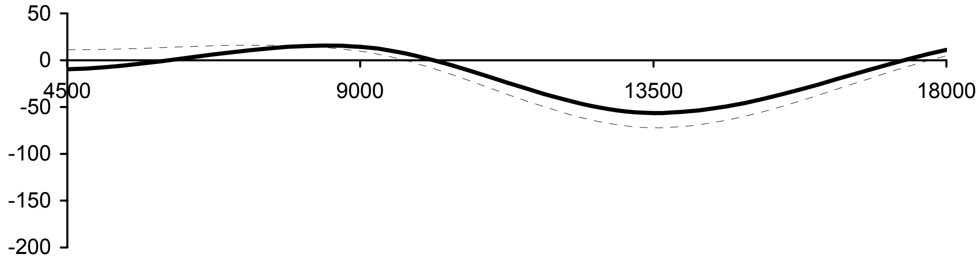

Figure E73: Deflected cross section slice E-E

As would be expected, the results for Case 4 (Position 3 in Figure E27are not dissimilar from the results for Case 3 (Position 4 in Figure E27).

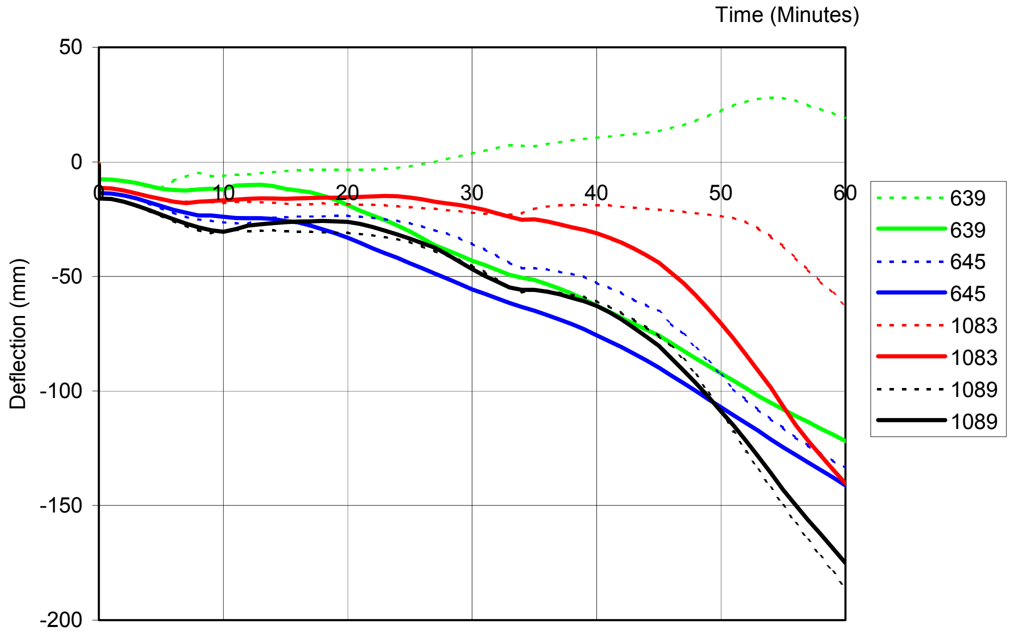

Figure E74: Deflections with respect to time

Figures E75 to E80 provide a comparison between the Base Design (no compartmentation) and Case 5, which has a compartment wall parallel and underneath one of the primary beams (Position 3 in Figure E27). The solid lines are for the compartmented case.

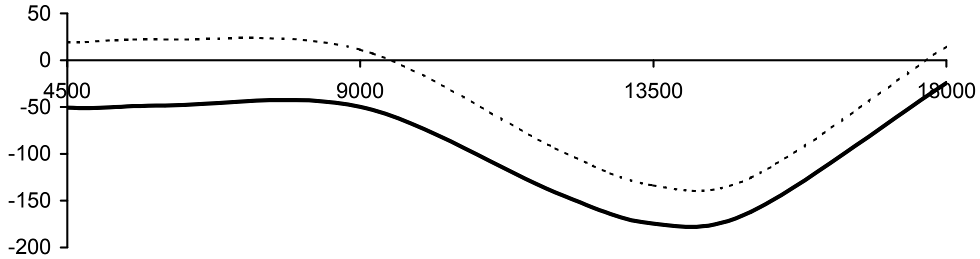

Figure E75: Deflected cross section slice A-A

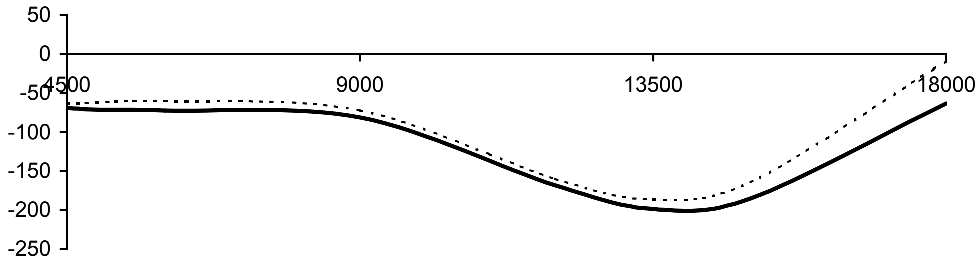

Figure E76: Deflected cross section slice B-B

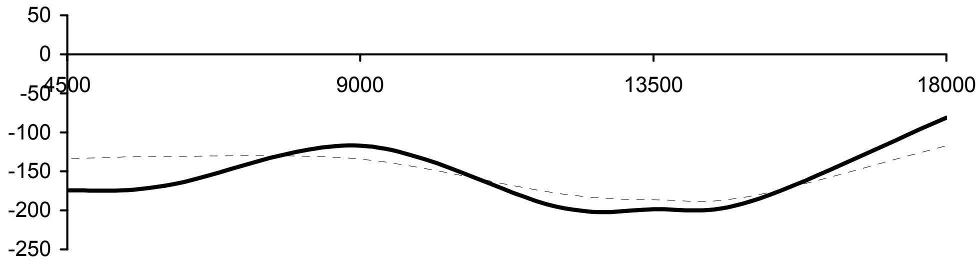

Figure E77: Deflected cross section slice C-C

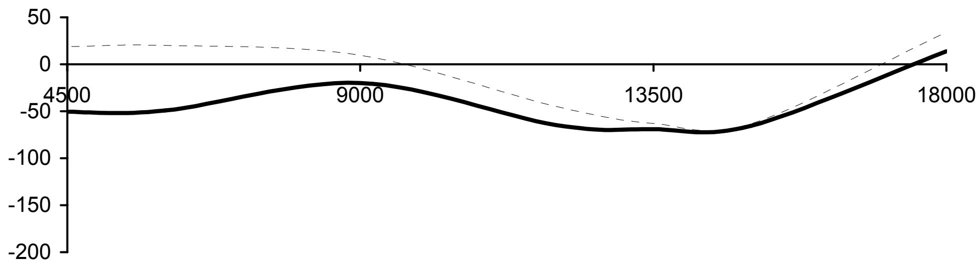

Figure E78: Deflected cross section slice D-D

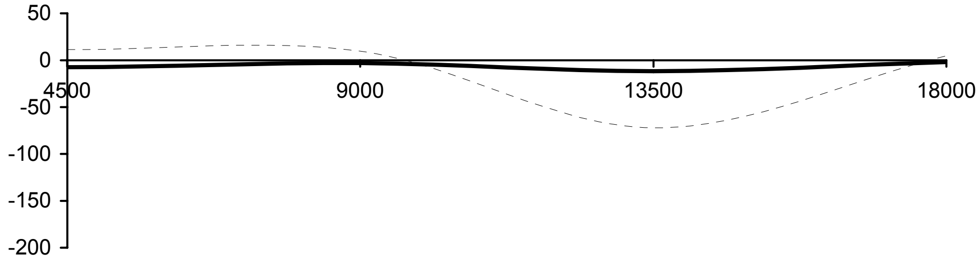

Figure E79: Deflected cross section slice E-E

Placing a compartment wall under the primary beam has very little impact on the deflections within the fire compartment. However, as can be seen from Section E-E, placing the compartment wall under the primary beam results in a significant reduction in the deflections that occur within the primary beam.

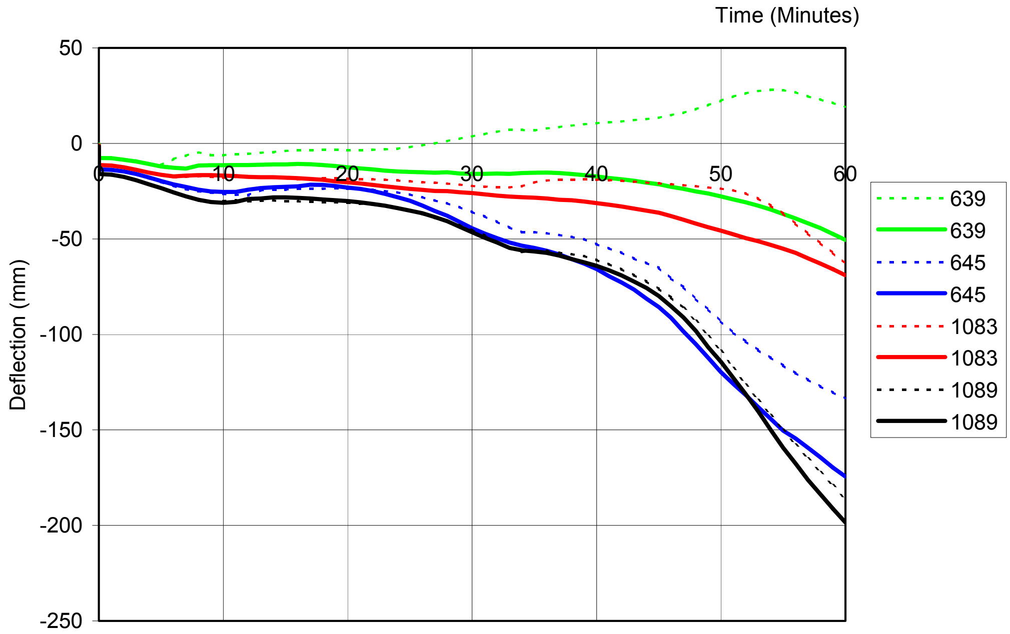

Figure E80: Deflections with respect to time

Partial Protection – Case 6

A study was conducted to assess the impact of unprotected beams on the likely deflections in fire scenarios (see figures E50 and E51). For the protected case, beams that do not frame into columns are not protected. All other beams are protected in accordance with Standard Fire Test requirements. This arrangement complies with the BRE design method. Figures E81 to E86 show the comparison between the fully protected case and the partially protected case. The partially protected case is represented by solid lines in the graphs.

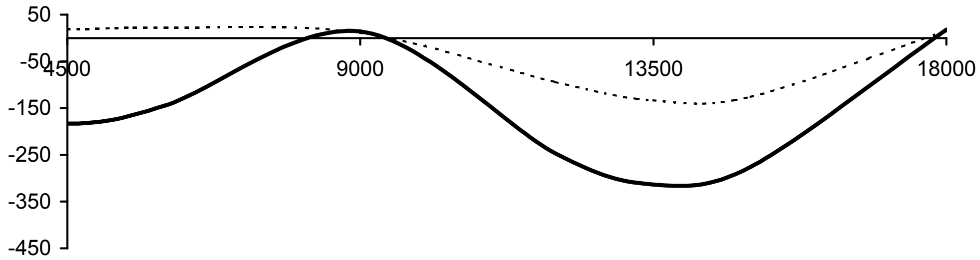

Figure E81: Deflected cross section slice A-A

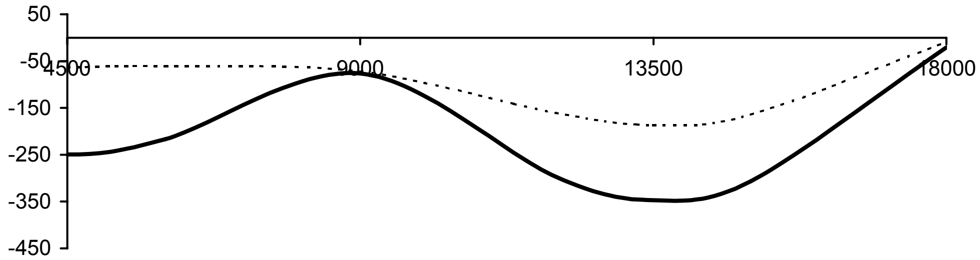

Figure E82: Deflected cross section slice B-B

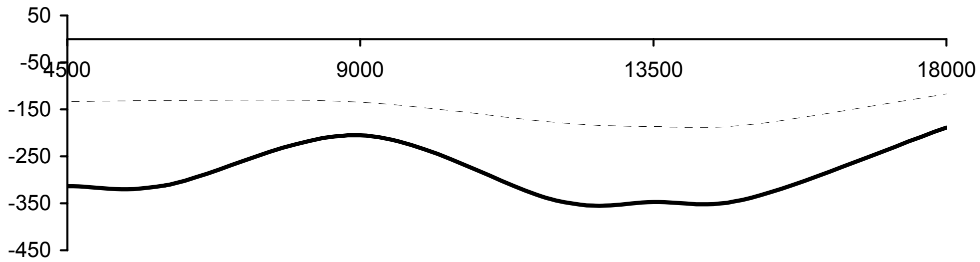

Figure E83: Deflected cross section slice C-C

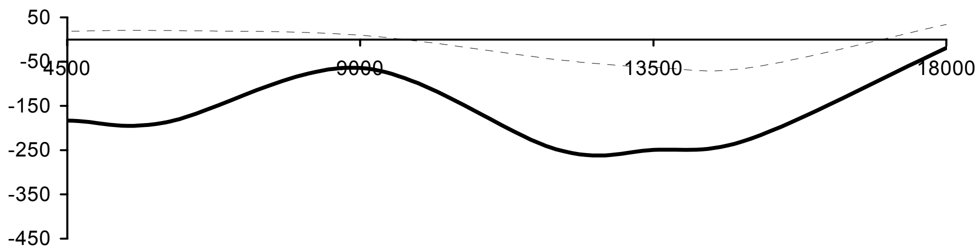

Figure E84: Deflected cross section slice D-D

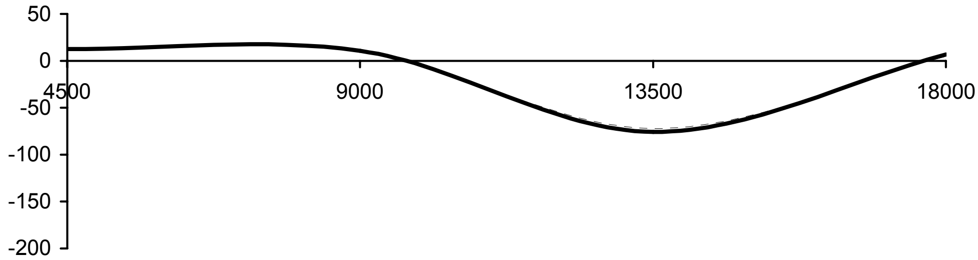

Figure E85: Deflected cross section slice E-E

Figures E81 to E84, which are for nodes in the centres of each bay, show that the deflection in the unprotected case are significantly greater than in the protected case. This would be expected due to the location of the unprotected beams. However, Figure E85 shows that there is negligible difference between the unprotected and the protected cases along Section E-E. This is because Section E-E is along the line of one of the protected beams. The maximum deflection is approximately 350mm which is less than the span/20 limitation (450mm) imposed by the BRE design method. This suggests that the BRE method delivers deflections equivalent to those that would be expected in a standard fire test.

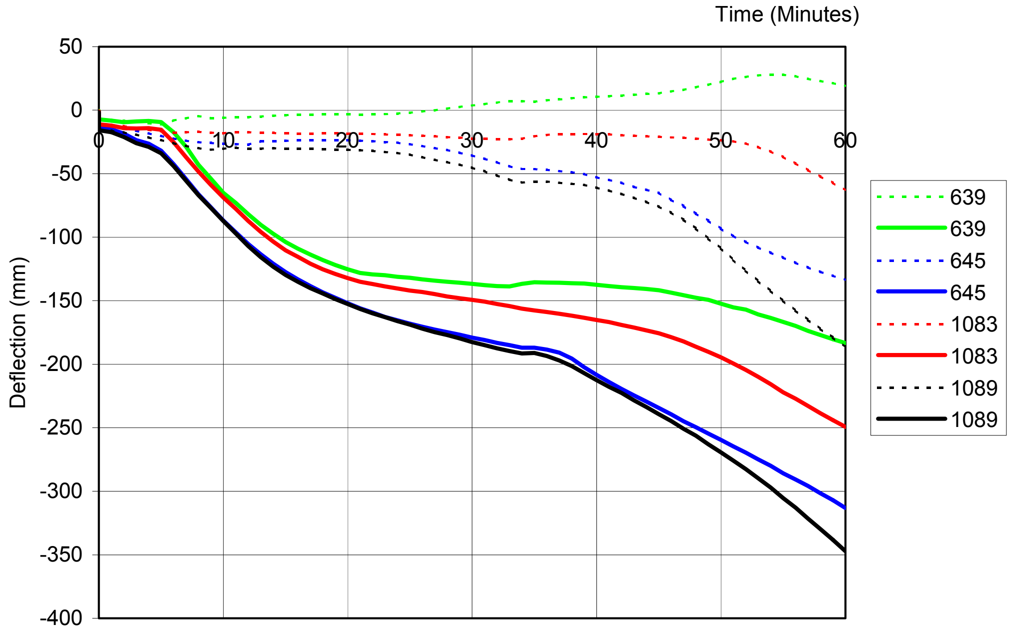

Figure E86: Deflections with respect to time

Design Fire – Cases 7 and 8

Historically, the fire protection requirements for structures have been determined using the Standard Fire Curve which is designed to represent a fully developed room fire. Whilst it has its uses, the Standard Fire Curve does not necessarily represent real fire behaviour. Therefore, a study was conducted to compare one particular natural fire scenario with 60 minute and 120 minute standard fire curves.

Figures E87 and E88 provide a comparison between the Base Design (no compartmentation) and Cases 7 and 8 respectively. Case 7 adopts a 120-minute Standard Fire and Case 8 adopts a natural fire instead of the Standard Fire Curve. In both cases, the dashed line represents the 60-minute Standard Fire (Base Case).

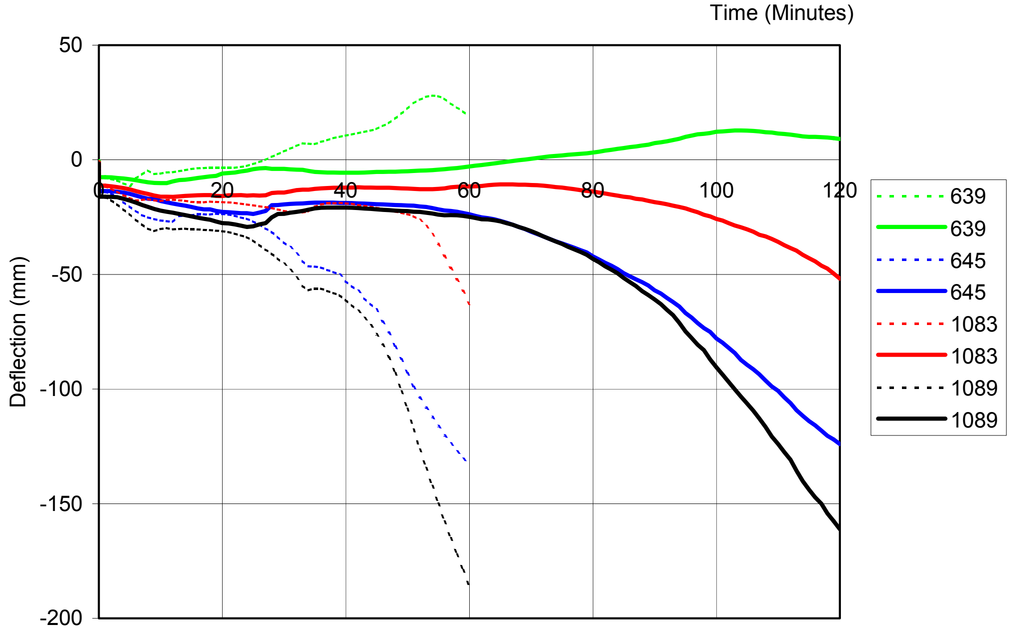

Figure E87: Deflections with respect to time

Figure E87 demonstrates comparable deflections for the 60-minute and 120-minute fire resistance periods. This is simply because the thickness of fire protection applied to the beams is increased in the 120-minute case.

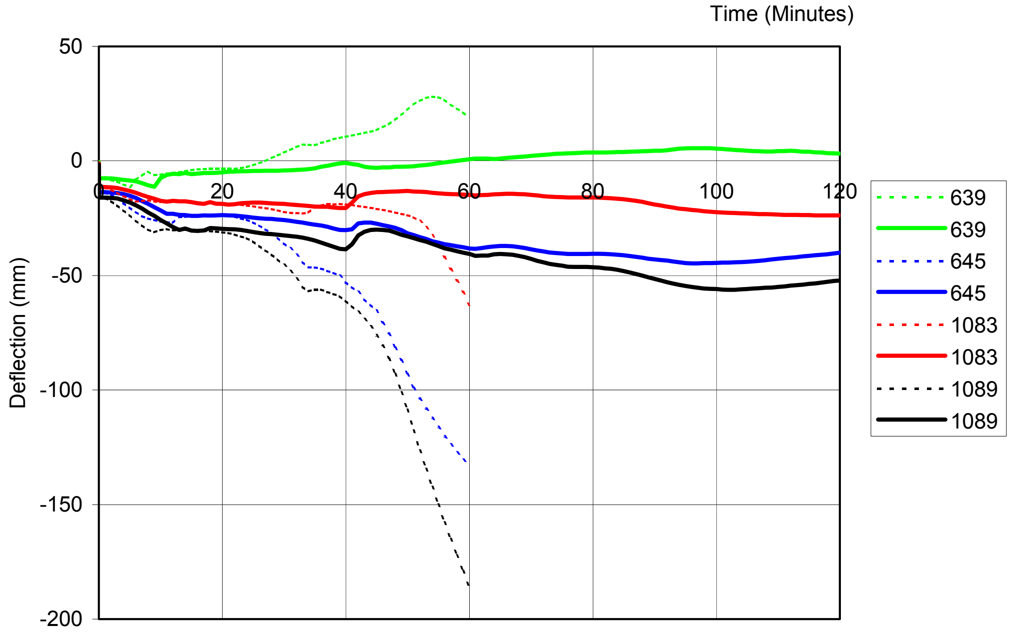

Figure E88: Deflections with respect to time

Figure E88 shows that maximum deflection that occurs in the realistic fire is similar to that of the standard fire scenarios. This is because parametric fire that was used has a time-equivalent period of 72 minutes and the beams were protected such that they achieve a 60-minute fire resistance period in accordance with the standard fire curve. If the time-equivalent period was less than 60-minutes, the maximum deflection would be less and visa-versa. The primary difference between natural fire and standard fire analyses is the time at which the maximum deflection occurs. This is because the maximum atmosphere temperature in the parametric fire occurs at 52 minutes as opposed to 60 minutes in the standard fire (for a 60-minute fire resistance period).

Design Loads – Cases 9 and 10

Figure E89 shows the comparison between an imposed load of 4 + 1 kN/m^2 (Base Case) and 2.5 + 1 kN/m^2. The solid line is for the reduced load condition.

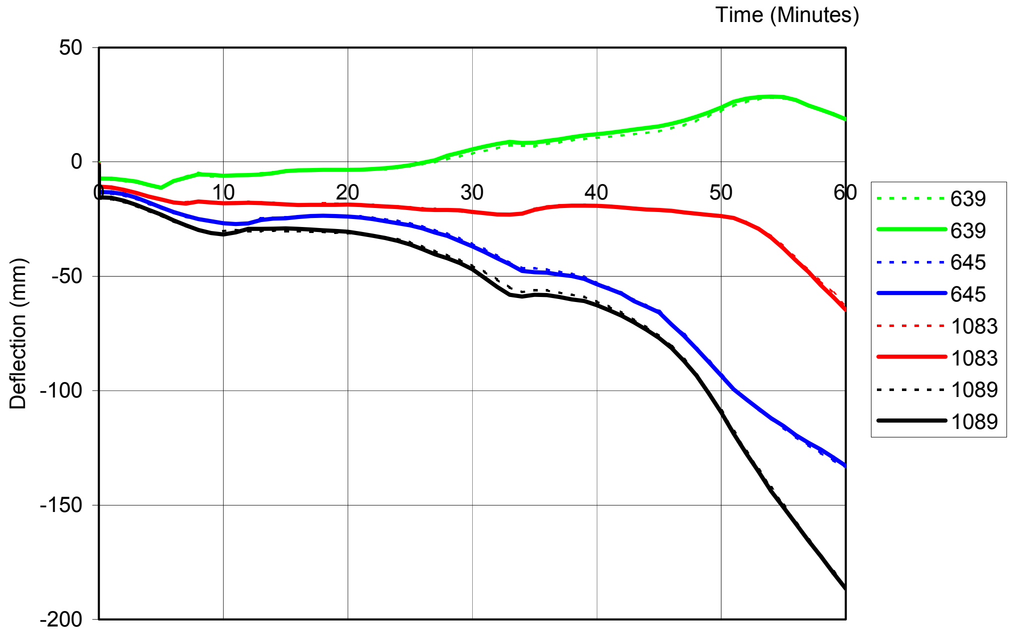

Figure E89: Deflection with respect to time.

Figure E90 shows the comparison between an imposed load of 4 + 1 kN/m^2 (Base Case) and 7.5 + 1 kN/m^2. The solid line is for the increased load condition.

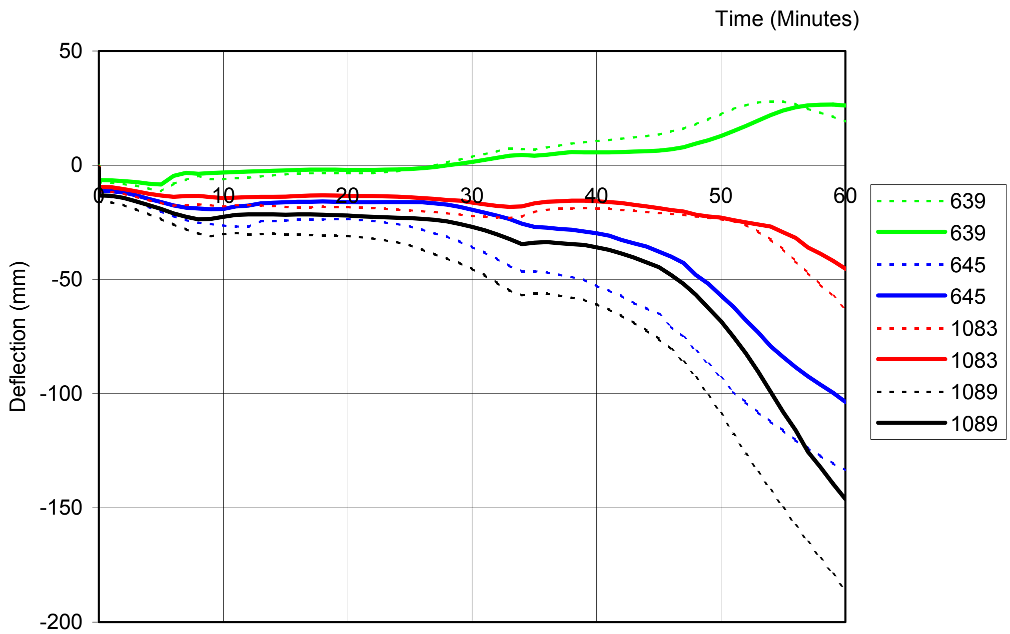

Figure E90: Deflection with respect to time.

It can be seen from Figures E89 and E90 that varying the load has a minimal impact on the magnitude of the maximum deflections. This is because the beam sizes have been changed to reflect the load conditions and therefore load ratio within the beams remains the same. It would be interesting to assess the impact of different load ratios within beams on the deflections that occur as it may be possible to reduce the minimum deflection-head requirement for compartment walls if the load ratio is reduced.

Grid Arrangements – Cases 11 and 12

Figure E91 shows a comparison between the central deflections for Bays 5, 6, 8 and 9 for the 9m x 9m and the 9m x 6m grids. The maximum deflections are approximately 185mm and 115mm for the 9m x 9m and 9m x 6m grids respectively. These deflections correspond to approximately span/50 in both cases.

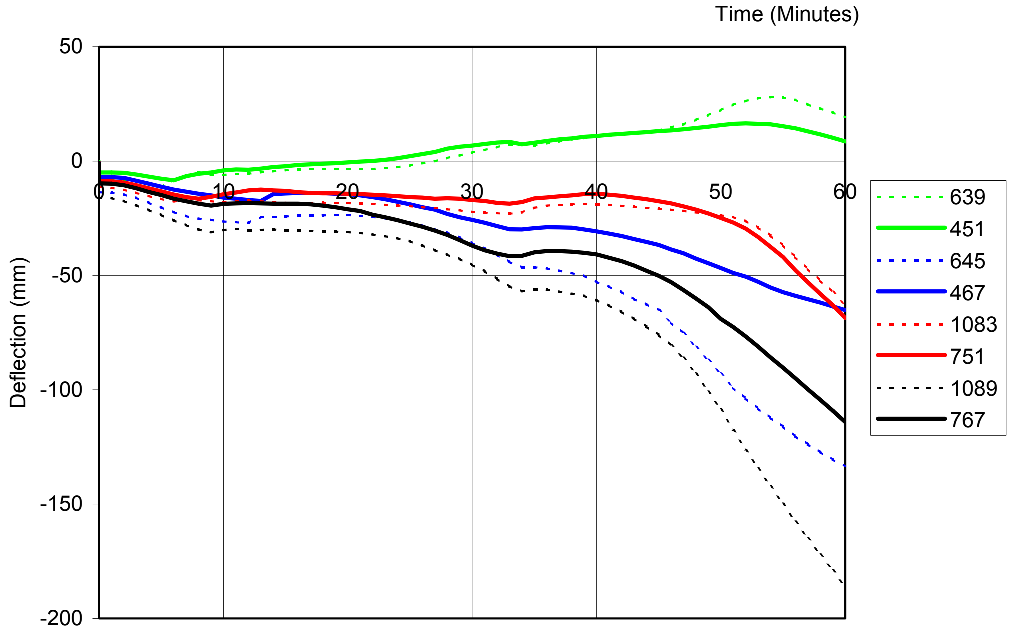

Figure E91: Comparison deflections for 9m x 9m (dashed) and 9m x 6m (solid) grids

Figure E92 shows a comparison between the central deflections for Bays 5, 6, 8 and 9 for the 9m x 9m and the 9m x 7.5m grids. The maximum deflections are approximately 185mm and 150mm for the 9m x 9m and 9m x 7.5m grids respectively. These deflections also correspond to approximately span/50 in both cases.

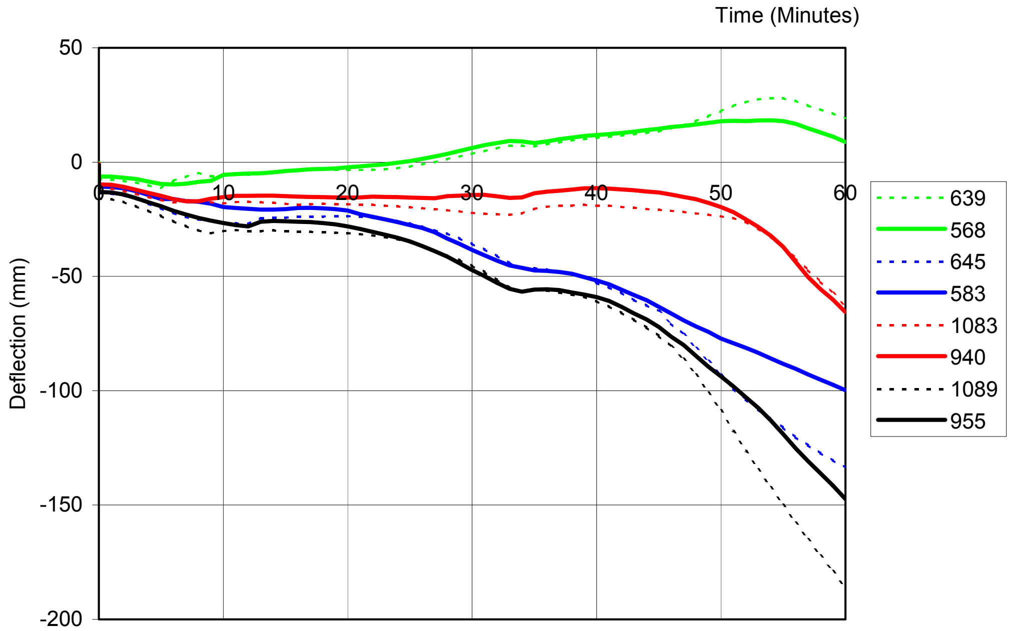

Figure E92: Comparison deflections for 9m x 9m (dashed) and 6m x 7.5m (solid) grids

The results of the study on different grid arrangements show that increasing the beam span increases the maximum deflection. This is expected. However, it can also be seen that the maximum deflection is approximately span/50 in all three cases. This suggests that the deflection-head requirements for compartment walls should be a function of the span under which they sit.

bre

Summary

Analysis	Maximum Deflection (mm)	Maximum Deflection on Compartment Line (mm)
1 – Base Case	185 (Span/49)	N/A
2 – Compartment 1	175 (Span/51)	85 (Span/106)
3 – Compartment 2	205 (Span/44)	40 (Span/225)
4 – Compartment 3	175 (Span/51)	55 (Span/164)
5 – Compartment 4	200 (Span/45)	15 (Span/600)
6 – Partial Protection	350 (Span/26)	N/A
7 – Natural Fire	56mm (Span/160)	N/A
8 – 120 Minute Fire	161mm (Span/56)	N/A
9 – 2.5 +1 kN/m^2	186mm (Span/49)	N/A
10 – 7.5 +1 kN/m^2	146mm (Span/61)	N/A
11 – 9m x 6m	115 (Span/52)	N/A
12 – 9m x 7.5m	150 (Span/50)	N/A

* 0 corresponds to no compartment walls and represents a worst-case scenario.

Table E7: Summary of maximum displacements

References for Appendix E

1. prEN 1993-1-2 Eurocode 3: Design of steel structures – Part 1.2: General rules – structural fire design, Stage 34 Draft, February 2002, CEN, Brussels

2. prEN 1994-1-2 Eurocode 4 – Design of composite steel and concrete structures – Part 1.2: General rules – Structural fire design, Stage 34 Draft, October 2003, CEN, Brussels

3. Welch, S. & Bailey, C. “Development of a validated engineering methodology for prediction of thermal and structural performance of masonry/concrete walls”, PiI Project report number 79330, Technology and Performance 38/19/179 cc 1841, 28 March 2001

4. Welch, S. (2000) "Developing a model for thermal performance of masonry exposed to fire", First International Workshop on "Structures in Fire", Copenhagen, June 2000

